A neuronal PIP3-dependent program of oligodendrocyte precursor recruitment and myelination

Dissertation

for the award of the degree

“Doctor rerum naturalium” (Dr. rer. nat.)

Division of Mathematics and Natural Sciences

of the Georg-August-Universität Göttingen

Basic program Biology

of the Georg-August University School of Science (GAUSS)

submitted by

Georg Wieser

born in

Satu Mare

Göttingen, 2016

Ph.D. thesis committee:

Prof. Klaus-Armin Nave Ph.D. (Reviewer)
Department of Neurogenetics,
Max-Planck-Institute of Experimental Medicine

Prof. Dr. Nils Brose (Reviewer)
Department of Molekulare Neurobiologie
Max-Planck-Institute of Experimental Medicine

Prof. Dr. Ralf Heinrich
Department of Cellular Neurobiology,
Schwann-Schleiden Research Centre

Extended Ph.D. thesis committee:

Prof. Dr. Dr. Hannelore Ehrenreich
Clinical Neuroscience,
Max-Planck-Institute of Experimental Medicine

Prof. Dr. Martin Göpfert
Department of Cellular Neurobiology,
Schwann-Schleiden Research Centre

Dr. Manuela Schmidt
Somatosensory Signaling Group,
Max-Planck-Institute of Experimental Medicine

Date of the oral examination: 15.12.2016

Declaration

I hereby declare that the PhD thesis entitled, "**A neuronal PIP3-dependent program of oligodendrocyte precursor recruitment and myelination**", has been written independently and with no other sources and aids than quoted. I would like to gratefully acknowledge collaborations with Sonia Spitzer and Ragnhildur Thóra Káradóttir (electrophysiological recordings), Kuo Yan and Dr. Ingo Bormuth (*in situ* hybridization) and Dr. Sven Wichert and Prof. Dr. Moritz Rossner (transcriptional profiling), as also indicated in the text. The material and methods part and most of the results are adapted from the publication "**A neuronal PI(3,4,5)P3-dependent program of oligodendrocyte precursor recruitment and myelination**", that has been published recently in *Nature Neuroscience* (Nat Neurosci. 2016 Oct 24. doi: 10.1038/nn.4425, PMID: 27775720).

Göttingen, 15.11.2016

Georg Wieser

Acknowledgments

I would like to convey my deep gratitude to Prof. Klaus-Armin Nave Ph.D., for giving me the opportunity to work in his department. He supported me during my PhD work in every possible way. I thank him a lot for sharing his scientific experience and knowledge.

I am sincerely grateful to Dr. Sandra Goebbels for her supervision and for endless valuable discussions. It was a unique experience to work on such an interesting and challenging project. With her influence, I developed personally and as a skilled scientist. I am greatly indebted to her for all the opportunities and thankful for her patience and support over the years.

I would like to thank Julia Edgar Ph.D. for her overwhelming support and help in the cell culture business. Her contributions were an important basis for my experiments and she influenced my way of thinking a lot.

I would like to thank Bettina Weege and Dr. Alexander Pieper for their contributions at the beginning of this project.

I am thankful to our collaborators, especially to Sonia Spitzer and Ragnhildur Thóra Káradóttir and Kuo Yan and Dr. Ingo Bormuth, Dr. Khalad Karram and Nicolas Renier Ph.D.

I would like to thank the members of my thesis committee, Prof. Dr. Nils Brose and Prof. Dr. Ralf Heinrich for their helpful discussions, advice and support.

I am deeply thankful to Ulli Bode, Hossein Hidaji, Elina Ott, Ramona Jung, Carolin Böhler and especially to Annette Fahrenholz for technical support in many ways.

I thank Torben Ruhwedel and Dr. Wiebke Möbius for teaching me the methods of electron microscopy. They were always very helpful and supported my experiments.

I would like to thank Dr. Sven Wichert and Dr. Magdalena Brzózka for help with the Laser-capture microdissection unit and Prof. Dr. Moritz Rossner with the help of the transcriptional profiling of laser captured GC layers.

I would also like to thank Cornelia Casper, Tanja Freerck, Bianca Nickel, Dr. Ursula Fünfschilling and Rainer Libal for providing an excellent mouse house and transgenic facility. I am grateful to Hajo Horn, Rolf Merker, Lothar Demel and Beate Beschke for all technical help regarding computer issues.

I would like to give special thanks to Michaela Schmalstieg and Gabriele Endo for help with administrative and bureaucratic issues.

During my time in the department of Neurogenetics, I had the opportunity to teach and help several rotation and master students. I therefore thank Ulrike Gerwig, Oleksandr Yagensky, Ole Jensen, Simon Merz, Markus Stahlberg, and Simon d'Aquin for their contributing effort.

I am grateful for the excellent working atmosphere, provided by every member of the Neurogenetics lab. I thank Dr. Julia Patzig, Ulrike Gerwig, Ramona Jung, Dr. Amit Agarwal, Dr. Markus Schwab and Dr. Tilmann Unterbarnscheidt for a fun and helpful environment.

Above all, I am indebted from the depth of my heart to my parents, my parents-in-law and especially to Julia, for their immense support, love and care.

Dedicated to Hannah Emilia Wieser

Content

Acknowledgments **4**

List of figures **8**

Abbreviations **10**

1. Abstract **13**

2. Introduction **14**

2.1. The central nervous system 14

2.2. Myelination 15

2.3 Regulation of myelination 17

2.4 PTEN 18

2.5 The architecture of the cerebellum 20

2.6 Cerebellar PTEN mutants 21

2.7 Aim of the study 23

3. Results **24**

3.1 *Pten* mutant GC trigger *de novo* myelination of Pf axons 24

3.2 *Pten* mutant GC trigger OPC proliferation and differentiation 31

3.3 Is ectopic myelination triggered by neuronal activity? 35

3.4 Is ectopic myelination triggered by down regulation of inhibitory cues? 36

3.5 Functional validation of selected candidate factors 38

3.5.1 Experimental design and hypothesis 38

3.5.2 *In vivo* uncoupling of brain derived neurotrophic factor (Bdnf) 40

3.5.3 *In vivo* uncoupling of Neuregulin 1 (Nrg1) 43

3.5.4 *In vitro* validation of selected candidate factors 45

3.5.4.1 Proliferation assay 45

3.5.4.2 Differentiation assay 46

3.5.4.3 Myelination assay 47

3.5.5 The cell type specific origin of selected candidate factors 49

3.5.5.1 No signs of gliosis in *NEX-CreERT2*Pten*$^{loxP/loxP}$ mice 51

3.5 Inactivation of *Pten* in CA3 neurons 52

3.6 Hamartoma formation in aged *Pten* mutants 54

4. Discussion **56**

4.1 Axon caliber and PI3K dependent induction of myelination 56

4.2 Regulation of OPC proliferation, differentiation and CNS myelination 58

4.3 Utilization of acquired knowledge from PI3K dependent *de novo* myelination 62

4.4 *Pten* deficiency in granular cells: A new mouse model for Lhermitte-Duclos disease 63

5. Material and Methods **64**

5.1 Mouse mutants 64

5.1.1 Genotyping primer for various mouse lines 64

5.2 BrdU labeling 65

5.3 Histology and immunohistochemistry 66

5.4 In situ hybridization 66

5.5 Electron microscopy 67

5.6 Electrophysiology 67

5.7 Synaptic current analysis 68

5.8 Laser-capture microdissection, RNA isolation and linear amplification, and microarray hybridization 68
5.9 RNA isolation, cDNA synthesis, and qRT-PCR....68
5.9.1 Quantitative real-time PCR primers....69
5.10 Mixed myelinating cocultures from mouse spinal cord....69
5.11 Mixed primary oligodendrocyte cultures....70
5.12 Recombinant proteins....71
5.13 Immunocytochemistry....71
5.14 Morphometry....71
5.15 G-ratio measurement....72
5.16 Protein analysis....72
5.17 Statistical analysis....73
6. References 76

List of figures

Fig. 1. Oligodendrocyte lineage cell development.

Fig. 2. Structure of myelinated axons in the CNS.

Fig. 3. Schematic diagram depicting the PI3K/Akt pathway.

Fig. 4. The cerebellar cytoarchitecture.

Fig. 5. Genetic loss of *Pten* in cerebellar granule cells triggers *de novo* myelination.

Fig. 6. *Pten* mutant granule cells stimulate the AKT1/mTOR pathway.

Fig. 7. Progressive enlargement of *Pten* mutant cerebella and increase in Pf diameter.

Fig. 8. Genetic loss of *Pten* triggers *de novo* myelination of parallel fibers.

Fig. 9. Progressive *de novo* myelination of *Pten* mutant parallel fibers.

Fig. 10. *De novo* myelination of parallel fibers and formation of node-like structures.

Fig. 11. Parallel fiber synapses onto Purkinje cell dendritic spines in the presence of myelin.

Fig. 12. G-ratio analysis.

Fig. 13. Local differentiation of OPCs induced by *de novo* myelination.

Fig. 14. Local proliferation of OPCs in the molecular layer.

Fig. 15. Early onset of proliferation.

Fig. 16. Ectopic myelination is not triggered by neuronal activity.

Fig.17. Cell type specific ablation of *Pten* in a small subset of cerebellar granule cells.

Fig.18. Experimental design to test candidate factors.

Fig.19. Histological *in vivo* validation of *Bdnf* uncoupling.

Fig. 20. Electron microscopy of *Pten* cKO and double mutants lacking *Pten* and *Bdnf.*

Fig. 21. Increased local proliferation of OPCs in double mutants lacking *Pten* and *Bdnf.*

Fig. 22. Neuregulin 1 is not required for Pf myelination in *Pten* mutant mice.

Fig. 23. Proliferation assay.

Fig. 24. Differentiation assay.

Fig. 25. Myelination assay.

Fig. 26. Fgf1 treatment of myelinating cocultures.

Fig. 27. Reactive gliosis and angiogenesis in *Pten* mutant mice.

Fig. 28. No activation of microglia and astrocytes in the *NEX-CreERT2*Pten*$^{loxP/loxP}$ cerebellum.

Fig. 29. *Pten* inactivation in principal neurons of the hippocampus.

Fig. 30. Enlargement of CA3 neurons upon *Pten* inactivation.

Fig. 31. *Pten* mutant mice as a model of Lhermitte-Duclos disease.

Abbreviations

°C	Degrees Celsius (centigrade)
BrdU	5'-bromo-2'-deoxyuridine
BSA	Bovine serum albumin
CNP	2'3'-cyclic nucleotide 3'phosphodiesterase
CNS	Central nervous system
DAB	3,3'-Diaminobenzidine
DAPI	4'-6-Diamidino-2-phenylindole
DCN	Deep cerebellar nuclei
ddH2O	Double distilled (or miliQ) water
DIV	Days in vitro
e.g.	Exempli gratia
EDTA	Ethylened acid
EM	Electron microscopy
f.c.	Final concentration
GL	Granular cell layer
GS	Goat serum
H&E	Haematoxylin-Eosin staining
HS	Horse serum
IHC	Immunohistochemistry
JXP	Juxtaparanode
kDa	Kilodalton
KO	Constitutive mutant
LDD	Lhermitte-Duclos disease
M	Molar
MBP	Myelin basic protein
ML	Molecular layer
mM	Millimolar
MS	Multiple sclerosis

n.s.	Non-significant
ng	Nanogram
nm	Nanometer
OL	Oligodendrocyte
OPC	Oligodendrocyte precursor cell
p	P-value
P	Postnatal day
PBS	Phosphate buffered saline
PCR	Polymerase chain reaction
Pf	Parallel fiber
PFA	Paraformaldehyde
PIP2	Phosphatidylinositol-4,5-bisphosphat
PIP3	Phosphatidylinositol (3,4,5)-trisphosphate
PL	Purkinje cell layer
PLP	Proteolipid protein
PMD	Pelizaeus-Merzbacher disease
Pn	Paranodal loop
PNS	Peripheral nervous system
PTEN	Phosphatase and tensin homolog
qRT-PCR	Quantitative real time PCR
Rpm	Revolutions per minute
RT	Room temperature
SC	Schwann cell
SD	Standard deviation
SDS	Sodium dodecyl sulfate
sec	Seconds
s.e.m.	Standard error of the mean
SPJ	Septate-like junction
TBS	Tris buffered saline

TEMED	Tetramethylendiamin
U	Unit, (for enzyme activities)
WM	White matter
WT	Wild type (control)
X-gal	5-bromo4-chloro-3-indolyl-β-D-galactoside
µg	Microgram
µl	Microliter
µM	Micromolar
µm	Micrometer

1. Abstract

Evolution of myelin has enabled rapid impulse propagation and development of complex brain circuitry. However, the *in vivo* mechanisms that trigger and orchestrate proliferation of oligodendrocyte precursor cells (OPCs), differentiation of OPCs into oligodendrocytes, and myelination in central nervous system (CNS) have remained unclear. Neuregulin-1/ErbB signaling, which controls virtually all aspects of peripheral myelination by Schwann cells is not essential for myelination in the CNS. Moreover, the identification of several promyelination factors made by astrocytes and microglial cells, the responsiveness of oligodendrocytes to ubiquitously expressed growth factors and their ability to myelinate artificial nanofibers has raised questions about the cellular origin of the key signals that control CNS myelination. To particularly address the impact of axonal signals *in vivo*, we studied the cerebellum of mice, in which the axons of granule cell neurons (referred to as “parallel fibers”) within the molecular layer are naturally of small caliber and unmyelinated. By conditional inactivation of the lipid phosphatase PTEN, we experimentally enhanced PI(3,4,5)P3-dependent Akt/mTOR downstream signaling specifically in granule cells, which subsequently lead to a significant increase in parallel fiber (Pf) diameters. Most importantly, this increase was tightly associated with the proliferation of OPCs, the differentiation of oligodendrocytes in the molecular layer, and the *de novo* myelination of up to 40% of all Pf at 1 year of age. While the synaptic input to OPCs was unchanged, gene expression profiling of laser captured mutant granule cell layers identified proteins, such as FGF1, Pleiotrophin, Timp3, Thymosin beta 4, and Activin A, as novel regulators of OPC proliferation, oligodendrocyte differentiation, and/or myelin growth. We conclude that activation of neuronal, PI(3,4,5)P3-dependent downstream signaling pathways can be sufficient to promote the entire program of OPC recruitment and CNS myelination.

2. Introduction

2.1. The central nervous system

The nervous system serves as a control center between the inner and the outer world. Composed of the central nervous system (CNS) and the peripheral nervous system (PNS), it constantly receives information, processes highly complex mechanisms and reacts in diverse patterns of behavioral control. The CNS is built by a variety of different cell types and is comprised of brain and spinal cord. It can be divided into white and gray matter. White matter mainly consists of myelinated fiber tracts and glial cells, while the gray matter is formed by neuronal cell bodies, dendrites and primarily unmyelinated axons.

Glial cells in the mammalian CNS can be subdivided into astrocytes, microglia, oligodendrocytes and chondroitin sulfate proteoglycan expressing NG2-Glia (Kettenmann and Ransom, 2005; Staugaitis and Trapp, 2009). Astrocytes usually exhibit a star shaped morphology and serve distinct functions, for example, the biochemical support of endothelial cells (the blood brain barrier forming cells), the support of neurons by transferring nutrients (e.g. lactate) and the removal of neurotransmitters from the synaptic cleft (Kettenmann and Ransom, 2005). Microglia cells are the resident innate immune cells of the CNS and are able to remove cellular debris or even parts of damaged cells (Kettenmann and Verkhratsky, 2011). Oligodendrocytes wrap long segments of axons with multilayered sheaths of extended cell membrane, the so-called “myelin sheaths” (Nave, 2010). By insulating axons at the internodes and thereby restricting action potentials to the nodes of Ranvier, they are providing the basis for the fast saltatory conduction of action potentials (Baumann and Pham-Dinh, 2001; Kettenmann and Ransom, 2005). Myelinated axons accelerate nerve conduction 20-100-fold compared to unmyelinated axons of the same diameter (Nave and Werner, 2014). Furthermore, reduced transverse capacitance and increased transverse resistance of the axonal plasma membrane is demonstrated by axons ensheathed with myelin. The restriction of action potentials to nodes of Ranvier reduces the ATP-dependent Na^+/K^+ exchange in preserving the resting potential of axonal membranes. In addition, oligodendrocytes maintain long-term axonal integrity and provide trophic axonal support. This is especially important for longer axons, where some myelinated segments can be even several meters away from the neuronal soma (Funfschilling et al., 2012; Lee et al., 2012; Nave, 2010; Nave and Werner, 2014).

2.2. Myelination

Myelination is an ongoing process that starts around birth and continues into the third decade of life in humans (Miller et al., 2012). During development, oligodendrocytes evolve from precursor cells that migrate throughout the spinal cord and brain, before they differentiate into postmitotic pre-myelinating oligodendrocytes and finally into myelin forming oligodendrocytes (**Fig. 1**). Oligodendrocyte precursor cells (OPCs) are produced from neuroepithelial cells in several distinct spatiotemporal waves in the spinal cord and brain (Rowitch and Kriegstein, 2010) and can be identified by the expression of marker proteins such as the NG2 proteoglycan and platelet-derived growth factor receptor alpha (PDGFRa). They remain to be present and are evenly distributed throughout the gray matter and white matter in the adult CNS (Kirby et al., 2006).

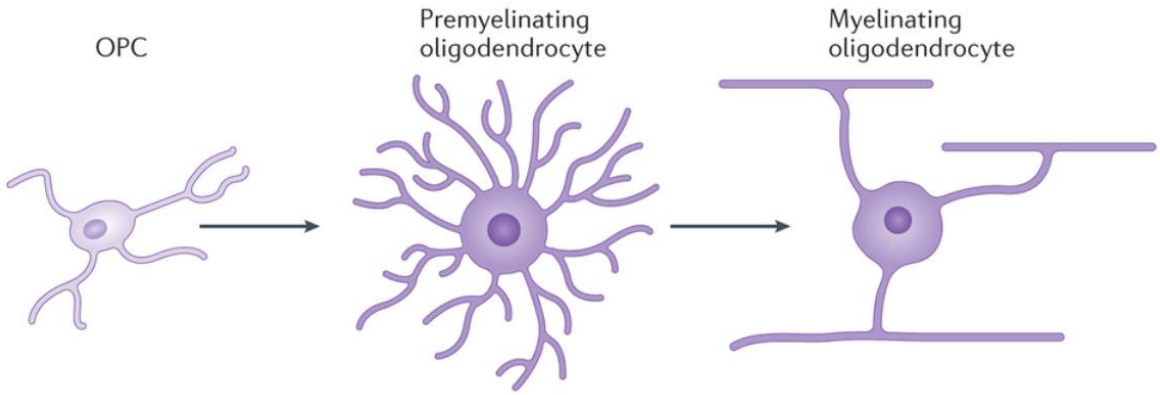

Fig. 1. Oligodendrocyte lineage cell development. Oligodendrocyte progenitor cells (OPCs) differentiate into multipolar premyelinating oligodendrocytes, which finally mature into myelinating oligodendrocytes. OPCs compose the majority of mitotic cells in the adult brain. Mature oligodendrocytes are the myelin forming glia cells in the CNS and are able to myelinate multiple axons simultaneously (adapted image from Fields, 2015).

Mature oligodendrocytes are capable of forming myelin sheaths that cover between 20 and 60 different axonal segments (Chong et al., 2012; Hildebrand et al., 1993; Matthews and Duncan, 1971) (**Fig. 2a**). In contrast, Schwann cells, the myelin forming glia cells in the PNS, are bipolar and enwrap only one axonal segment each. Data from zebrafish experiments suggests, that the wrapping of single axonal segments takes only a couple hours (Czopka et al., 2013). The half-life of myelin proteins is very long and myelinating oligodendrocytes can remain for more than 5 decades in humans (Savas et al., 2012; Yeung et al., 2014). Nevertheless, OPCs are also abundant in the mature brain, and account for approx. 5% of all brain cells (Bergles and Richardson, 2016). They continue to proliferate

and differentiate into mature myelinating oligodendrocytes (Richardson et al., 2011). that for example replace dying oligodendrocytes or intercalate among existing myelin sheaths. Furthermore, adult-born oligodendrocytes, might be involved in the myelination of previously unmyelinated axons and thereby contribute to neuronal plasticity. In humans and mice there is evidence, that myelin remodeling contributes to motor learning (McKenzie et al., 2014; Yeung et al., 2014; Young et al., 2013). For example, changes in white matter structures could be correlated with extensive piano practice and juggling (Hu et al., 2011; Scholz et al., 2009).

Myelin is a highly specialized, fundamental compartment of the oligodendrocyte, which can further be subdivided in compact and non-compact myelin (Arroyo and Scherer, 2000; Poliak and Peles, 2003). Compact myelin consists of several layers of adhesive plasma membrane. Proteolipid protein (PLP) is the most abundant protein of the CNS myelin, with a role in the compaction, stabilization and maintenance of myelin sheaths (Boison et al., 1995; Klugmann et al., 1997). Analysis of mice lacking PLP and its splice isoform DM20 revealed physically unstable CNS myelin (Boison et al., 1995; Klugmann et al., 1997). In patients, mutations in the *PLP* gene causes Pelizaeus-Merzbacher disease (PMD), an X-linked dysmyelinating disorder (Inoue et al., 1996). Another essential adhesion protein is Myelin basic protein (MBP) (Dupouey et al., 1979), with a potential zipper function for the cytoplasmic leaflets (Nawaz et al., 2009). In mutant mice lacking MBP expression (*shiverer*), oligodendrocytes fail to assemble compact myelin and display hypomyelination in the CNS (Rosenbluth, 1980). The non-compact myelin compartment is lacking these adhesion proteins and is comprised of adaxonal myelin, abaxonal myelin, paranodal loops and additional nanochannels (**Fig. 2b**). Paranodal loops form septate-like junctions (SpJ) with the axonal membrane and directly influence the distribution of sodium channels at the node of Ranvier and potassium channels at the juxtaparanode (JXP) (Poliak and Peles, 2003; Rasband, 2011). A large proportion of the axon at the juxtaparanodes and the internodes is covered by the adaxonal membrane of the oligodendrocyte.

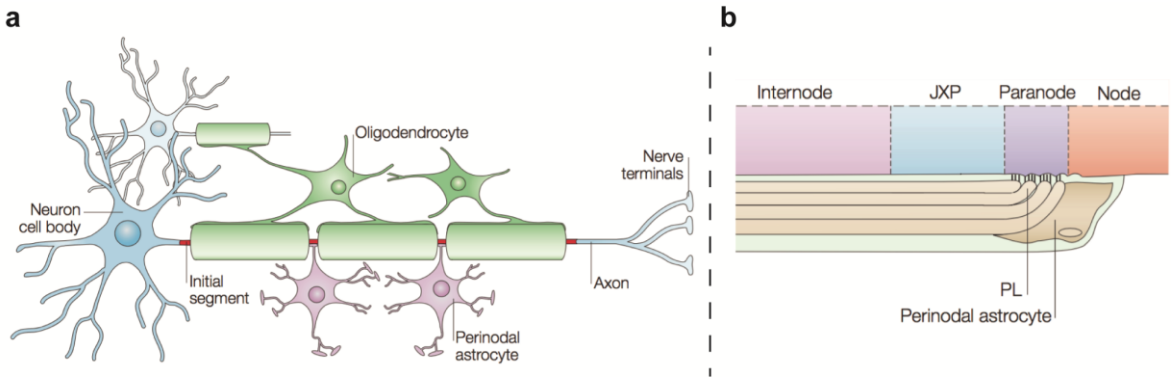

2.3 Regulation of myelination

Suggestively, differentiation of oligodendrocytes and myelination is regulated by a plethora of intrinsic and extrinsic cues. These signals include growth factors, protein kinases and extracellular matrix molecules, influencing epigenetic modifications, transcriptional and translational regulation and the actin cytoskeleton in oligodendrocytes (Bercury and Macklin, 2015). In contrast to cultured Schwann cells, which clearly require axonal signals for differentiation, oligodendrocyte development, at least *in vitro,* follows more a “default pathway”. Oligodendrocytes can differentiate and even produce myelin components in the absence of neurons and axons (Dubois-Dalcq et al., 1986; Mirsky et al., 1980; Temple and Raff, 1986). Later it was shown that they can even myelinate artificial carbon nanofibers and micropillars (Lee et al., 2012; Mei et al., 2014). These findings may raise the question to which extend axonal signals are required at all to regulate oligodendrocyte differentiation and myelination. On the other hand, several lines of experiments have indeed suggested an instructive role of neuron-derived signals at various stages of oligodendrocyte development *in vivo* (Barres and Raff, 1999; Simons and Trajkovic, 2006; Taveggia et al., 2010). For example, killing axons significantly reduced the number of oligodendrocytes and supplying the transected optic nerve with exogenous ciliary neurotrophic factor (CNTF) prevented the reduction of oligodendrocytes (Barres et al., 1993). Transgenic mice, in which the number of optic nerve axons was genetically increased also harbored more oligodendrocytes (Burne et al., 1996). In other experiments electrical activity of axons has increased the number of OPCs and supported myelination, possibly as a response to the axonal release of adenosine (Barres and Raff, 1993; Demerens et al., 1996; Gibson et al., 2014; Stevens et al., 2002). However, in contrast to Schwann cells, which are always in close axonal contact during migration CNS oligodendrocyte lineage cells develop largely without close axonal contact. Myelination in the CNS begins with OPC recruitment and expansion, followed by oligodendrocyte differentiation, all steps without axonal contact.

Different growth factors and cytokines, including Pdgf, Fgf2, Igf1, Bdnf, Nt3, Cntf and Lif, have been identified over the last decades as regulators of the proliferation and differentiation of oligodendrocyte lineage cells (Baron et al., 2005; Barres and Raff, 1994; Carson et al., 1993; Ishibashi et al., 2006; Miller, 2002).

Fig. 2. Structure of myelinated axons in the CNS. (**a**) Oligodendrocytes cover multiple axonal segments and provide the basis for saltatory signal propagation. (**b**) Schematic longitudinal cut through a myelinated fiber heminode. The node, paranode, juxtaparanode (JXP) and internode are labelled and are structurally specialized axonal segments upon myelination (modified image from Poliak and Peles, 2003).

Most of these identified factors are produced by astrocytes. However, *in vitro* experiments also revealed the capability of endothelial cells to promote the survival and proliferation of OPCs by soluble growth factors (Arai and Lo, 2009). In contrast to the PNS, no neuronally expressed “regulator” has been identified so far that would control myelination in the CNS. With respect to it's instructive role in PNS myelination, a possible candidate, however, was neuronal Neuregulin1 (Nrg1). This axonal growth factor activates ErbB receptor tyrosine kinases on glial cells, and is required for Schwann cell survival, differentiation and myelination (Jessen and Mirsky, 2005; Michailov et al., 2004; Nave and Salzer, 2006; Taveggia et al., 2005). The role of Nrg1 in the CNS is still somewhat controversially discussed. Earlier reports suggested a role for Nrg1 and ErbB receptors in OPC proliferation, oligodendrocyte survival, and myelination (Taveggia et al., 2008; Vartanian et al., 1999). However, intensive genetic analyses of mice lacking Nrg1 from CNS neurons or the corresponding ErbB3/4 receptors from oligodendrocytes revealed normal oligodendrocyte numbers and intact CNS myelination (Brinkmann et al., 2008). Neuronally expressed proteins that are able to influence oligodendroglial functions can also be found in the group of secretases. Disintegrin and metalloprotease (ADAM) proteins have been implicated in PNS myelination (Sagane et al., 2005; Wakatsuki et al., 2009). The β-site amyloid precursor protein cleaving enzyme 1 (BACE1) demonstrated a role in PNS and CNS myelination (Hu et al., 2006; Willem et al., 2006). Oligodendrocyte development in the CNS can furthermore be limited by interaction between Jagged-Notch. Jagged is expressed by neurons at early developmental stages and by binding to Notch1 (only expressed by oligodendrocytes) OPC differentiation and myelination is inhibited (Genoud et al., 2002; Givogri et al., 2002; Wang et al., 1998; Zhang et al., 2007).

2.4 PTEN

Phosphatase and tensin homolog *(Pten*) is a tumor suppressor gene that was first discovered by Li et al. 1997 in a variety of different breast, prostate gland and brain tumors (Li et al., 1997). The protein encoded by this gene is a phosphatidylinositol-3,4,5-trisphosphate 3-phosphatase. PTEN antagonizes the PI3K induced activation of Akt/mTor downstream signaling, by converting PIP3 (Phosphatidylinositol (3,4,5)-trisphosphate) into PIP2 (Phosphatidylinositol-4,5-bisphosphat) (Stiles et al., 2004b; Suzuki et al., 2008). Loss of PTEN function leads to over-activation of Akt and in general a hyperactivated PI3K downstream signaling as a consequence of accumulation of PIP3 in the plasma membrane (Cantley and Neel, 1999) (**Fig. 3**). In several *in vivo* studies the deletion of PTEN in neurons induced an increase in cell nuclei and cell soma (Backman et al., 2001; Fraser et al., 2004;

Groszer et al., 2001; Kwon et al., 2006). Differentiated neurons of the cerebral cortex and hippocampus lacking PTEN elicited a macrocephaly in mice and a neuronal hypertrophy (Kwon et al., 2001). Transgenic mice expressing Cre-recombinase under a *GFAP* promotor crossed to mice with floxed PTEN, resulted in *PTEN* deletion primarily in astrocytes, cerebellar granule cells and granule cells of the dentate gyrus of the hippocampus. Similar to findings in human Lhermitte-Duclos disease (LDD), this genetic modification induced enlarged brains, increased neuronal cell size and lead to abnormal neuronal organization (Backman et al., 2001; Kwon et al., 2001). LDD is a rare brain tumor, also known as dysplastic cerebellar gangliocytoma and is characterized by abnormal development and enlargement of the cerebellum. Although the exact cause in patients is unknown, mutations in the *PTEN* gene have been identified (Blumenthal and Dennis, 2008). Astrocytes, next to neurons show a similar cell growth when PTEN is deleted specifically in astrocytes in the cerebral cortex (Fraser et al., 2004). In mouse mutants selectively lacking PTEN in oligodendrocytes enlargement of all white matter tracts and hypermyelination at the single cell level was a prominent finding (Goebbels et al., 2010). Similar, the ablation of PTEN in from Schwann cells caused a hypermyelination of small-caliber axons and a focal hypermyelinating pathology in larger axons (Goebbels et al., 2010; Goebbels et al., 2012).

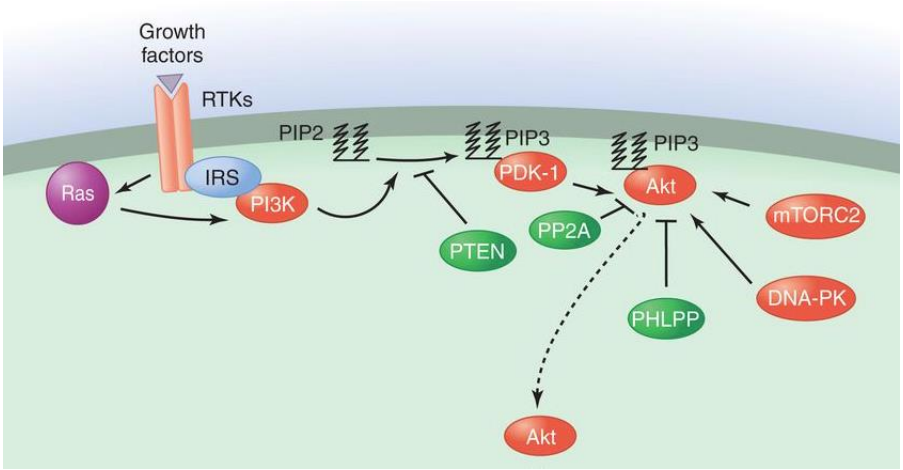

Fig. 3. Schematic diagram depicting the PI3K/Akt pathway. Binding of growth factors to G protein-coupled receptors and tyrosine kinase receptors (RTKs) triggers the phosphorylation of PIP2 by PI3K to generate PIP3. PTEN is the antagonist of PI3K and removes the 3′ phosphate of PIP3. Activated PDK1 phosphorylates AKT and promotes survival, migration, cell cycle progression, and cell growth (adapted image from Hemmings, 2015).

2.5 The architecture of the cerebellum

The cerebellum is a structure of the CNS and plays an important role in motor control. Cerebellar dysfunctions often present with motor abnormalities, such as ataxia. Coordination, precision and timing of movements are associated with the cerebellum. The vermis, a narrow midline area, divides the cerebellum into two hemispheres. The cerebellum consists of the cerebellar cortex and the deep cerebellar nuclei (DCN). Tightly folded layers of the cortex, with white matter underneath form the gross anatomy of the cerebellum. The cytoarchitecture is highly uniform and characterized by the molecular layer (ML), the Purkinje cell layer (PL) and granular cell layer (GL) (**Fig. 4a**). The ML is the outermost layer and contains stellate and basket cell interneurons. Parallel fibers (Pf), the granule cell axons, form a large number of excitatory synapses onto the dendrites of Purkinje cells and dendrites of basket cells and stellate cells. Pf belong to the thinnest known vertebrate axons and are normally unmyelinated, possibly because their size is below a critical threshold. From mouse to macaque, the average unmyelinated Pf diameter is between 0.2 µm and 0.3 µm and it scales up slightly with brain size (Wyatt et al., 2005) (**Fig. 4b**). The PL contains the large Purkinje cell bodies the Bergmann glia. Purkinje cell dendrites harbor a larger number of spine branches spreading up into the ML. Each Purkinje cell can be innervated by 100000-200000 parallel fibers (Ito, 2006). Additionally, and in contrast to the high number of parallel fiber inputs, Purkinje cells receive input from exactly one climbing fiber of the inferior olivary nucleus (Barmack and Yakhnitsa, 2011). The GL contains the cell bodies of the small granule cells, unipolar brush cells and the Golgi cells. The mossy fibers form excitatory synapses with the granule cells and the cells of the cerebellar nuclei (Nicoll and Schmitz, 2005). Granule cells are the most abundant neurons in the human brain (Purves, 2012).

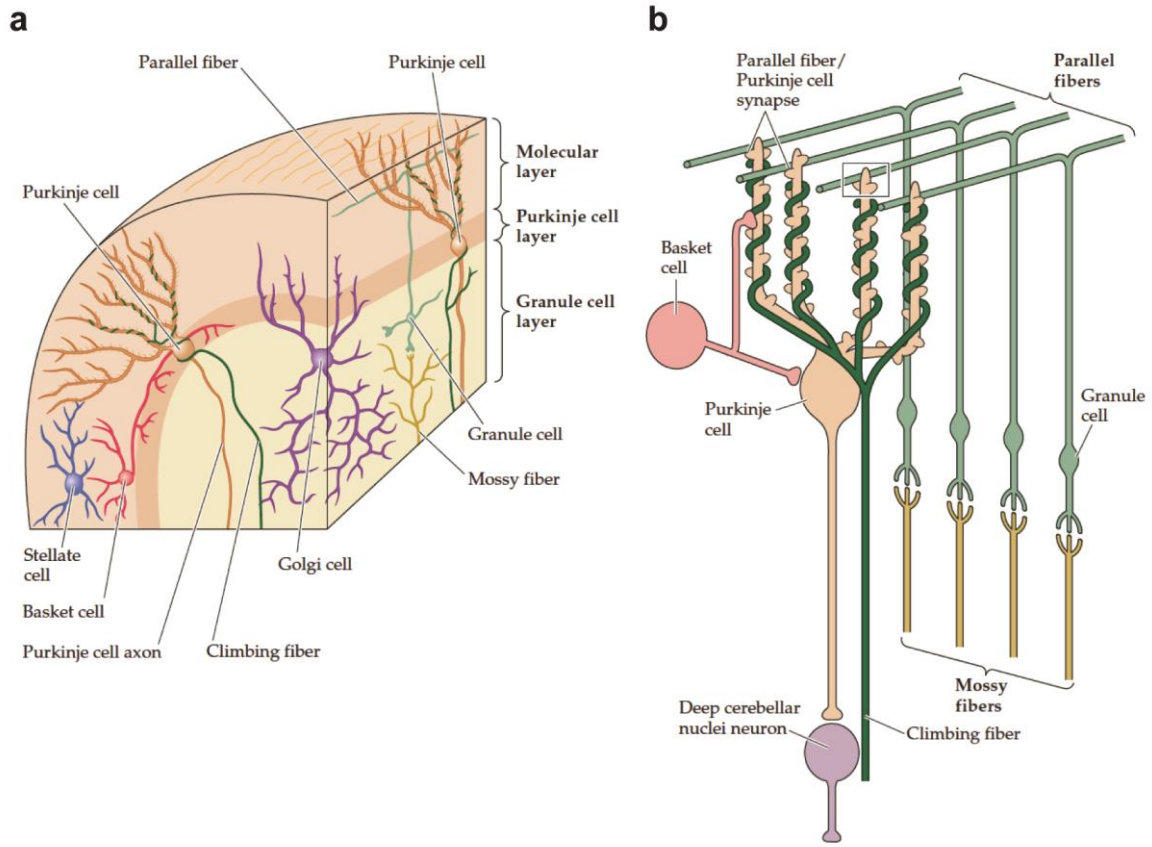

Fig. 4. The cerebellar cytoarchitecture. (**a**) The cerebellum can be clustered into the molecular layer, the Purkunje cell layer, the granule cell layer and underneath the cerebral cortex, the white matter. (**b**) The diagram elucidates the inputs from parallel fibers onto a Purkinje cell. Parallel fibers are the unmyelinated axons from the granule cells (modified image from Purves, 2012).

2.6 Cerebellar PTEN mutants

Throughout the body, the genetic loss of *Pten* can trigger enhanced mTOR-dependent cell growth (Backman et al., 2001; Fraser et al., 2004; Groszer et al., 2001; Kwon et al., 2006). Preliminary results were generated by B. Weege and Dr. A. Pieper (in the Department of Neurogenetics, subgroup "Developmental Neurobiology") by Intercrossing *Pten*-floxed mice (Lesche et al., 2002) with mice that express Cre recombinase (under control of the GABAA receptorα6 subunit promoter) selectively in cerebellar granule cells (Funfschilling and Reichardt, 2002). Experimental inactivation of *Pten* enlarged cerebellar granule cells and their axons (**Fig. 5a**). The diameter of parallel fibers increased over time, as quantified by electron microscopy (EM), reaching 0.61±0.009 µm in *Tg(mα6)-Cre*Pten*$^{loxP/loxP}$ mice (mutant) over 0.16±0.002 µm in *Pten*$^{loxP/loxP}$ mice (control) at 1 year of age (**Fig 5b**). More importantly the deletion of *Pten* in granule cells was sufficient to trigger *de novo* myelination

of the enlarged parallel fibers in the cerebellar molecular layer by wildtype oligodendrocytes, as indicated by Gallyas silver impregnation (Gallyas, 1979) (**Fig. 5c**).

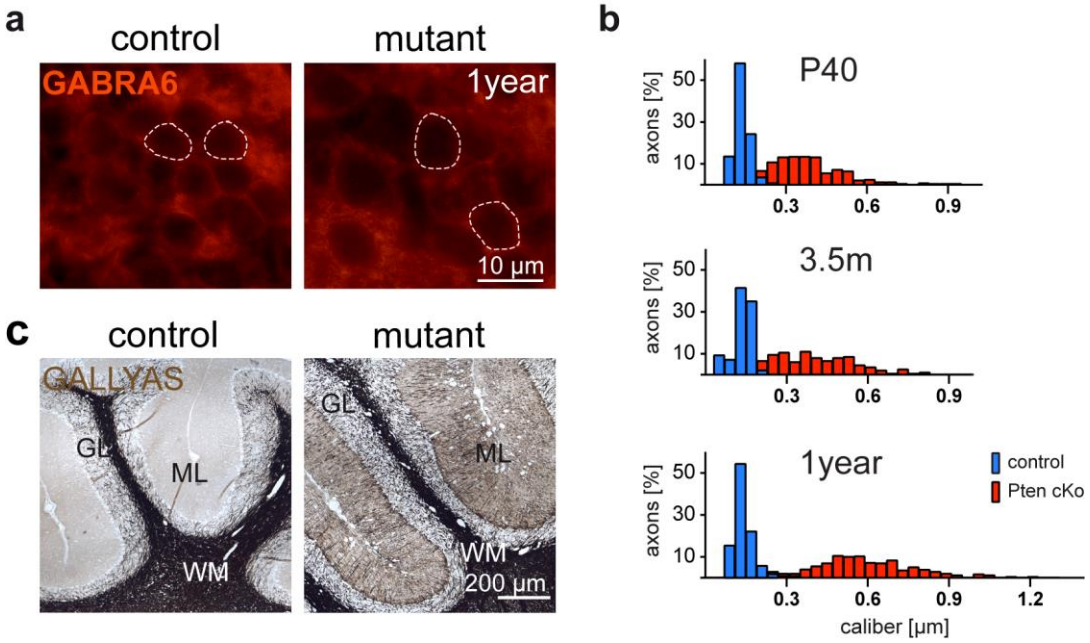

Fig. 5. Genetic loss of *Pten* in cerebellar granule cells triggers *de novo* myelination by progressive enlargement of granule cells and parallel fibers. (**a**) Immunostaining for $GABA_A$ receptor α6 subunit (in red), a cerebellar GC marker, at 1 year. Increased cell size in the mutants is indicated by dashed lines. (**b**) Progressive enlargement of Pf calibers in the mutant molecular layer (ML) over time as determined by EM (n=3 per genotype and age, 140 Pf quantified per animal). (**c**) *De novo* myelination of normally unsheathed parallel fibers in the cerebellum. In comparison to control brains (left), without myelin in the molecular layer (ML), Gallyas silver impregnation (Gallyas, 1979) of myelin demonstrates the presence of robust levels of ectopic myelin in the molecular layer (ML) of mutant mice. GL, granule cell layer; ML, molecular layer; WM, white matter.

2.7 Aim of the study

In the vertebrate nervous system, myelin decreases the electrical capacity of axonal membranes and enables rapid salutatory impulse propagation. The failure of oligodendrocytes and Schwann cells to achieve normal myelination causes severe neurological diseases, including leukodystrophies and peripheral neuropathies (Boespflug-Tanguy et al., 2008; Suter and Scherer, 2003). Moreover, in myelin diseases such as multiple sclerosis (MS), the remyelination of axons is often inefficient. This leads to axonal degeneration and persistent clinical disability (Franklin and Ffrench-Constant, 2008). Thus, it is of major importance to develop therapies that stimulate rapid and efficient myelin repair by oligodendrocytes. The finding that the number of oligodendrocyte precursor cells (OPCs) found in MS plaques is apparently not the limiting problem of remyelination (Bauer et al., 2012; Franklin and Ffrench-Constant, 2008), accentuates the need for a precise identification of signals that might stimulate OPCs differentiation and myelination *in vivo*. Thus the aim of the study is to understand how OPC proliferation, differentiation and myelination in the developing and adult brain is controlled and in what way axon-derived signals are instrumental to this process.

3. Results

3.1 *Pten* mutant GC trigger *de novo* myelination of Pf axons

Cell size is regulated by the Akt/mTOR pathway, which itself is stimulated by phosphatidylinositol-3,4,5-trisphosphate [PI(3,4,5)P3] (Laplante and Sabatini, 2012) (**Fig. 6a**). Loss of the lipid phosphatase PTEN can therefore increase cell size (Stiles et al., 2004a). To specifically enlarge cerebellar granule cells (GC) and their axonal projections (Pf), we deleted *Pten* in a novel line of *Tg(mα6)-Cre*Pten*$^{loxP/loxP}$ mice that express Cre under control of the $GABA_A$ receptor α6 subunit promoter (Funfschilling and Reichardt, 2002; Lesche et al., 2002). As demonstrated by reporter gene expression in *Tg(mα6)-Cre* mice, recombination starts at around P9 in predominantly postmitotic and postmigratory GC (Funfschilling and Reichardt, 2002). By quantitative RT-PCR and Western blot analyses the cerebellum of *Tg(mα6)-Cre*Pten*$^{loxP/loxP}$ mice (hereafter termed *Pten* cKO or "mutants") revealed a significant loss of *Pten* mRNA (by 63%) (**Fig. 6b**) when compared to *Pten*$^{loxP/loxP}$ mice (hereafter termed "controls"). To determine if indeed expression of PTEN was disrupted in *Pten* mutant mice, immunoblot analysis with antibodies specific for PTEN was performed using cerebellar lysates of control and mutant mice at the age of 3.5 months. The protein abundance of PTEN was reduced by 80% (p=0.0025) in *Pten* cKo (**Fig. 6c**). Loss of PTEN resulted in enhanced phosphorylation of AKT, GSK3β, mTor and S6 (**Fig. 6a,d**), verifying the overall hyperactivation of the PI3K pathway.

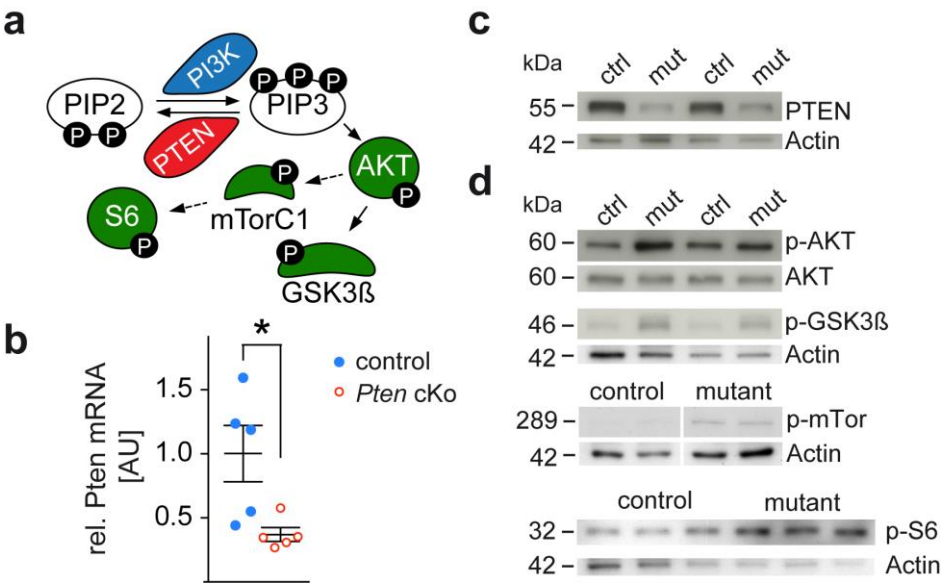

Pten mutant mice were born in the expected Mendelian ratio and appeared healthy during the first months of life (Video 1, can be found on the included CD-ROM or on Nature Neuroscience webpage http://www.nature.com/neuro/journal/vaop/ncurrent/fig_tab/nn.4425_SV1.html). During postnatal development the cerebellum of *Pten* mutant mice became progressively enlarged (**Fig. 7a**). Hematoxylin and eosin staining (H&E) of parasagittal sections at P14 revealed no detectable difference between control and mutant mice, whereas at 2.5 months of age the size increase became obvious and revealed to be progressive, when analyzed at 1 year of age. The diameter of parallel fibers in the ML, next to bigger granule cells immunostained for $GABA_A$ receptor α6 subunit (**Fig. 5a**) also increased over time, as quantified by electron microscopy, reaching 0.61±0.009 µm in mutants versus 0.16±0.002 µm in controls at 1 year of age (**Fig. 7b).**

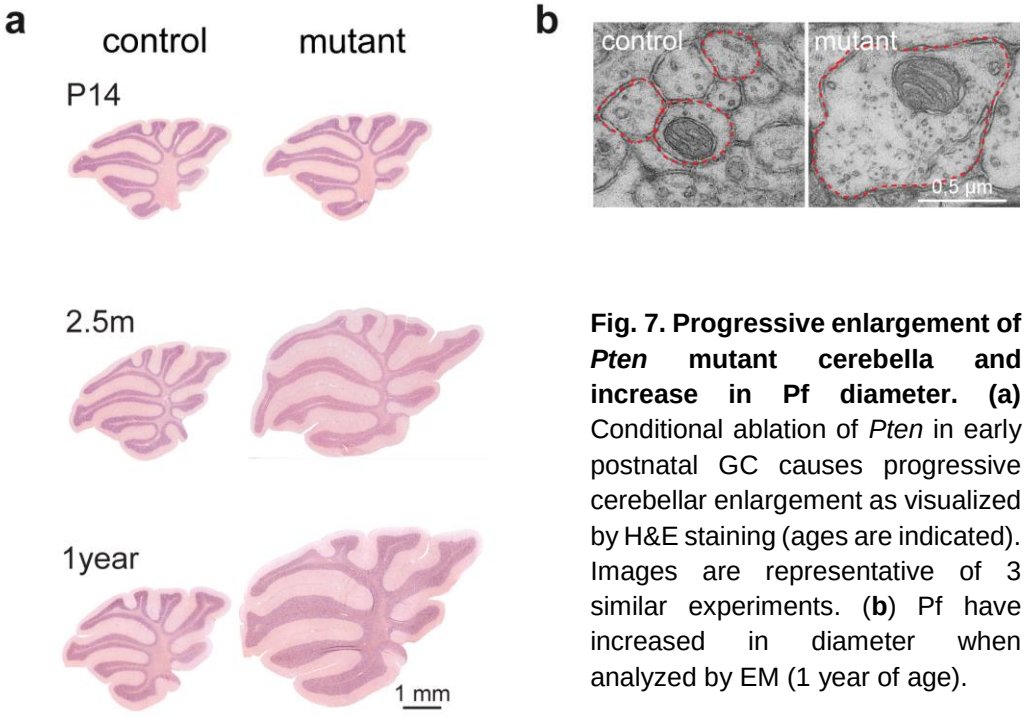

Fig. 7. Progressive enlargement of *Pten* mutant cerebella and increase in Pf diameter. (a) Conditional ablation of *Pten* in early postnatal GC causes progressive cerebellar enlargement as visualized by H&E staining (ages are indicated). Images are representative of 3 similar experiments. (**b**) Pf have increased in diameter when analyzed by EM (1 year of age).

Fig. 6. ***Pten* mutant granule cells stimulate the AKT1/mTOR pathway. (a)** Schematic representation of selected candidates of PI3K/AKT1/mTORC1 signaling. **(b)** By qRT-PCR *Pten* transcripts containing the floxed exon 5 are decreased in the cerebellum of conditional *Pten* mutants (age 3.5 months). Means ± s.e.m. n=5 mice each genotype (p=0.0231, two-tailed unpaired Student's t-test). **(c)** On Western blots PTEN levels are decreased in the cerebellum of mutants (age 3.5 months, cropped blot images). (**d**) Phosphorylation (p-) of the PI3K downstream effectors AKT1, GSK3β, mTOR and S6 is enhanced in *Pten* mutant mice (age 3.5 months, cropped blot images).

To determine, whether ablation of *Pten* from cerebellar granule cells and the subsequent increase in their axonal diameter was sufficient to induce myelination of parallel fibers in the molecular layer, immunohistochemistry with antibodies directed against CNP and Parvalbumin was performed using parasagittal sections of control and mutant mice at the age of 1 year. Interestingly and in contrast to controls, chromogenic staining for CNP

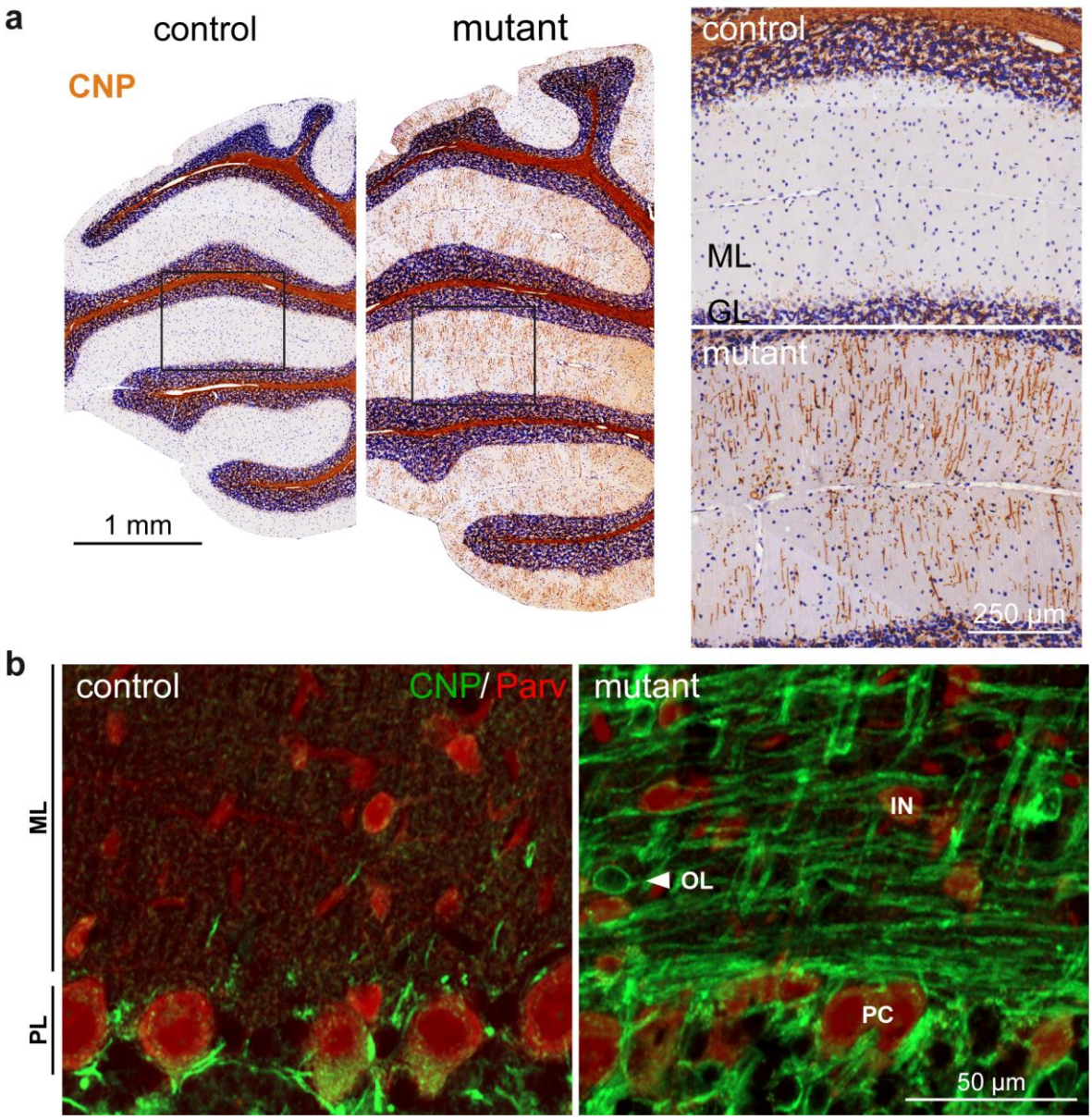

Fig. 8. Genetic loss of *Pten* triggers *de novo* myelination of parallel fibers. (a) Hematoxylin and CNP immunhistochemistry on sagittal cerebellar sections of 3.5 month old animals revealed *de novo* myelination of normally non-myelinated parallel fibers in the cerebellum. In comparison to control brains (top), without myelin in the molecular layer (ML), immunohistochemistry specific for CNP demonstrates the presence of robust levels of ectopic myelin in the molecular layer (ML) of mutant mice (bottom). (**b**) Myelinated parallel fibers in mutant brains (right) immunostained for CNP (green). Both Purkinje cells (PC) and molecular layer interneurons (IN) are Parvalbumin (red) positive (age 1 year). Note the absence of myelin in the molecular layer (ML) of control brains (left). Arrowhead points to an oligodendrocyte (OL) cell body.

demonstrated a massive accumulation of myelin in the molecular layer of *Pten* mutant mice (**Fig. 8a**). By fluorescent double immunohistochemistry for CNP and Parvalbumin, a marker of Purkinje cells and ML interneurons, this finding of *de novo* myelination of parallel fibers (**Fig. 8b**) was validated. Beginning at P40 the number of mutant parallel fibers that became myelinated (labeled by immunostaining of CNP) progressively increased over time (**Fig. 9**).

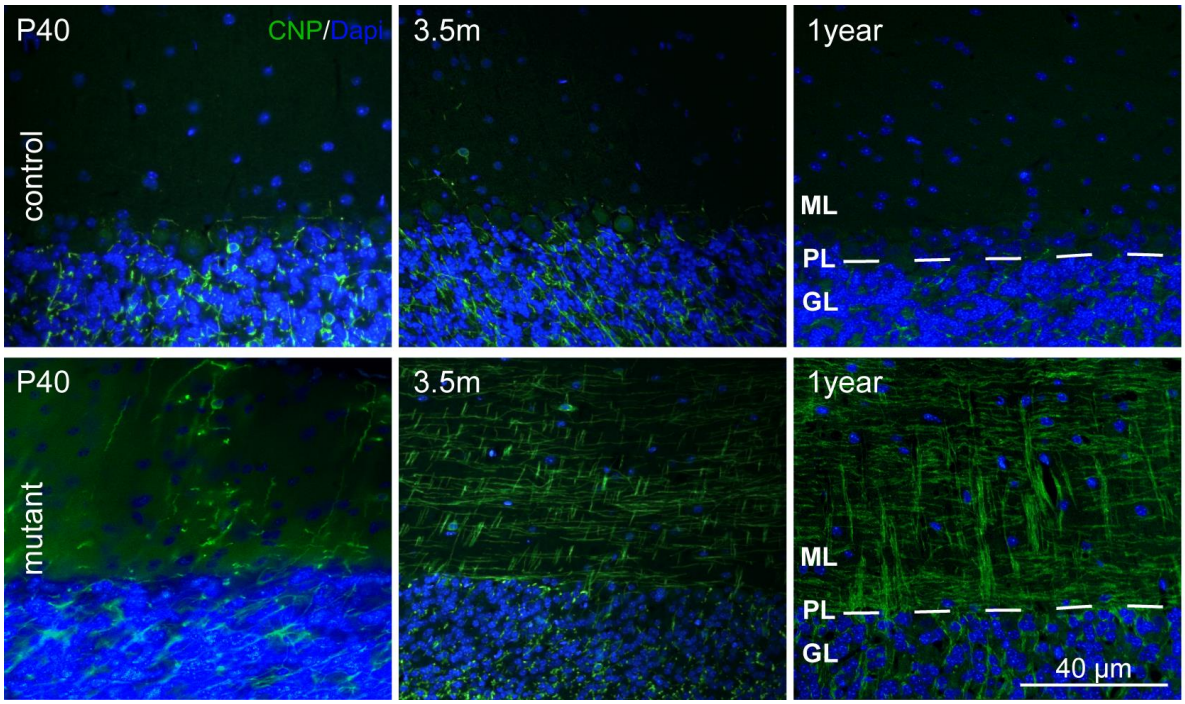

Fig. 9. Progressive *de novo* myelination of *Pten* mutant parallel fibers. In comparison to control brains, without myelin in the molecular layer (ML), immunostaining of myelin protein CNP (green) demonstrates the presence of robust levels of ectopic myelin in the molecular layer of mutant mice. Myelination increases significantly over time. PL, Purkinje cell layer; GL, granule cell layer; ML, molecular layer.

To illustrate newly formed myelin on a single cell level and to analyze how de novo myelination affected Pf morphology, we performed electron microscopic analyses of 1 year old *Pten* mutant mice. Indeed also by EM we could identify *de novo* myelinated Pf (marked by asterisks) that were presumably ensheathed by the depicted oligodendrocyte in close proximity (**Fig. 10a).** Myelination of parallel fibers induced the ectopic formation of node-like structures on Pf that were flanked by paranodal myelin loops (Pn). Furthermore EM analysis revealed the formation of septate-like junctions of the inner myelin leaflet with the Pf membrane (**Fig. 10b**). EM images of myelinated Pf axons also demonstrated that the newly formed myelin restricted the synaptic contact of Pf to Purkinje cell dendritic spines, causing

these synapses to reside in the newly established nodal regions. These "en passant" synapses harbored presynaptic vesicles (arrowhead) (**Fig. 11**).

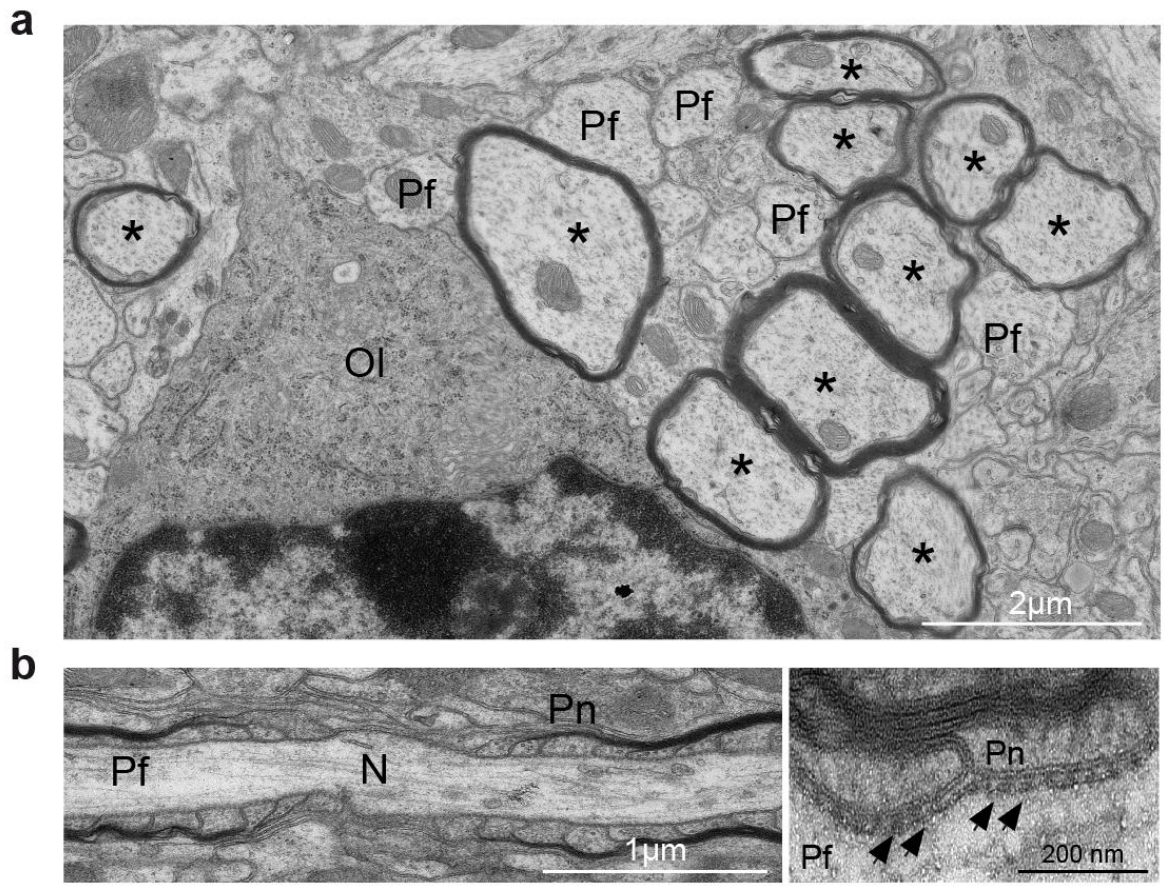

Fig. 10. *De novo* myelination of parallel fibers and formation of node-like structures. (a) By electron microscopy (EM) normally unmyelinated parallel fibers (Pf) become *de novo* myelinated in mutant mice. Asterisks mark myelinated Pf (age, 1 year). Note the formation of a node of Ranvier (N), flanked by paranodal (Pn) loops (in **b,** black arrows).

By EM analysis the amount of newly formed myelin in *Pten* mutants was measured by dividing the inner myelin diameter by the outer myelin diameter (g-ratio, **Fig. 12a**). The g-ratio was plotted against the axonal caliber. Note that a g-ratio of 1 denotes an unmyelinated axon. An electron micrograph in **Fig. 12b** shows one of the smallest detected myelinated parallel fiber and by subsequent analyses we determined a size threshold for myelination in the mutants of approx. 0.25 µm (**Fig. 12c**). By morphometry and g-ratio analysis of controls and mutants, up to 40±3% of Pf in the ML were myelinated at 1 year of age. At that age, mutant Pf exhibited an average g-ratio of 0.84. The first myelinated parallel fibers appeared at the age of P40 (2.3±0.6%). Further analysis at 3.5 months revealed up to 9.5±1% myelinated parallel fibers (**Fig. 12c**). At all analyzed ages, axons larger than 0.45 µm in diameter were preferentially myelinated.

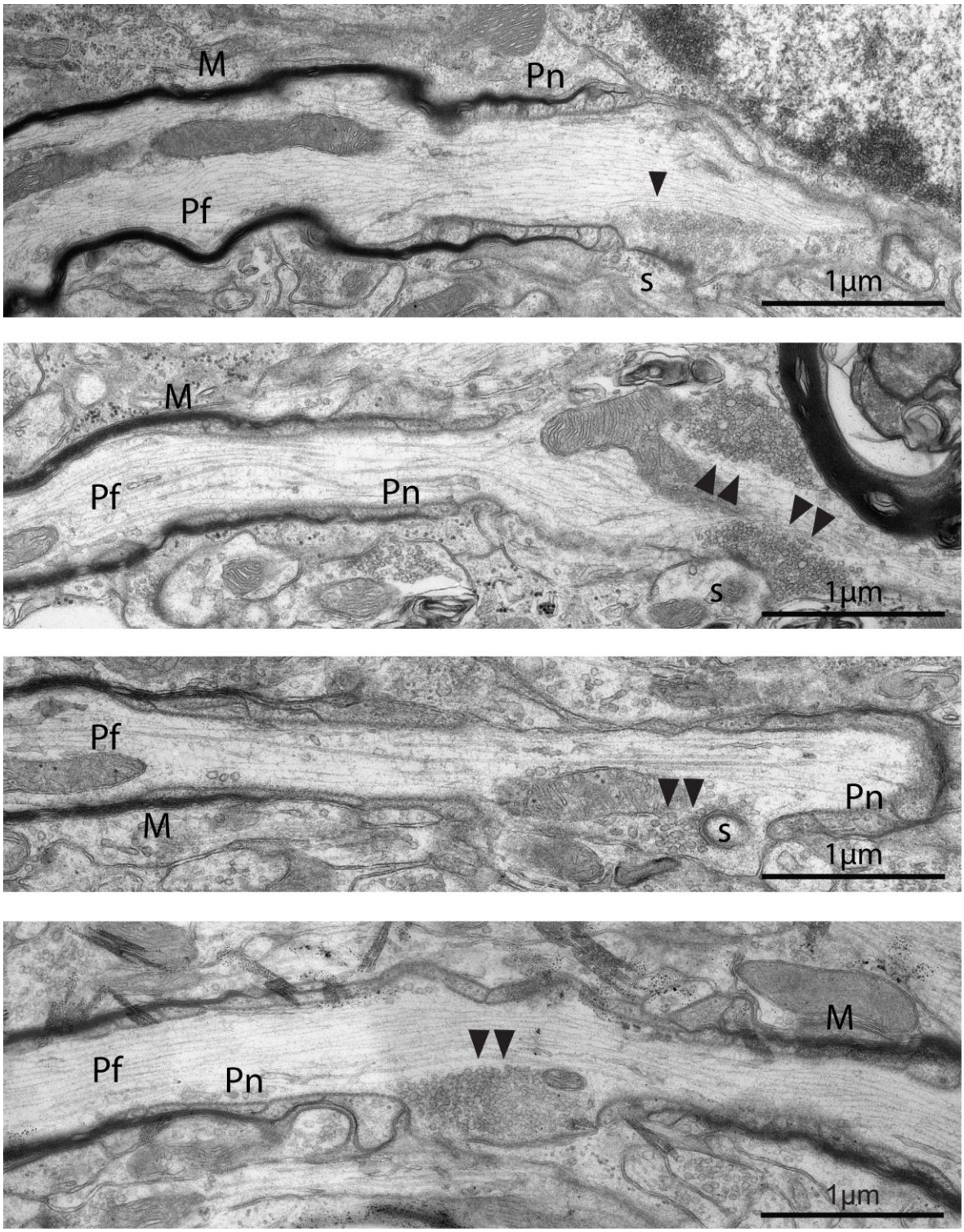

Fig. 11. Parallel fiber synapses onto Purkinje cell dendritic spines in the presence of myelin. EM images of *de novo* myelinated Pf in mutants at 1 year of age. The “en passant” synapses of Pf on Purkinje cells spines appeared restricted to the newly established nodal regions. Arrowheads point to presynaptic vesicles. M, myelin; Pf, parallel fiber axon; Pn, paranodal loop; s, dendritic spine.

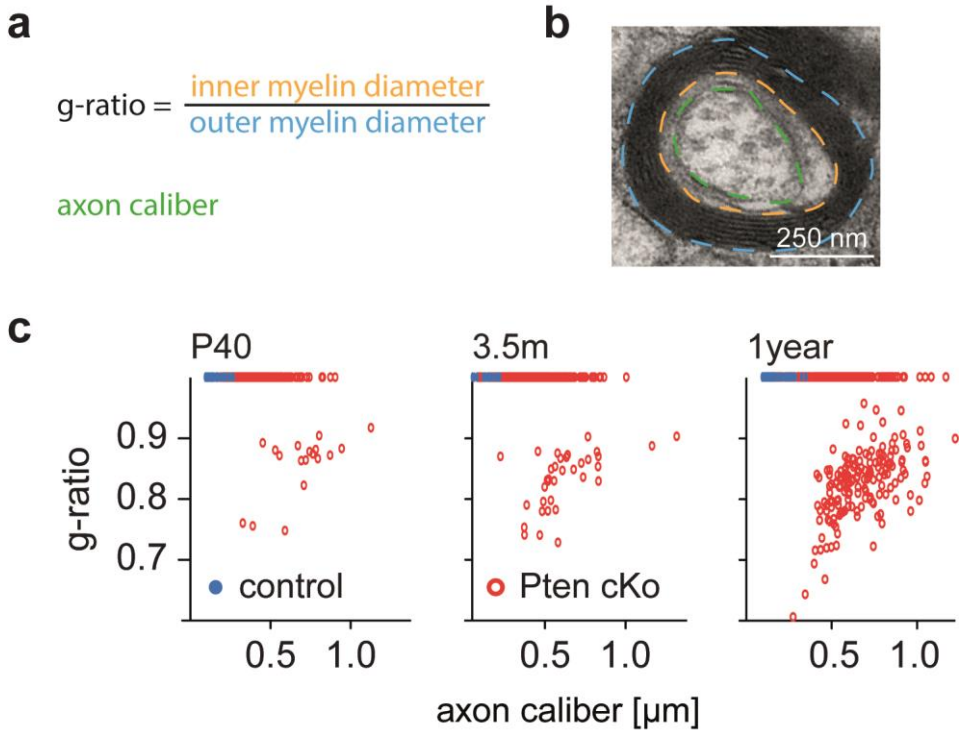

Fig. 12. G-ratio analysis. (**a**) The amount of myelin was measured by dividing the inner myelin diameter by the outer myelin diameter. (**b**) By EM, *de novo* myelination of mutant Pf requires a minimum axonal caliber of 0.25 µm. We never observed thinner myelinated axons than the one shown (age 1 year). (**c**) Progressive myelination as quantified by g-ratio analysis of myelin thickness at the indicated ages. Note that a g-ratio of 1 denotes for unmyelinated axons. There is continuous increase in the number of myelinated fibers in mutants (red dots). In controls (blue dots) myelin profiles are virtually absent (n=3 per genotype and age, 140 Pf quantified per animal).

Taken together, activation of the PI3K/AKT/mTOR pathway in cerebellar granule cell neurons of conditional *Pten* mutant mice was sufficient to induce a granule cell hypertrophy, a thickening of their associated axons and a progressive *de novo* myelination of the normally unmyelinated Pf by genetically wildtype oligodendrocytes.

3.2 *Pten* mutant GC trigger OPC proliferation and differentiation

The ML harbors normally hardly any oligodendrocytes and only scattered NG2 positive cells, as demonstrated in *Plp1-DsRed*Ng2-EYFP* double-transgenic mice (Hirrlinger et al., 2005; Karram et al., 2008) (**Fig. 13a**). Immunohistochemistry with an antibody directed against carbonic anhydrase (CAII), a marker of mature oligodendrocytes, revealed significantly more oligodendrocytes in the GL (+33%) and ML (+750%) of *Pten* mutants. Unaltered numbers of CAII positive cells were detected in the WM of *Pten* mutants as compared to controls, when quantified at P45 (**Fig. 13b**).

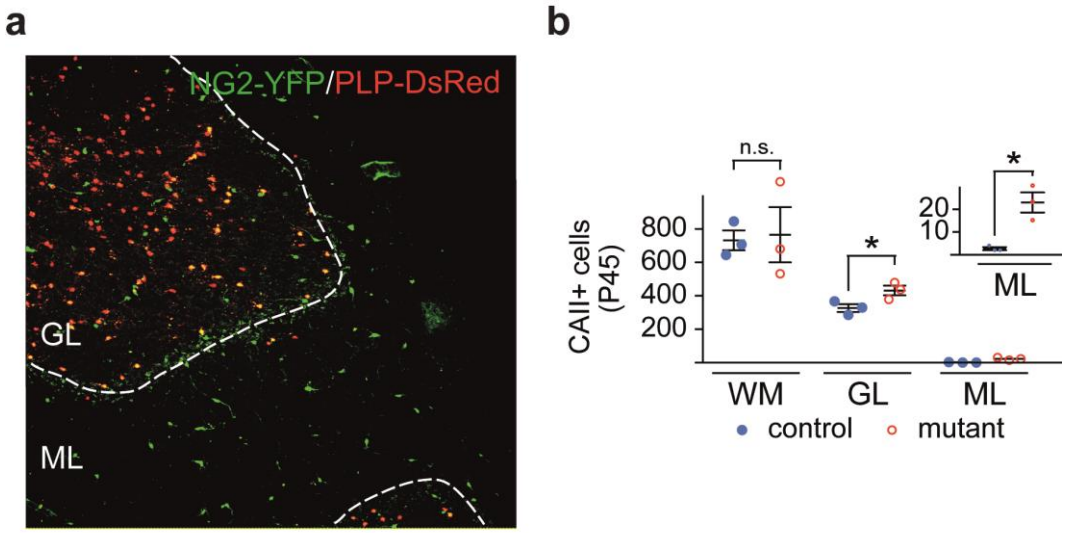

Fig. 13. Local differentiation of OPCs induced by *de novo* myelination. (a) The normal cerebellar ML is devoid of oligodendrocytes (red), but contains scattered NG2+ OPCs (green), as revealed by DsRed and EYFP fluorescence, respectively, in double-transgenic *Plp1-DsRed*Ng2-EYFP* mice. The depicted picture was kindly provided by Dr. Khalad Karram from the Institute for Molecular Medicine, Mainz, Germany. GL, granule cell layer; ML, molecular layer. (**b**) Mature oligodendrocytes (carbonic anhydrase/CAII-positive) are more numerous in the mutant granule cell layer (p=0.0498) and molecular layer (p=0.0103), but not in cerebellar white matter (WM; p=0.8581). All analyses at age P45 (n=3 per genotype). Data are means ± s.e.m. *p<0.05, student's t test. GL, granular cell layer; ML, molecular layer; WM, white matter.

To determine whether *Pten* deficient axons induce OPC proliferation within the ML or whether OPCs are recruited from the GL below, we used 5'-bromo-2'-deoxyuridine (BrdU) labeling detection, in combination with antibodies directed against specific oligodendroglial marker antigens (**Fig. 14a**). BrdU is a thymidine analog that incorporates into dividing cells during DNA synthesis (Wojtowicz and Kee, 2006). Once it is incorporated into the new DNA, BrdU will remain in place and will be passed down to daughter cells following division (Wojtowicz and Kee, 2006).

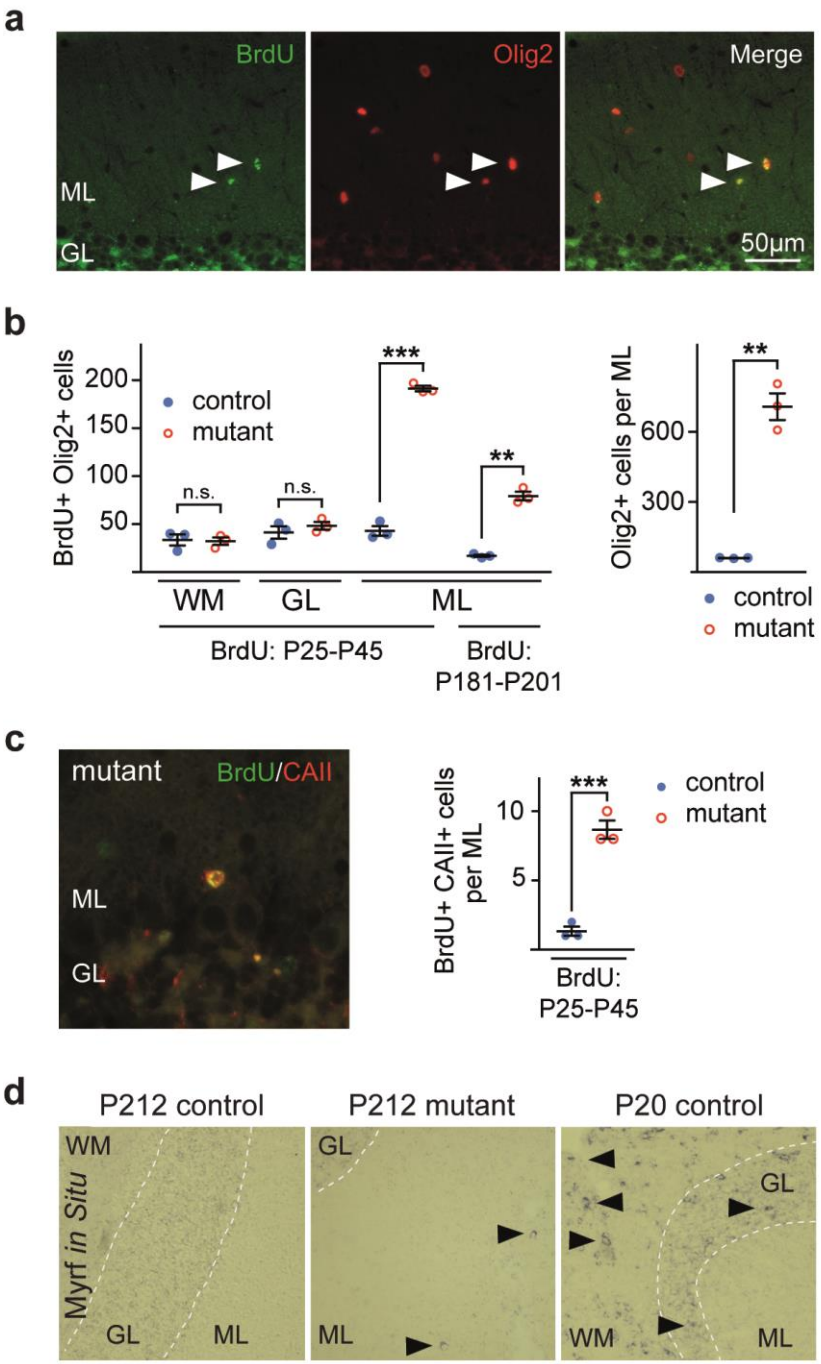

Fig. 14. Local proliferation of OPCs in the molecular layer. **(a)** In the cerebellar ML of *Pten* mutant mice, many OPCs (Olig2+, red) nuclei can be co-labeled for BrdU (green, arrowheads), following daily BrdU administration between P25-P45. **(b)** At age P45, the density of proliferating OPC (BrdU+;Olig2+) is only increased in the ML (n=3 per genotype; p=0.0004), but proliferation remains elevated at age P201 (n=3 per genotype; p=0.0016). Thus, by P201 the total number of Olig2+ oligodendrocyte lineage cells in the ML is 10-fold higher than in controls (n=3 per genotype; p=0.0031). (**c**) After daily BrdU injections (between P25 and P45) newly generated OPC of the ML also turn into mature oligodendrocytes, as revealed by quantifying cells that are co-labelled for BrdU (green) and CAII (red). N=3 per genotype (p=0.0006). (**d**) By chromogenic *in situ* hybridization, *Myrf* mRNA can be detected in single differentiating oligodendrocytes of the mutant ML (arrowheads in middle panel), suggesting ongoing differentiation. Myrf+ differentiating OL were never detected in the control ML. Right: section from a developmental stage (P20) as a positive control for *Myrf* expression. Data are means ± s.e.m, $^{**}P < 0.01$; $^{***}P < 0.001$, student's *t* test**.**

We injected BrdU intraperitoneally (i.p.) from P25-P45, if not mentioned otherwise. When the number of BrdU+;Olig2+ cells was analyzed at P45 (i.e. after 20 days of daily BrdU injection) and compared between mutants and controls, OPC proliferation was not significantly different in the GL and the WM of mutant mice (**Fig. 14b**). However, in the ML BrdU+;Olig2+ cells were 4.4-fold increased (**Fig. 14b**). Even at 6-7 months, the 20-day BrdU treatment protocol (i.p. injection of BrdU from P181-P201) revealed a 4.7-fold increase of BrdU+;Olig2+ cells in the mutant ML (**Fig. 14b**). At that age the total number of oligodendrocyte lineage cells had reached a 10-fold increase compared to controls (**Fig. 14b**). Importantly, double-labeling of BrdU and CAII confirmed that newly generated OPCs that had incorporated BrdU during the 20 day period of BrdU injection, differentiated into CaII expressing mature oligodendrocytes (**Fig. 14c)**. In a collaboration with Kuo Yan at the Institute of Cell Biology and Neurobiology, Berlin (Germany), we performed a chromogenic *in situ* hybridization for *Myrf* mRNA on parasagittal sections of the cerebellum. *Myrf* (Myelin Regulatory Factor) is a membrane-associated transcription factor and is required for the generation of CNS myelin during development (Bujalka et al., 2013). *Myrf* is required for the final stages of oligodendrocyte differentiations and is expressed exclusively by maturating oligodendrocytes. In fully mature oligodendrocytes *Myrf* is almost undetectable (personal communication with Ben Emery, Jungers Center for Neurosciences Research, Department of Neurology, Oregon USA). With this in situ hybridization we could confirm that even at 7 months of age the ML in mutant brains still contained some maturating oligodendrocytes (**Fig. 14d)**. As a positive control for *Myrf* expression we used parasagittal cerebellar sections of a P20 wild type mouse.

To better define the timing of OPC proliferation in *Pten* deficient mice, we injected BrdU from P15-P20 and quantified BrdU+,Olig2+ cells in the ML of control and mutant mice. At P20 there was no detectable difference in the number of double positive cells (**Fig. 15a)**. Using a slightly later BrdU injection protocol (P20-P30) we identified a time window at which proliferation of OPCs was already increased but the number of mature (CNP+) oligodendrocytes was not (**Fig. 15b)**. This indicates that OPC proliferation is independently activated by the genetically modified granule cells and not just a mere homeostatic mechanism to replace OPCs that have matured to the myelinating state. This result was validated by immunohistochemical analysis at P45 (and after BrdU administration between P25-P45) with antibodies directed against MBP and BrdU. Here, we found that BrdU labeled OPCs were uniformly distributed over the mutant ML and not in close proximity to mature oligodendrocytes and their associated myelin sheaths (**Fig. 15c**).

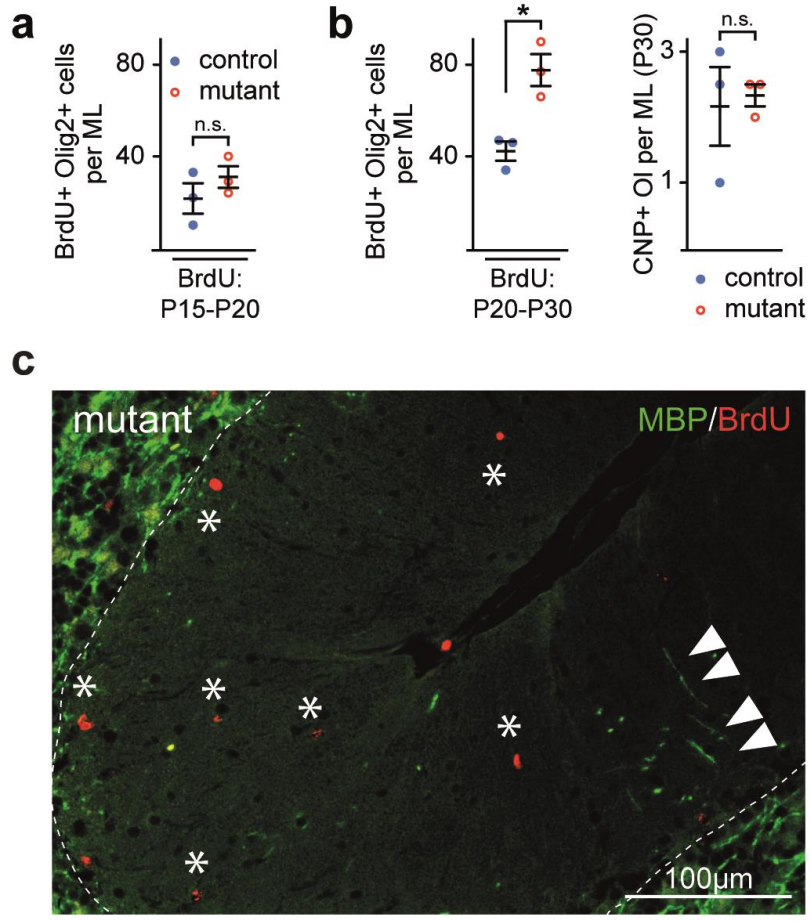

Fig. 15. Early onset of proliferation (**a**) The number of proliferating OPCs (BrdU+Olig2+) in the ML following daily BrdU administration from P15 to P20 is similar in mutants and controls (p=0.3161). (**b**) In contrast, after daily BrdU administration between P20 and P30 (analyzed at P30) the number of proliferating OPCs (BrdU+,Olig2+) in the ML is increased in the mutants (p=0.0120). However, at that age, the number of mature oligodendrocytes expressing CNP is unchanged between control and mutants (p=0,8025), indicating that proliferation of OPCs proceeds the differentiation of OPCs to oligodendrocytes. (**c**) OPCs labeled for BrdU (asterisks) distribute evenly in the ML of *Pten* mutants and are not preferentially close to newly generated oligodendrocytes and their myelin sheaths (arrowheads). N=3 per genotype, Data are means ± s.e.m. *p<0.05, student's *t* test.

Taken together, the inactivation of *Pten* in cerebellar granule cells increased Pf caliber above a "threshold" of 0.25 µm and was sufficient to induce OPC proliferation, OPC differentiation, and oligodendrocyte maturation and myelination.

3.3 Is ectopic myelination triggered by neuronal activity?

Proliferation of OPCs and myelination in the CNS can be triggered by neuronal activity (Gibson et al., 2014; Li et al., 2010). OPCs receive synaptic input from Pf in the cerebellar ML (Lin and Bergles, 2004) and altered synaptic input modulates OPC proliferation (Mangin et al., 2012) and myelination (Wake et al., 2011). To test the hypothesis if the *de novo* myelination upon *Pten* deficiency in granular cells is triggered by neuronal activity, we started a collaboration with Sonia Spitzer and Ragnhildur Thóra Káradóttir from the University of Cambridge, UK. Here, *Pten* mutants were tested for altered Pf electric activity picked up by OPCs in the ML. Using acute slices from mutant and control mice that additionally expressed the *Ng2-EYFP* transgene (Karram et al., 2008), our colleagues whole-cell patch clamped both Purkinje cells, that receive input dominantly from Pf, and fluorescent OPCs in the ML. This allowed them to determine GC activity and the spontaneous synaptic inputs from the Pf to the OPCs. However, no differences were found between mutants and controls in the spontaneous postsynaptic inward currents recorded from NG2-EYFP expressing OPCs (**Fig. 16a,b**) nor in the frequency of the spontaneous synaptic input to the OPCs (**Fig. 16c**). Similar the frequency of spontaneous inputs to Purkinje cells showed no significant difference (**Fig. 16d**). Taken together, the data of our collaborators suggest that *de novo* myelination of parallel fibers in young *Pten* mutants is not triggered by neuronal activity.

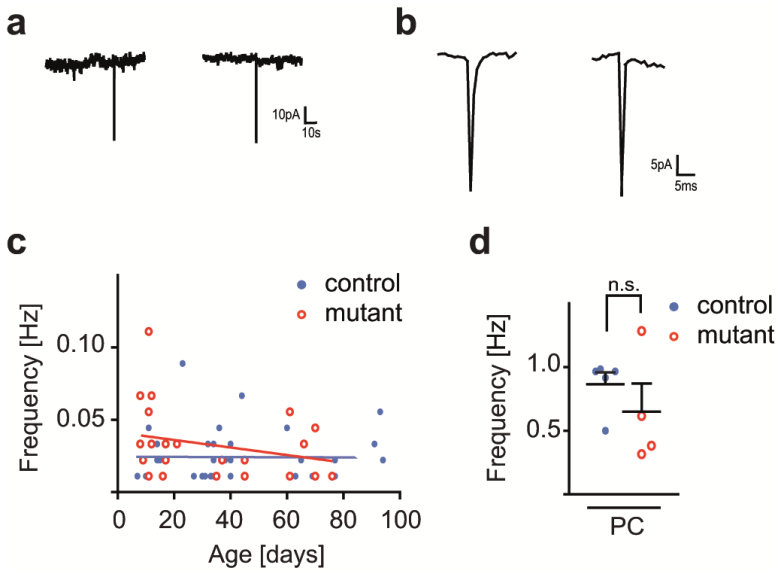

Fig. 16. Ectopic myelination is not triggered by neuronal activity. **(a)** Spontaneous postsynaptic inward currents recorded from NG2-EYFP expressing OPCs clamped at -74mV in the ML of control and *Pten* mutant mice. (**b**) Inward currents appeared at an expanded time scale. (**c**) The average frequency of detectable spontaneous events in OPCs is comparable between controls (n=5; $0.02\pm7x10^{-3}$ Hz) and mutants (n=6; $0.02\pm4x10^{-3}$ Hz) (p=0.94). (**d**) Similarly, there is no significant difference in the frequency of spontaneous inputs in Purkinje cells (PC), which are predominantly from Pf (control, n=5, $0.8\pm7x10^{-2}$ Hz; mutant, $0.6\pm2x10^{-2}$ Hz n=4) (p=0.32). Analysis of covariance in **c**, chi-squared test in **d.**

3.4 Is ectopic myelination triggered by down regulation of inhibitory cues?

Some reports in the literature suggest that axon–bound signaling proteins are not essential for regulation of CNS myelination. For example, it has been reported that oligodendrocytes can ensheath synthetic nanofibers *in vitro* (Lee et al., 2012). Hence, we hypothesized that (i) axons have to meet a 0.25 µm "size threshold" to become myelinated (Lee et al., 2012), and that (ii) oligodendrocytes respond with myelination to instructive diffusible factors or to the down regulation of inhibitory cues that could be axon-bound or diffusible.

To test for possible inhibitory axonal cues, we intercrossed floxed *Pten* mutants (Lesche et al., 2002) to a *Nex-CreERT2* driver line (Agarwal et al., 2012). In contrast to *Tg(mα6)-Cre* mice (which recombine more than 90% of cerebellar granule cells) the Nex gene promoter targets Cre only in a minor fraction of all granule cells (Agarwal et al., 2012). Indeed, after 5 consecutive days of tamoxifen treatment (P10-P15), reporter gene expression was detectable in less than 4% of all cerebellar granule cells (**Fig. 17a**). However, when analyzed 28 weeks later (**Fig. 17b**), loss of PTEN in this small fraction of granule cells was sufficient to significantly increase the number of mature oligodendrocytes, expressing CNP (**Fig. 17c,d)**. Importantly, these mature oligodendrocytes, similar to our previous findings in *Tg(mα6)-Cre*Pten$^{loxP/loxP}$* mice, participated in *de novo* myelination of parallel fibers. Accordingly, a significantly larger MBP positive area could be quantified in *Nex-CreERT2*Pten$^{loxP/loxP}$* mutants compered to age matched controls (**Fig. 17e,f)**.

Since 96% of the Pf were non-recombined in *Nex-CreERT2*Pten$^{loxP/loxP}$* mice and thus wildtype with regard to the expression of potential inhibitory, diffusible cues, our data strongly suggests that the induction of *de novo* myelination of parallel fibers is unlikely triggered by the down regulation of diffusible inhibitory cues from the axons.

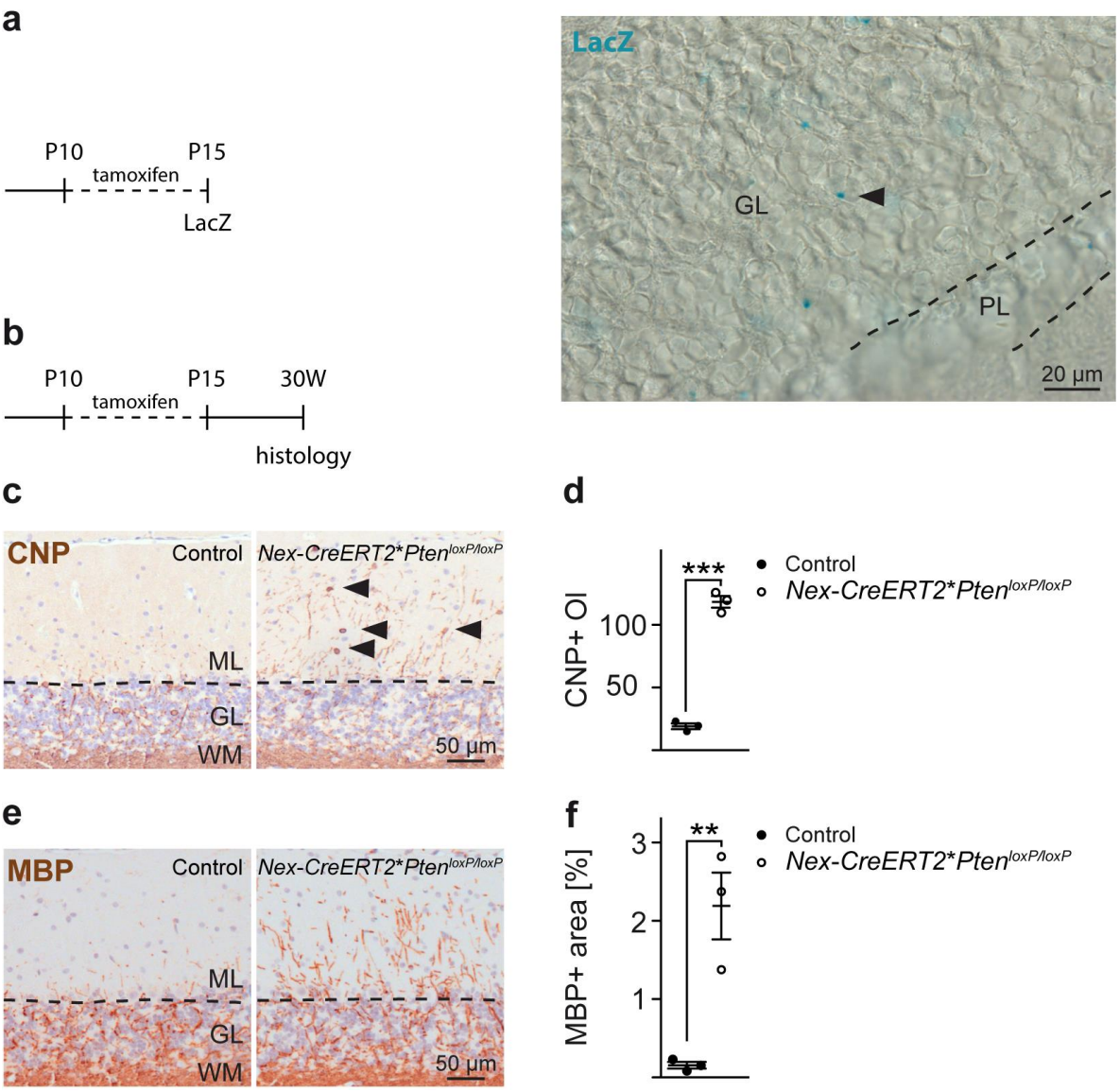

Fig.17. Cell type specific ablation of *Pten* in a small subset of cerebellar granule cells. (**a**) Tamoxifen treatment of *Nex-CreERT2*Rosa26*-lacZ mutant mice induces Cre-mediated activation of a lacZ reporter gene in a small subset of GC. (**b**) Tamoxifen treatment scheme for *Nex-CreERT2*Pten$^{loxP/loxP}$* mutant mice. (**c,d**) *Nex-CreERT2*Pten$^{loxP/loxP}$* mutants harbor significantly more CNP positive oligodendrocytes (arrowheads) in the ML, when compared to controls. (**e,f**) Targeted ablation of *Pten* by *Nex-CreERT2* induced a significantly larger MBP positive area in the ML when compared to controls (quantitated in parasagittal sections of the cerebellar vermis; n=3 per genotype and indicated age). Data are means ± s.e.m. **p<0.01; ***p<0.001, student's *t* test (d,f). GL, granule cell layer; ML, molecular layer; WM, White matter.

3.5 Functional validation of selected candidate factors

3.5.1 Experimental design and hypothesis

Pten deficient mice and their controls were further used as a tool, helping to find promyelinating factors in the CNS. We used laser captured microdissection and obtained stripes of the GL from cerebellar cryosections of 3.5 month-old mutants and age-matched controls (**Fig. 18a**). We isolated RNA for global transcriptome analyses using microarrays (Affymetrix Mouse Genome 430A 2.0 Array). Transcriptome analysis resulted in a first list of candidate factors upregulated in *Pten* cKO (**Fig. 18b**). Candidate transcripts were selected by several criteria, including magnitude of upregulation in the transcriptome of *Pten* mutant GL vs. control GL (>1.4 fold, n=3 per genotype), level of significance ($p<0.05$) and annotation. The resulting candidate list included e.g. neurotensin (Nts; 32.8-fold), inhibin beta-A (Inhba, forming the biologically active dimer Activin A; 4.4-fold), thymosin beta 4 (Tmsb4x, 2.4-fold), tissue inhibitor of metalloproteinase 3 (Timp3, 2.1-fold), secreted protein, acidic and rich in cysteins-like 1 (Sparcl1, 1.9-fold), vascular endothelial growth factor c (Vegfc, 1.9-fold), fibroblast growth factor 1 (Fgf1, 1.6-fold), pleiotrophin (Ptn or heparin-binding growth factor 8/Hbfg-8, 1.5-fold) and brain-derived neurotrophic factor (Bdnf, 1.4-fold). The database from http://web.stanford.edu/group/barres_lab/brain_rnaseq.html (Zhang et al., 2014) was used to indicate which cell type showed the highest expression of the corresponding gene. For example, Nts is mainly expressed by neurons and endothelia cell; Inhba, by OPCs, neurons and astrocytes; Tmsb4x, by endothelia cells and microglia; Timp3, Sparcl1, FGF1 and Ptn, by astrocytes; Vegfc, by endothelia cells and Bdnf, by neurons and astrocytes (Zhang et al., 2014). To further validate the obtained transcriptome data, some differentially expressed candidate genes were further analyzed by qRT-PCR. *Nts*, *FGF1*, *Ptn*, *Timp3* and *Inhba* showed a significantly higher mRNA abundance in cerebellar lysates from *Pten* cko compared to controls (**Fig. 18c**).

a

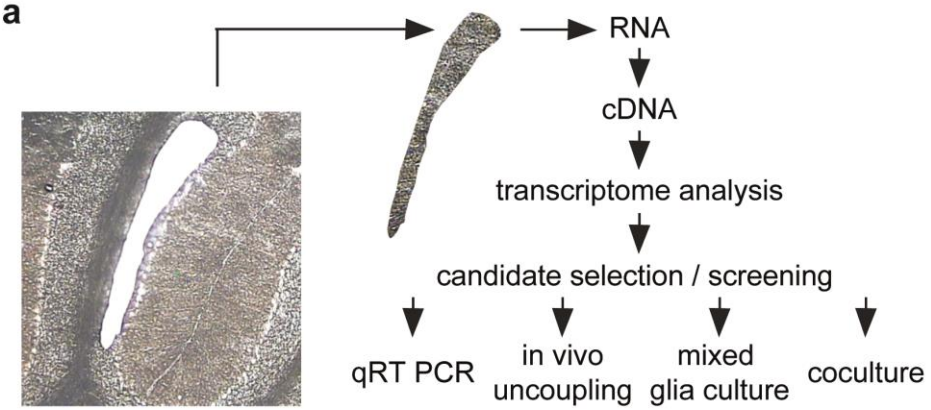

b

Gene ID	FC	Cell type	Gene ID	FC	Cell type	Gene ID	FC	Cell type
Nts	32.8	N; E	Tmsb4x	2.4	E; M	Igfbp7	1.7	E
Igfbp4	7.2	M; E	Adamts1	2.3	E; M	Sfrp4	1.6	N; A
Cd163	7.0	M	Ninj1	2.1	M	Tgfb3	1.6	A; N; OPC
Mcam	6.0	E; NFO; MO	Bmp6	2.1	N; OPC	Timp2	1.6	N; M
Fstl1	4.6	A; E	Timp3	2.1	A	Fgf1	1.6	A
Inhba	4.4	OPC; N; A	Igfbp2	2.0	A	Thbs2	1.6	N
Dll1	3.7	OPC	Sparc	1.9	E; M	Adam23	1.6	OPC; NFO; N
Nrg3	2.8	N	Sparcl1	1.9	A	Ptn	1.5	A
Ctgf	2.8	E; A; N	Adamts5	1.9	A; OPC	Fgf18	1.5	N; A
Dkk3	2.6	N; A	Vegfc	1.9	E	Bdnf	1.4	A; N
MMP17	2.5	OPC; N	Apcdd1	1.8	E			
Igfbp3	2.4	OPC; E	Fmod	1.7	OPC; E; N			

c

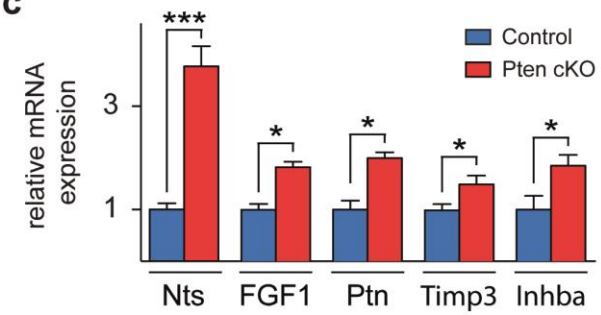

Fig.18. Experimental design to test candidate factors which were identified in conditional GC-specific *Pten* mutant mice and may have an impact on oligodendrocyte development. (**a**) Laser capture microdissection (LCM) was used to obtain the granular cell layer from serial cerebellar sections at the age 3.5 months (representative section shown). (**b**) Candidate transcripts were selected by several criteria, including magnitude of upregulation in the transcriptome of *Pten* mutant GL vs. control GL (>1.4-fold, n=3 per genotype), level of significance ($p<0.05$) and annotation. The third column indicates the cell type with the highest expression of the corresponding gene, according to the database: http://web.stanford.edu/group/barres_lab/brain _rnaseq.html (Zhang et al., 2014). A, astrocyte; N, neuron; OPC, oligodendrocyte precursor cell; NFO, newly formed oligodendrocyte; MO, myelinating oligodendrocyte; M, microglia; E, endothelial cells; FC, fold change. (**c**) qRT-PCR analysis of mRNAs encoding for some differentially expressed candidate genes. Analyzing cerebellum lysates from *Pten* cko and control mice, revealed a significantly higher mRNA abundance of *Nts*, *FGF1*, *Pt*n, *Timp3* and *Inhba* (age 3.5 months). Data are means ± s.e.m. *$p<0.05$; ***$p<0.001$, student's *t* test, n=3-5 per genotype.

Some mRNAs encoded secreted proteins that had been associated with oligodendrocyte development before, at least *in vitro*, such as Bdnf (Xiao et al., 2010), Vegfc (Le Bras et al., 2006), Ctgf (Stritt et al., 2009) and Tmsb4x (Santra et al., 2012). Other factors, including Fstl1, IGFBP-4, Dkk-3, Apcdd1, and Sfrp4, are new but known as antagonists of Wnt and Bmp signaling (Cruciat and Niehrs, 2013; Sylva et al., 2013), i.e. negative regulatory pathways of oligodendrocyte differentiation (He and Lu, 2013). Also modulators of insulin-like growth factor (IGF) signaling (IGFBPs 2, 3, and 7), which is thought to play a role in oligodendrocyte development (Taveggia et al., 2010), were upregulated. Finally, the metallopeptidases MMP17 and Adamts1 showed enhanced expression. The latter is relevant for myelination, as these proteases serve functions in remodeling the extracellular matrix and in the degradation of those proteins (such as chondroitin sulfate proteoglycans) that inhibit remyelination (Lau et al., 2013).

We hypothesized that *de novo* myelination of the cerebellar molecular layer in *Pten* mutant mice is initiated by a neuronal developmental program. The increase of axon size is PI3K/Akt/mTOR-dependent and associated with the upregulated expression of numerous genes, identified by transcriptional profiling of laser captured GC layers.

3.5.2 *In vivo* uncoupling of brain derived neurotrophic factor (Bdnf)

To address the significance of our candidate list, we selected Brain derived neurotrophic factor (Bdnf) for an *in vivo* analysis. Bdnf is a member of the nerve growth factor family (Levimontalcini and Angeletti, 1968) that supports existing neurons and influences growth and differentiation of new neurons and synapses (Acheson et al., 1995; Huang and Reichardt, 2001). The role of Bdnf and its receptor TrkB for oligodendroglia survival, differentiation, and myelination has been previously studied *in vitro* and *in vivo.* Till now no full picture about its functions has emerged yet, but Bdnf is thought to have a promyelinating effect (Xiao et al., 2010).

Floxed *Bdnf* mice (Rauskolb et al., 2010) were kindly provided by Michael Sendtner (Institute for Clinical Neurobiology, University of Würzburg). We generated triple-mutant mice by *Tg(mα6)-Cre* mediated targeting of *Pten* (for ectopic myelination) in combination with the floxed *Bdnf* gene. We hypothesized that if *Bdnf* is essential for myelination, its conditional inactivation in double mutant granule cells should result in reduced *de novo* myelination.

Surprisingly, at both analyzed ages (7 and 10 weeks) *Tg(mα6)-Cre*Pten$^{loxP/loxP}$*Bdnf$^{loxP/loxP}$* mice (hereafter termed *Pten* cKO, *Bdnf* cKO or *Pten*Bdnf* double mutants) exhibited a

significantly higher (not lower) number of mature (CNP+) oligodendrocytes in the ML than *Pten* single mutants (Pten cKO) (**Fig. 19a,b**). Also the (MBP+) myelinated area of the ML was significantly larger (not smaller), when quantified by immunostaining at the age of 7 and 10 weeks (**Fig. 19c,d**). Interestingly, even *Pten* het**Bdnf* cKO showed significantly more CNP+ oligodendrocytes at 7 weeks of age than control mice. This difference is undetectable at 10 weeks of age.

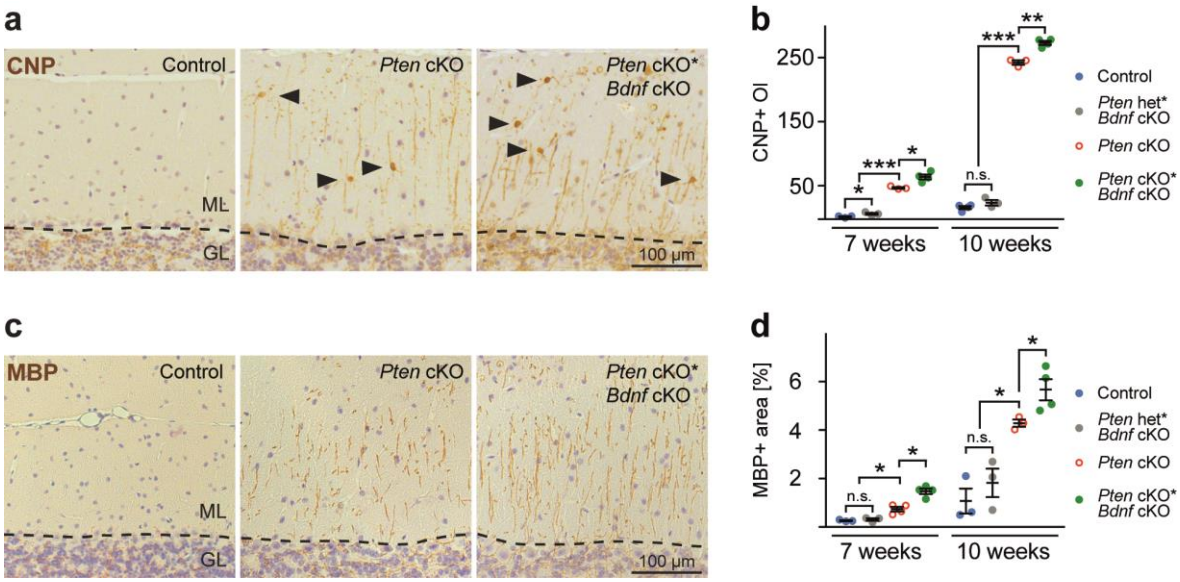

Fig.19. Histological *in vivo* validation of *Bdnf* uncoupling. (**a**) CNP was labeled on cerebellum slices of 10 weeks old control *Pten* cKO and *Pten*Bdnf* double mutant mice. (**b**) Double mutants lacking both *Pten* and *Bdnf* in cerebellar granule cells harbour significantly more CNP positive oligodendrocytes, at both time points (7 weeks: p=0.0132, 10 weeks: p=0.0012). (**c,d**) Immunohistochemistry for MBP exhibited a larger MBP positive area (7 weeks: p=0.0024, 10 weeks: p=0.0476) in the ML of double mutants, when compared to single *Pten* mutants (quantitated in parasagittal sections of the cerebellar vermis; n=3-4 per genotype and indicated age). Data are means ± s.e.m. *p<0.05; **p<0.01; ***p<0.001, one-way analysis of variance (ANOVA) followed by Bonferroni test (b,d). GL, granule cell layer; ML, molecular layer.

By electron microscopy we confirmed that the Pf calibers, independent from whether myelinated or unmyelinated, were as enlarged as in *Pten* single mutants (**Fig. 20a**). However, by g-ratio analysis at the age of 10 weeks the thickness of myelin was slightly but significantly reduced (indicated by a bigger g-ratio, p=0.0259) in *Pten*Bdnf* double mutants (**Fig. 20b,c**) when compared to single *Pten* mutants.

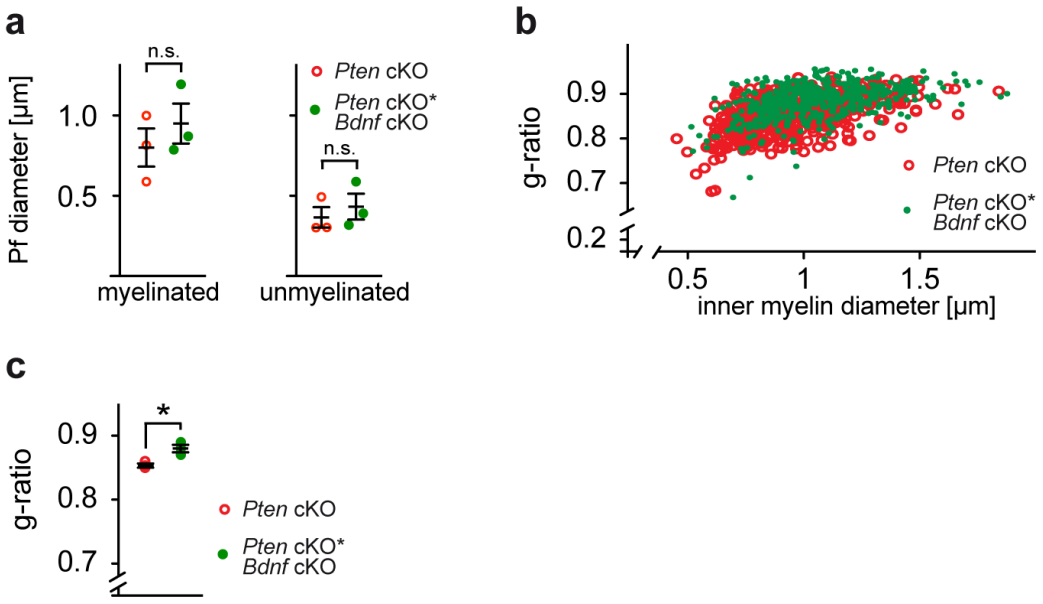

Fig. 20. Electron microscopy of *Pten* cKO and double mutants lacking *Pten* and *Bdnf*. (**a**) Caliber measurements of myelinated (p=0.4339) and unmyelinated (p=0.5558) Pf diameters demonstrated no detectable difference between single *Pten* mutants and double mutants lacking both *Pten* and *Bdnf*. (**b,c**) G-ratio analysis of ML myelin in *Pten* single mutants and *Pten*Bdnf* double mutants revealed a slightly reduced myelin sheath sickness (indicated by a bigger g-ratio, p=0.0259). Data are means ± s.e.m, *p<0.05, student's *t* test, n=3 per genotype.

Taken together, in the absence of *Bdnf* expression from *Pten* mutant granule cells, radial axonal growth was not altered, mature oligodendrocytes became more numerous and the observed ectopic myelin was thinner. Our data suggests that neuronally expressed Bdnf is as a coregulator of CNS myelination, which demonstrates the relevance of our experimental approach. Nevertheless, the double mutant phenotype was puzzling and had to be defined in more detail.

As a working hypothesis we took into account that OPCs *in Pten* mutants receive both, "pro-proliferation" and "pro-differentiation" signals and that the simultaneous reaction of an OPC to both conflicting stimuli is impossible. Assuming that Bdnf is one of the "pro-differentiation" signals for OPCs in the mutants, its loss in double mutants would increase the weight of the "pro-proliferative" signals and thereby increase the number of OPCs generated in the ML. However, at a later stage the remaining "pro-differentiation" factors would still suffice to trigger OPC differentiation and myelin sheath formation, possibly with some temporal delay. This would explain our seemingly paradoxic result of more ectopic myelin in the conditional *Pten*Bdnf* double mutant mouse.

To test this hypothesis, we determined OPC proliferation at the age of 7 weeks in conditional double mutants and in *Pten* single mutants that had received daily BrdU injections between P25 and P45 (**Fig. 21a**). Indeed, double mutants showed 34% more BrdU labeled Olig2+ OPCs in the ML than *Pten* single mutants (p=0.0426, n=4 per genotype) (**Fig. 21b**). We noted that a lack of *Bdnf* also induced a higher proliferation of OPCs in heterozygous *Pten* mutants when compared to controls. This suggested a role of Bdnf to control the number of cerebellar OPCs, which are likely to turnover in the absence of other myelination promoting factors.

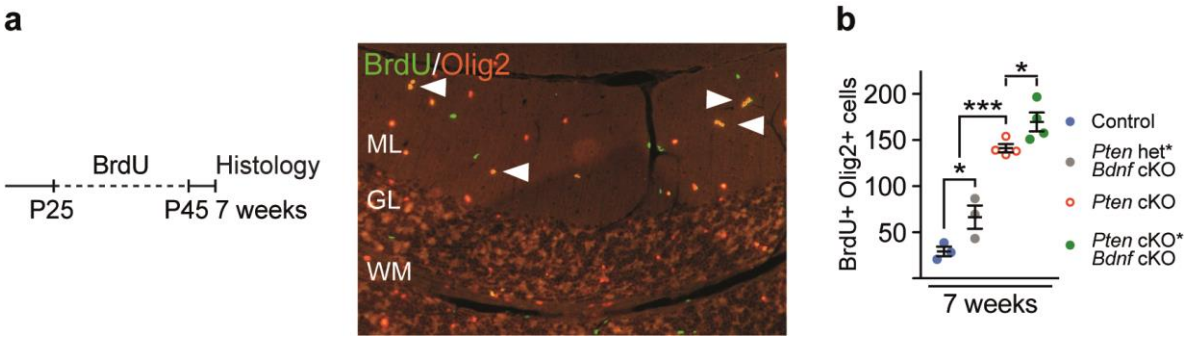

Fig. 21. Increased local proliferation of OPCs in double mutants lacking *Pten* and *Bdnf*. (**a**) BrdU was administered by intraperitoneal (i.p.) injection from P25-P45 and histology was performed 4 days later. Double positive cells are labelled with an arrowhead. (**b**) Quantitation of BrdU positive Olig2 expressing cells in the ML of parasagittal sections of the cerebellar vermis revealed significantly more double positive cell in *Pten* cKO**Bdnf* cKO mice compared to single *Pten* mutants (n=3-4 per genotype, p=0.0426). Data are means ± s.e.m. *p<0.05; ***p<0.001, one-way analysis of variance (ANOVA) followed by Bonferroni test. ML, molecular layer; GL, granule cell layer; WM, white matter.

3.5.3 *In vivo* uncoupling of Neuregulin 1 (Nrg1)

Nrg1 is another interesting axonal grow factor, since it is essential for myelination by Schwann cells in the PNS. As detailed in the introduction, its role in CNS myelination is still under debate. As a second *in vivo* uncoupling experiment we generated *Tg(mα6)-Cre*Pten*$^{loxP/loxP}$**Nrg1*$^{loxP/loxP}$ double mutant mice (hereafter termed *Pten* cKO**Nrg1* cKO). When compared to *Pten* single mutants at 10 weeks of age we found no difference in the number of (CNP+) oligodendrocyte (**Fig. 22a**). Analysis of MBP+ area also revealed no significant differences between single *Pten* mutants and *Pten* cKO**Nrg1* cKO (**Fig. 22b**). Additionally, g-ratio analysis and quantification of Pf calibers (myelinated and unmyelinated fibers) on electron microscopic sections at the age of 10 weeks showed no detectable differences (**Fig. 22c-e**).

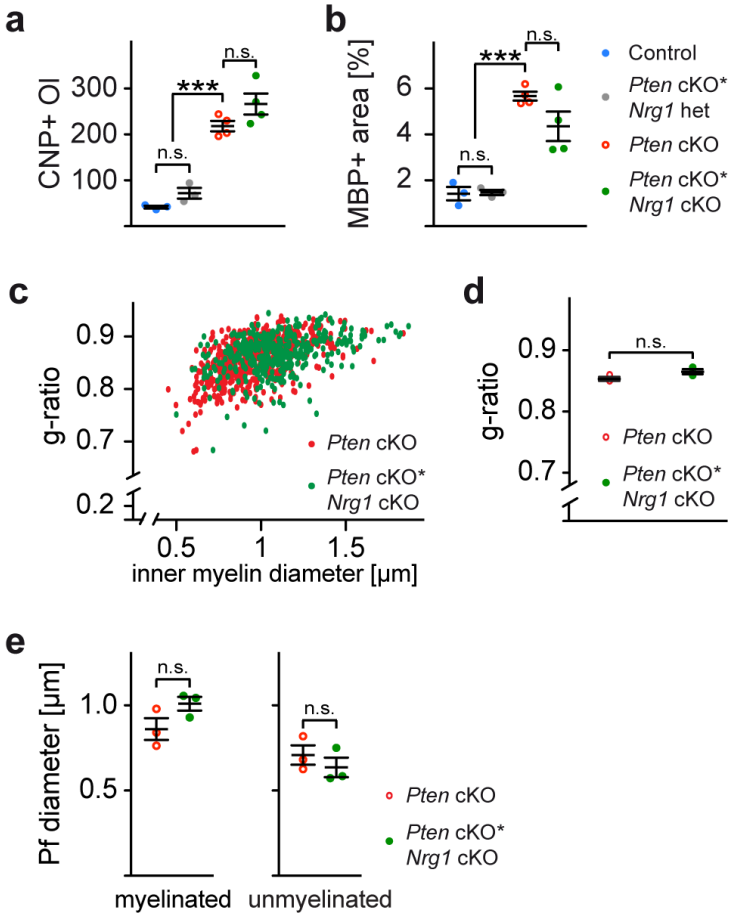

Fig. 22. Neuregulin 1 is not required for Pf myelination in *Pten* mutant mice. (**a**) Double mutants lacking both *Pten* and *Nrg1* in cerebellar granule cells (*Pten* cKO**Nrg1* cKO) do not differ from single *Pten* mutants (*Pten* cKO), when comparing oligodendrocyte numbers in the ML (CNP positive cells, p=0.1068). (**b**) Quantification of MBP+ area revealed no difference between single *Pten* mutants and double mutants lacking *Pten* and *Nrg1* (p=0.0982). Quantified were parasagittal sections of the cerebellar vermis (n=3-4 per genotype; 10 weeks of age). (**c,d**) G-ratio analysis derived from electronmicrographs of *Pten* cKO and *Pten* cKO**Nrg1* cKO mutants showed no significant difference (n=3 mice each genotype; 10 weeks of age; p=0.0581). (**e**) Caliber measurements of myelinated and unmyelinated Pf revealed no significant difference (n=3 per genotype; 10 weeks of age). Data are means ± s.e.m. ***p<0.001, student's *t* test (d,e) or one-way analysis of variance (ANOVA) followed by Bonferroni test (a,b).

3.5.4 *In vitro* validation of selected candidate factors

Because of the complexity of myelination control *in vivo*, we turned to simpler assay systems for proof-of-principle and to assess if our selected candidates indeed affect the fate of OPCs and oligodendrocytes. We used either mixed primary oligodendrocyte cultures (devoid of axons) from spinal cord of 4 day-old mouse pups or neuron-glia cocultures (that myelinate *in vitro*) prepared from E13 mouse spinal cord. Recombinant candidate proteins (chosen by diffusibility of the encoded protein, extent of upregulation, annotation, and overall plausibility) were added to the media at either 10 ng/ml (Sparcl1, Ptn) or 100 ng/ml (all other factors). After 3 and 5 days OPCs and oligodendrocytes in mixed cultures were quantified with antibodies against Olig2 (a pan-OL lineage marker) and the Adenomatosis polyposis coli (Apc) gene product (clone APC-CC1), a marker of postmitotic oligodendrocytes. Numbers and proliferation of oligodendrocyte lineage cells as well as *in vitro* myelination in neuron-glia cocultures were scored after 25 days by using antibodies against Olig2, Ki67 (a proliferation marker), MBP, and phosphorylated neurofilament as an axonal marker antigen (SMI31). In these experiments, our selected factors triggered different responses in oligodendrocyte lineage cells.

3.5.4.1 Proliferation assay

OPC proliferation was induced by adding recombinant acidic Fgf1 to myelinating cocultures. (**Fig. 23a,b**). The numerical increase in OPCs correlated with a 1.5-fold higher number of Ki67 positive Olig2+ cells (**Fig. 23c,d**). Other factors tested (including Sparcl1, Vegfc, Pleiotrophin, Tmsb4x, Timp3 and Activin A) showed no pro-proliferative effect. The OPC-mitogen Pdgf served as a positive control and significantly increased the relative percentage of Olig2+ cells in the culture **(Fig. 23b)**.

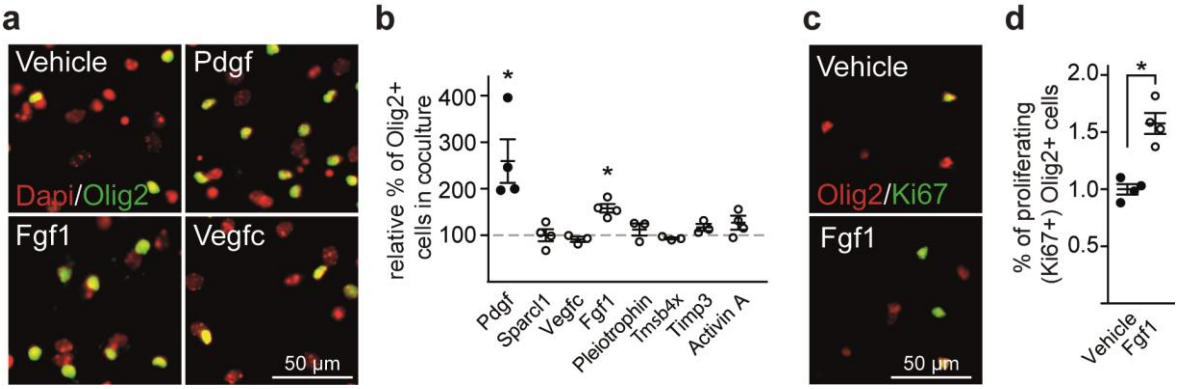

3.5.4.2 Differentiation assay

When determining the fraction of OPCs in primary mixed cultures (**Fig. 24a**) that had turned into mature postmitotic (APC/CC1+) oligodendrocytes after 3 (or 5) days of treatment, this number was significantly increased when Activin A was added (**Fig. 24b**). However, none of the other factors tested including Klotho (400ng/ml), which enhanced OPC maturation of rat OPCs *in vitro* (Chen et al., 2013) and was therefore used as a control, had any such effect.

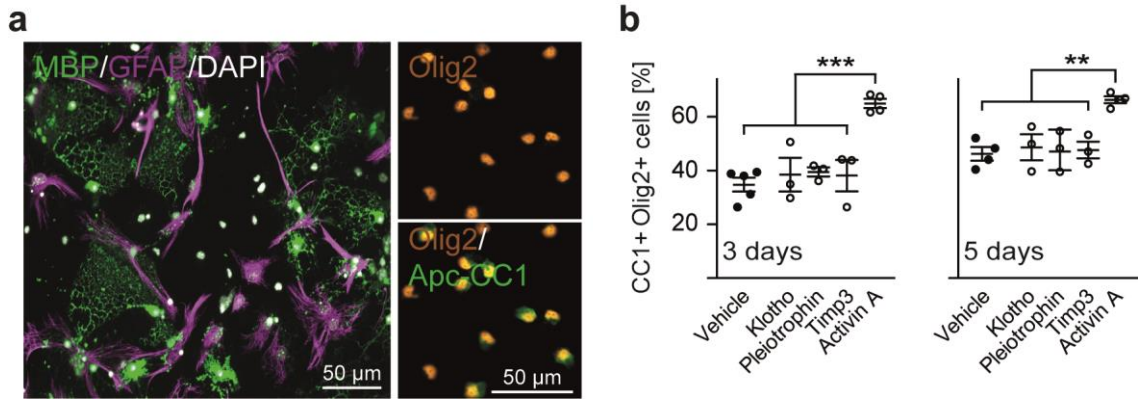

Fig. 24. Differentiation assay. (**a**) Representative images of a mixed primary oligodendrocyte cultures, co-immunostained for GFAP and MBP (left) or Olig2 and Apc-CC1 (right) after 3 days in culture. (**b**) Quantitation of the percentage of CC1 expressing cells in relation to Olig2 positive cells after 3 and 5 days treatment with either vehicle or one of the indicated recombinant proteins (n=3-5 for both time points). Klotho was included as a positive control (Chen et al., 2013), although the addition showed no significant effect (3 days: Vehicle vs. Klotho, p=0.5403; 5 days: Vehicle vs. Klotho, p=0.6483). Adding the recombinant form of Activin A to the mixed primary oligodendrocyte cultures increased (both time points) significantly the percentage of CC1 expressing cells in relation to Olig2 positive cells (3 days: Vehicle vs. Activin A, p=0.0003; 5 days: Vehicle vs. Activin A, p=0.0026). Pleiotrophin and Timp3 showed no such effect (3 days: Vehicle vs. Pleiotrophn, p=0.2397, Vehicle vs. Timp3, p=0.5629; 5 days: Vehicle vs. Pleiotrophin, p=0.8878, Vehicle vs. Timp3, p=0.7308). Data are means ± s.e.m. **p<0.01; ***p<0.001, Wilcoxon matched pairs test.

Fig. 23. Proliferation assay. (**a**) Representative images of cocultures treated with recombinant proteins and immunostained for Olig2 (pseudocolored in green) 13 days later. Cell nuclei are counterstained with DAPI (pseudocolored in red). (**b**) Quantitation of Olig2 positive cells after treatment of cocultures with the indicated selected factors between 12 and 25 days *in vitro* (DVI). The relative percentage of Olig2 positive cells was calculated by dividing the number of Olig2+ cells by the total cell number (determined by DAPI) and by normalization to vehicle treated cultures that were set to 100% (dashed line). The OPC-mitogen Pdgf served as positive control (n=3-4 independent experiments, Pdgf: p=0.0113; Sparcl1: p=0.9947; Vegfc: p=0.3451; Fgf1: p=0.0179; Pleiotrophin: p=0.4774; Tmsb4x: p=0.3125; Timp3: p=0.1766; Activin A: p=0.0869). Treating cocultures with the recombinant form of Fgf1 increased the number of Olig2+ cells. (**c**) Representative images of cocultures treated with vehicle (top) or Fgf1 (bottom) and costained for Olig2 (pseudocolored in red) and Ki67 (pseudocolored in green). (**d**) Addition of Fgf1 to the coculture increased the percentage of Ki67 positive Olig2+ cells (n=4 independent experiments, p=0.0153). Data are means ± s.e.m. *p<0.05. Wilcoxon matched pairs test (in b and d).

3.5.4.3 Myelination assay

Finally, in neuron-oligodendrocyte cocultures (**Fig. 25a**) we studied whether any of the recombinant proteins promoted terminal oligodendrocyte differentiation and myelin sheath formation by quantifying (for each culture) the myelin-representing (MBP+) territory relative to the size of the underlying axonal (SMI31+) network. Using this system, several of our candidates, including Pleiotrophin, Tmsb4x, Timp3 and Activin A significantly increased the myelinated area, and emerged as novel pro-myelinating factors (**Fig. 25b**). We note that Fgf1 increased both Olig2 cell numbers and myelinated area (**Fig. 23b, Fig. 25b**). However, and in contrast to the other factors tested, we scored many more MBP+ flat membrane sheaths instead of compacted myelin wraps (**Fig. 26**). Both enhanced cell number and flat membrane sheaths distorted the true “pro-myelinating” effect, when analyzed by an automated ImageJ plug in.

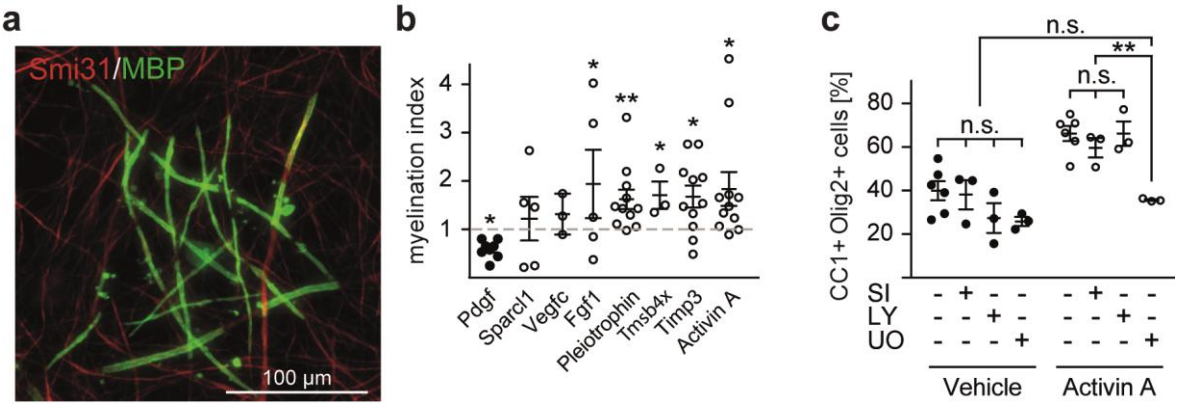

Fig. 25. Myelination assay. (**a**) Representative image of a myelinating coculture (neuron/oligodendrocyte, 25 days *in vitro*) immunostained for MBP and Smi31. (**b**) The “myelination index” was calculated by dividing the MBP positive area by the Smi31 positive area and defining this ratio as 1 in vehicle treated controls (dashed line) (n=3 for Vegfc, n=6 for Sparcl1 and Fgf1, n=11 for Pdgf, Ptn, Timp3 and Activin A). 5 added factors in this assay showed a singnificantly increased pro-myelinatin activity (Fgf1: p=0.0498, Pleiotrohin: p=0.0005, Tmsb4x: p=0.025, Timp3: p=0.0264 and Activin A: p=0.0132). Adding the recombinant form of Pdgf, as a known “pro-proliferative" signal significantly reduced the calculated myelination index (Pdgf: p=0.0049). Sparcl1 and Vegfc showed no effect (Vegfc: p=0.8806, Sparcl1: p=0.5781). (**c**) Mixed primary oligodendrocyte cultures treated for 3 days with Activin A in combination with either 2.5 µM SIS3 (SI), 0.5 µM LY294002 (LY) or 10 µM UO126 (UO) were co-immunostained for Olig2 and Apc-CC1. Quantification (n=3) of the percentage of CC1 expressing cells in relation to Olig2 positive cells after 3 days of treatment, revealed a significant abolishment of the Activin A effect by the specific inhibitor UO (Activin A vs. Activin A+UO: p=0.0005). SI and LY showed no significant reduction (Activin A vs. Activin A+SI: p=0.3050; Activin A vs. Activin A+LY: p=0.9959). Data are means ± s.e.m. *p<0.05; **p<0.01; ***p<0.001, Wilcoxon matched pairs test (b), or one-way analysis of variance (ANOVA) followed by Bonferroni test (c).

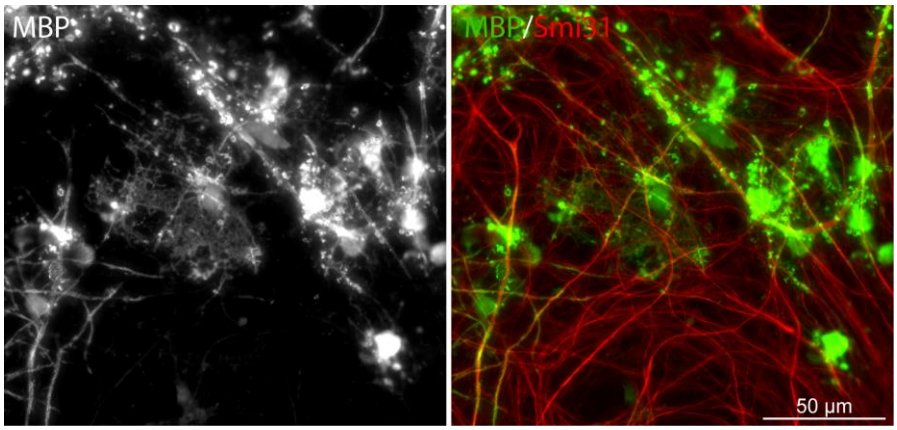

Fig. 26. Fgf1 treatment of myelinating cocultures favors "myelin-like" flat sheaths over compacted myelin wraps. Representative images of a myelinating coculture treated with Fgf1 between DIV 12 and DIV 25 in culture and immunostained for MBP and Smi31. Compare to **Fig. 25a.**

All *in vitro* studies described, were not optimized for any factor nor designed to characterize their function, but they provide "proof-of-principle" for the validity of a genetic approach that used ectopic myelination *in vivo* as its readout. However, for Activin A we used mixed primary oligodendrocyte cultures, to gain additional mechanistic insight (**Fig. 24a**). The TGF-like glycoprotein signals via type I and type II receptor serine/threonine kinases and the downstream transcription factors Smad2 and Smad3 (Tsuchida et al., 2009). Additionally, Smad-independent Activin A signaling involving p38 MAPK, ERK1/2, and AKT has been reported (Do et al., 2008; Tsuchida et al., 2009), i.e. pathways independently implicated in myelination control (Flores et al., 2008; Goebbels et al., 2010; Ishibashi et al., 2006). To determine which downstream mechanism is most critical, we treated mixed primary OL cultures with recombinant Activin A in the presence or absence of different inhibitors. Inhibition of MEK1/2 with UO126 (UO) completely abolished the pro-differentiation effect of Activin A, whereas inhibition of PI3K with LY294002 (LY) or inhibition of SMAD3 with SIS3 had no effect (**Fig. 25c**).

3.5.5 The cell type specific origin of selected candidate factors

Based on our experimental approach, we have no formal proof, that the cellular origin of the newly identified “differentiation/myelination factors" is neuronal. Indeed, by our transcriptome analysis of *Pten* cKO mutants and controls we identified several upregulated immune modulatory factors, e.g. Nts (neurotensin) and Ninj1 (**Fig. 18b**) with a role in immune cell migration (Ifergan et al., 2011; Katsanos et al., 2008). However, general microglia and macrophage marker antigens, including *Aif1*/*Iba1* (allograft inflammatory factor 1/ionized calcium-binding adapter molecule 1), *Cd68* (cluster of differentiation 68), or *Itgam*/*CD11B* (Integrin alpha M/cluster of differentiation 11B) were not differentially regulated (**Fig. 27a**). This is in line with immunohistochemical analysis of microglial marker antigens (Iba1, Mac-3) in the GL of *Pten* cKO (**Fig. 27b**). Similar, the quantification revealed no difference in cell numbers, between mutants and controls at the age of 2.5 month (**Fig. 27b,c**). Nevertheless, *Cd163* (Cluster of differentiation 163), which is considered a marker of anti-inflammatory or immunoregulatory M2 (alternatively activated) microglia/macrophages was 7-fold upregulated at the RNA level in the mutant GL (**Fig. 27a**). Interestingly, M2 microglia and macrophage derived Activin A has recently been reported to drive oligodendrocyte differentiation (Miron et al., 2013). Additionally, moderate changes of Iba1 and Mac-3 positive cells could be identified in the ML of *Pten* cKO (**Fig. 27b,c**). Quantification of GFAP+ area revealed the similar results (**Fig. 27d**). Furthermore, by immunohistochemistry for CD31 (cluster of differentiation 31/ PECAM-1, platelet endothelial cell adhesion molecule) we found significantly enhanced angiogenesis in the mutant GL at the age of 2.5 months (**Fig. 27e**).

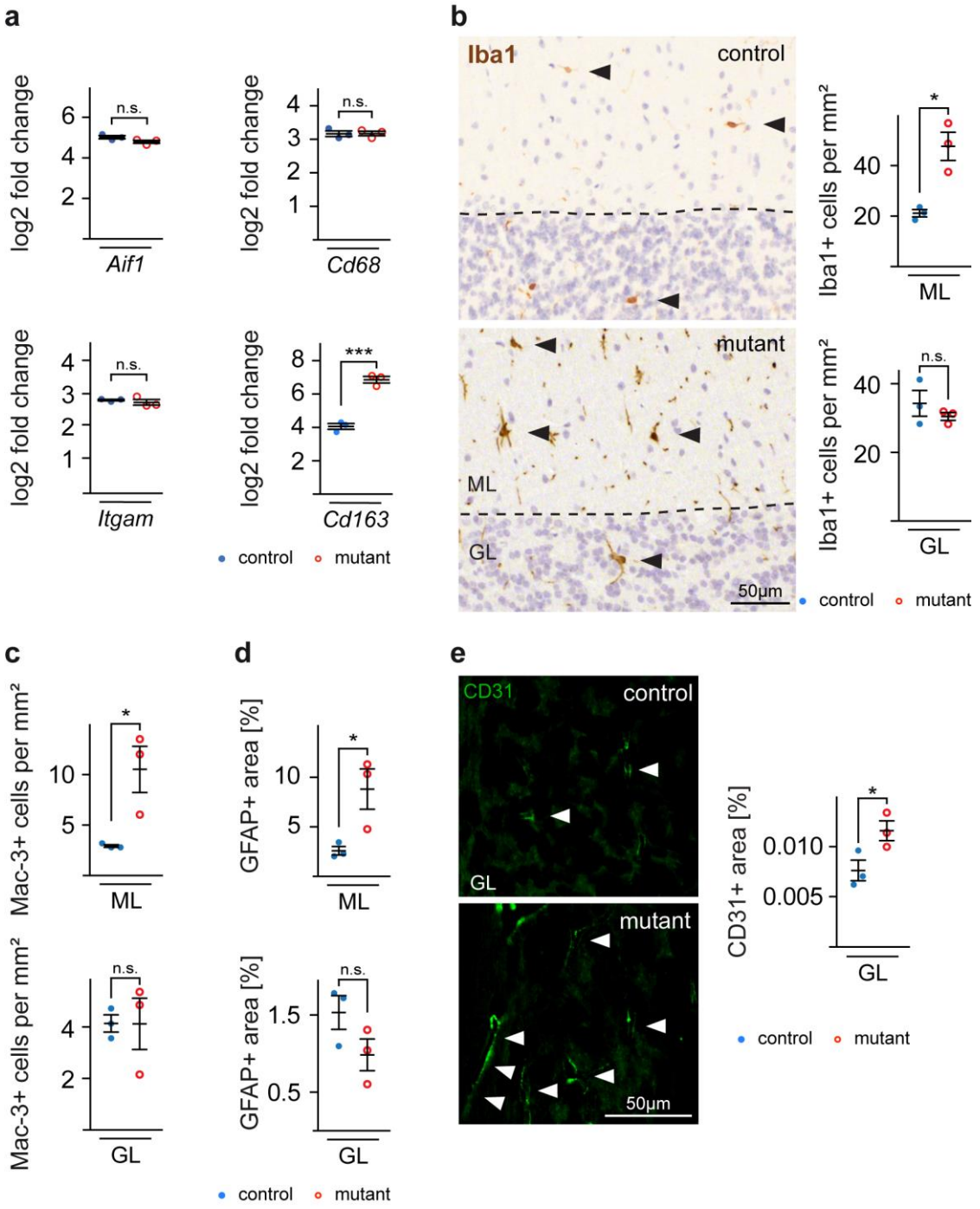

Fig. 27. Reactive gliosis and angiogenesis in *Pten* mutant mice. (**a**) Transcriptome analysis of *Pten* cKO and controls revealed no general upregulation of microglia and macrophage antigens, such *Aif1* (Iba1, p=0.1083), *Cd68* (p=0.9555), *Itgam* (CD11B, p=0.4901). *Cd163* a marker of anti-inflammatory or immunoregulatory M2 microglia/macrophages demonstrated a 7-fold upregulated at the RNA level in the mutant GL (p=0.0004) (**b**) Immunohistochemistry and quantification of Iba1 revealed a significant difference in the ML of *Pten* cKO mutants, compared to controls (p=0.0413), whereas the numbers in the GL are unchanged (p=0.5484). (**c**,**d**) Likewise, the number of Mac-3 positive microglia cells and the GFAP+ positive are is increased in the mutant ML (Mac-3: p=0.0295; GFAP+ area: p=0.0406) but not in the GL (Mac-3: p=0.9888; GFAP+ area: p=0.141). (**e**) Percentual area covered by microvessels is increased in the *Pten* mutant GL when compared to controls (quantitated on lobe 5 of cerebellar parasagittal paraffin sections immunostained for the endothel cell marker CD31). N=3 per genotype; age: 2.5 months. Data are means ± s.e.m. *p<0.05; ****P* < 0.001**,** student's *t* test.

3.5.5.1 No signs of gliosis in *NEX-CreERT2*Pten$^{loxP/loxP}$* mice

Since we found minor changes of Iba1, Mac-3 and GFAP in the *Pten* cKO ML (**Fig. 27b,c,d**) we analyzed *Nex-CreERT2*Pten$^{loxP/loxP}$* mutants with only 4% GC recombination (**Fig. 17a**), but significant myelination (**Fig. 17c-f**). Quantification for "gliosis" markers revealed no detectable differences in the ML and GL of *Nex-CreERT2*Pten$^{loxP/loxP}$* mutants compared to controls (**Fig. 28a-c**), even 28 weeks after recombination (**Fig. 17b**). This suggests, that the upregulation of Iba1+, Mac-3+ and GFAP+ cell numbers in the ML of *Pten* cKO are not a necessary primary trigger for *de novo* myelination.

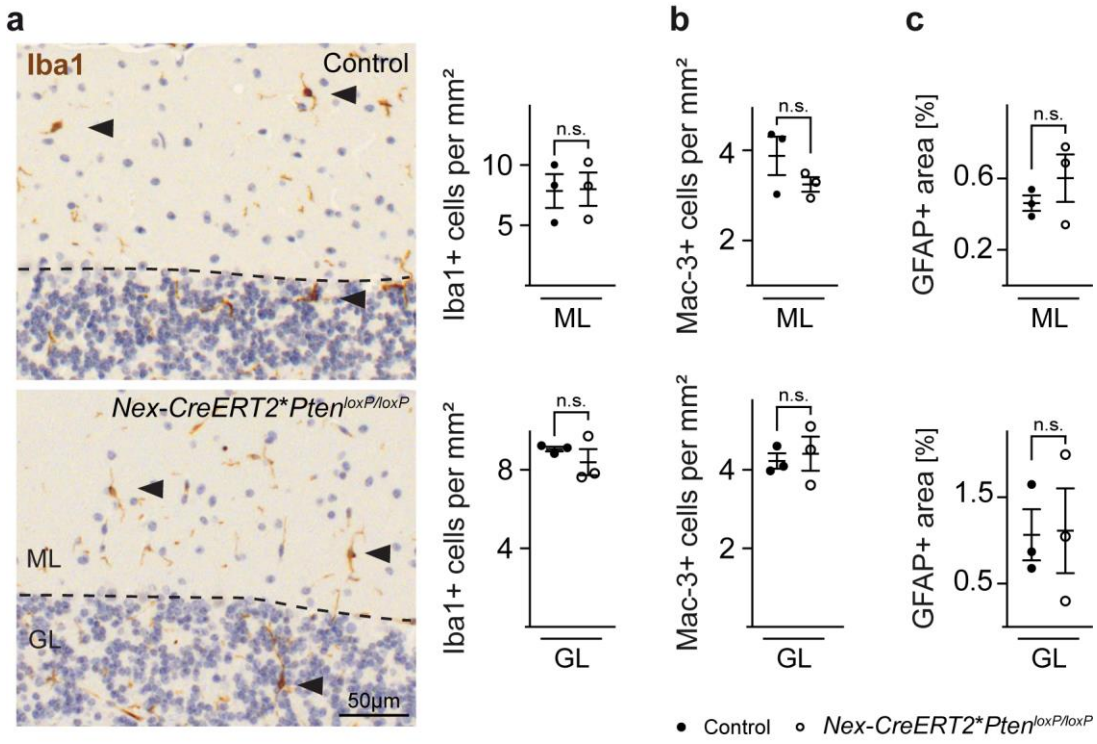

Fig. 28. No activation of microglia and astrocytes in the *NEX-CreERT2*Pten$^{loxP/loxP}$* cerebellum. (**a**) *Nex-CreERT2*Pten$^{loxP/loxP}$* mutants do not exhibit more Iba1+ microglia in the ML (p=0.8886) nor in the GL (p=0.516). (**b**) Quantification of Mac-3+ cell revealed no significant difference (ML: p=0,1494; GL: p=0,7067). (**c**) Similarly, GFAP+ area is similar in *Nex-CreERT2*Pten$^{loxP/loxP}$* mutant and control GL (p=0.9487) and ML (p=0.4998). Quantifications were performed on parasagittal sections of the cerebellar vermis; n=3 per genotype; age, 30 weeks. Data are means ± s.e.m.; student's *t* test; GL, GC layer; ML, molecular layer.

3.5 Inactivation of *Pten* in CA3 neurons

Are all CNS axons subject to *de novo* myelination when the Akt/mTOR pathway is artificially hyperactivated in the corresponding neuron? To target this question, we inactivated *Pten* in the forebrain, using the *Nex-CreERT2* driver line intercrossed with floxed *Pten* mutants (Lesche et al., 2002). In contrast to the sparse recombination of cerebellar granule cells (see **Fig. 17a**) almost all hippocampal pyramidal neurons recombine after 5 consecutive days of tamoxifen treatment (P10-P15) (Agarwal et al., 2012) (**Fig. 29a,b**). However, when analyzed 28 weeks after tamoxifen induced inactivation of *Pten,* no ectopic OPC proliferation and no *de novo* myelination of CA3 Schaffer collaterals (**Fig. 29c**) could be observed. Furthermore, quantification of the total number of CNP positive cells and MBP+ area in the hippocampus of controls and *Nex-CreERT2*Pten*$^{loxP/loxP}$ mutants revealed no significant difference (**Fig. 29d,e**).

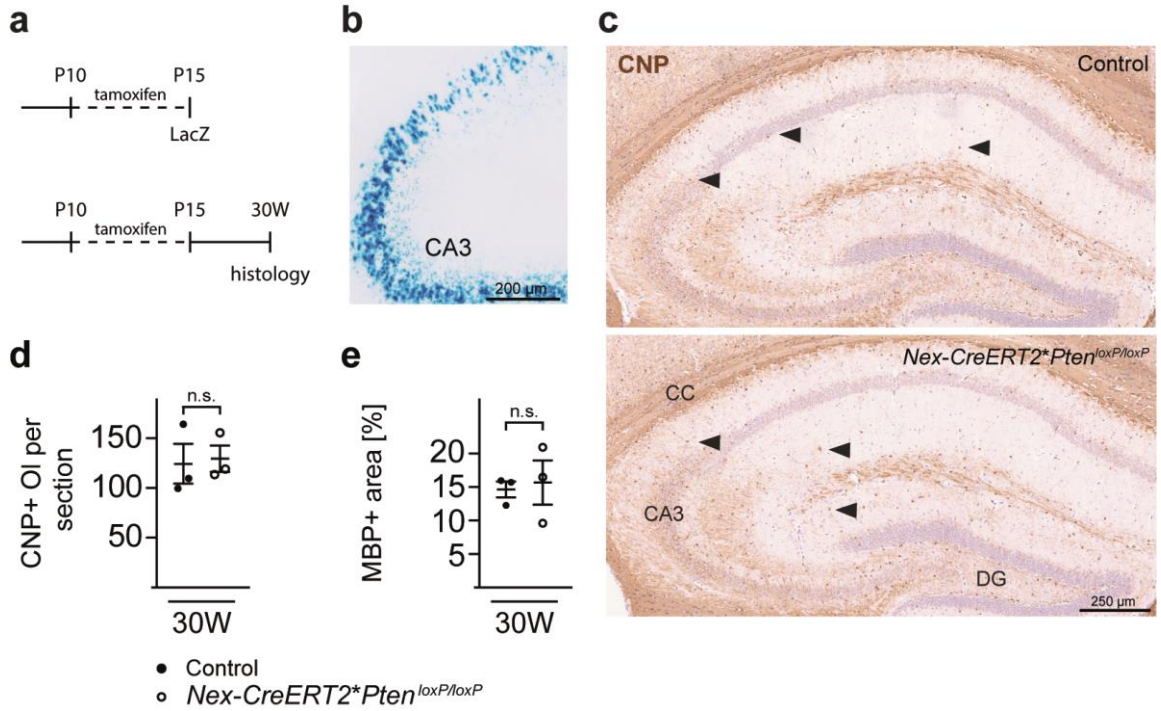

Fig. 29. *Pten* inactivation in principal neurons of the hippocampus. (**a**) Tamoxifen treatment schemes of *Nex-CreERT2*Pten*$^{loxP/loxP}$ mutant mice. Cre-mediated activation of a lacZ reporter gene in CA3 neurons (CA3) revealed almost a 100% recombination efficiency upon tamoxifen treatment from P10-P15 (**b**). For further analysis, *Nex-CreERT2*Pten*$^{loxP/loxP}$ mutant mice and controls were injected with tamoxifen from P10-P15 and analysed 28 weeks later. (**c**) *Nex-CreERT2*Pten*$^{loxP/loxP}$ mutant mice exhibited the identical distribution of CNP+ oligodendrocytes in the hippocampus. (**d**) Quantification of CNP+ oligodendrocytes revealed no significant difference (p=0.8451). (**e**) Similar, the MBP+ area is unchanged in *Nex-CreERT2*Pten*$^{loxP/loxP}$ mutant mice compared to controls (p=0.7849). Quantified on coronal sections of the forebrain; n=3 mice each genotype and age. Data are means ± s.e.m., student's t-test. CC, corpus callosum; DG, dentate gyrus.

Since somata of *Nex-CreERT2*Pten*$^{loxP/loxP}$ mutant CA3 neurons were enlarged when quantified on H&E stained paraffin sections and on electron micrographs (**Fig. 30a,b**) we argue that hyperactivation of PI3K/Akt/mTOR pathway is not always sufficient to trigger CNS myelination. Inhibitory signals may "protect" forebrain neurons, as myelination can interfere with axonal sprouting and neuronal plasticity in the adult brain (Schwab and Strittmatter, 2014). However, we have no formal proof that the Schaffer collaterals were sufficiently enlarged. Electron micrographs and serial block-face scanning electron microscopy did not allow us to unequivocally identify Schaffer collaterals.

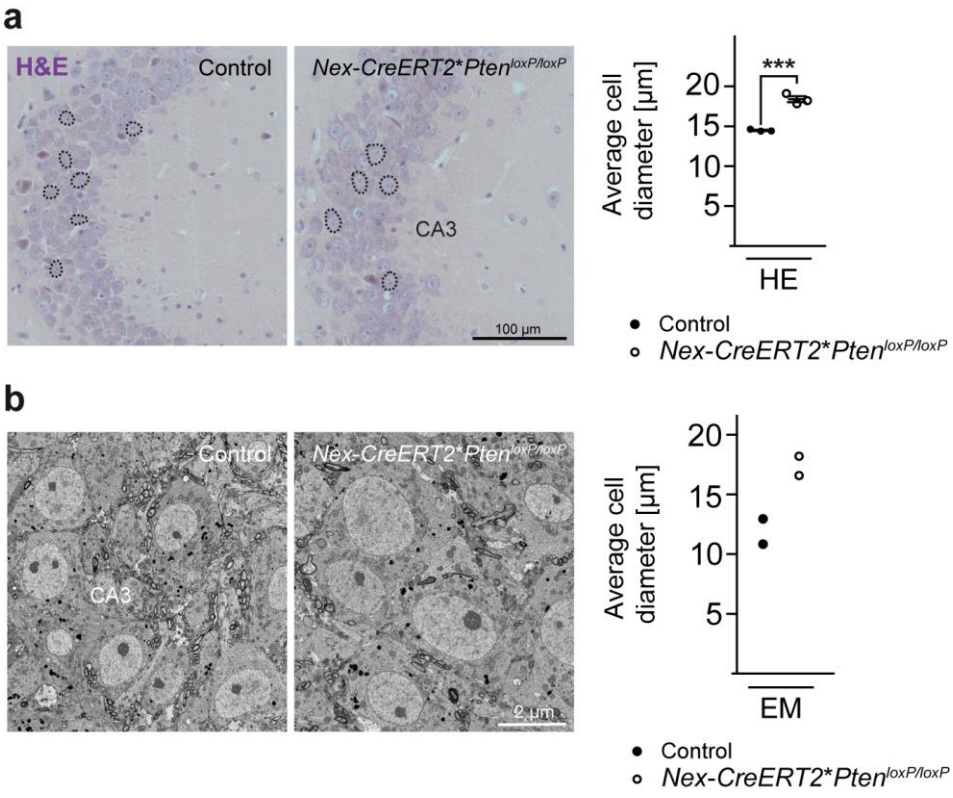

Fig. 30. Enlargement of CA3 neurons upon *Pten* inactivation. (a) *Nex-CreERT2*Pten*$^{loxP/loxP}$ mutant mice exhibited significantly enlarged hippocampal CA3 neurons, when quantified in H&E stained paraffin sections. *Pten was inactivated* by injecting tamoxifen from P10-P15. Quantification was done 28 weeks later (n=3 per genotype; 40 cells per animal, p=0.0005). (**b**) Similar enlarged cell diameters were obtained by electron microscopy (n=2 per genotype; 10-15 cells per animal).

3.6 Hamartoma formation in aged *Pten* mutants

We note that later in life, many mice older than 11 months developed ataxia and hindlimb paralysis (Video 2, can be found on the included CD-ROM or on Nature Neuroscience webpage http://www.nature.com/neuro/journal/vaop/ncurrent/fig_tab/nn.4425_SV2.html), possibly due to cerebellar hamartomas at that older age, which preferentially affected the inferior and posterior lobes (**Fig. 31a**). Granular cells, preferentially located in the inferior and posterior lobes of the cerebellum, developed a secondary and focal hyperplasia that was clearly more pronounced than the hypertrophy underlying the myelination phenotype (**Fig. 31b**). Calbindin immunohistochemistry revealed a Purkinje cell loss (**Fig. 31c**), next to reduced central white matter (immunostained for CNP, oligodendrocyte and myelin specific marker) (**Fig. 31d**) and signs of inflammation (activated microglia cells, immunostained for Mac-3). Furthermore, vascularization was enhanced (**Fig. 31e**). These features collectively model features of human Lhermitte Duclos disease (LDD), a dysplastic gangliocytoma of the cerebellum associated with *PTEN* gene mutations.

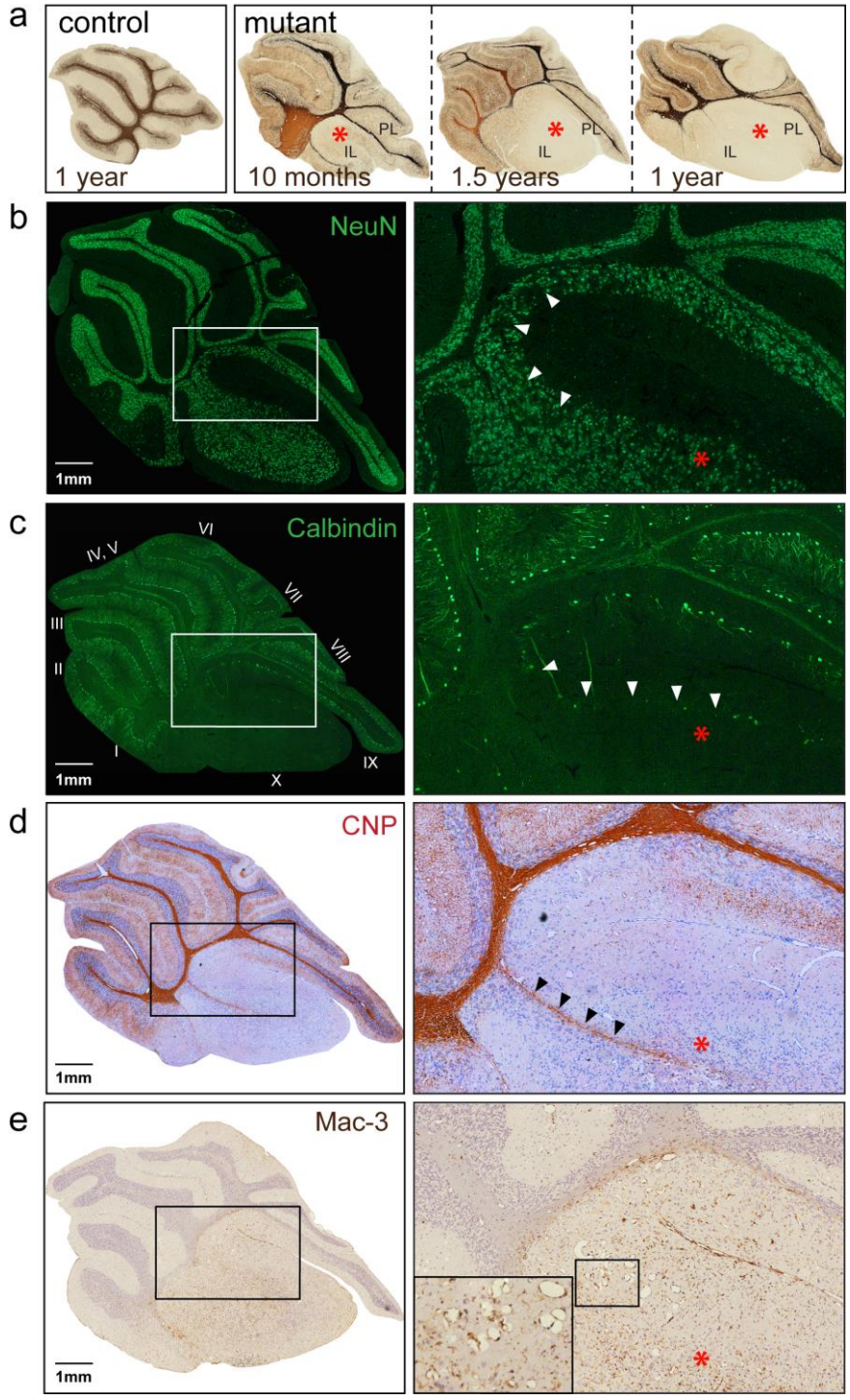

Fig. 31. ***Pten*** **mutant mice as a model of Lhermitte-Duclos disease. (a)** Gallyas silver impregnation of cerebellar parasagittal sections reveals a focal pathology (asterisks) in aged *Pten* mutants that is preferentially localized to the inferior lobe (IL) and the posterior lobe (PL). Pathology is characterized by secondary focal hypergrowth of GC immunostained for NeuN (arrowheads in **b**; age 1 year; boxed area magnified on the right), loss of Purkinje cells immunostained for Calbindin (arrowheads in **c**; age, 1 year; boxed area magnified on the right), loss of central white matter immunostained for CNP (arrowheads in **d**; age, 1 year; boxed area magnified on the right), and presence of activated microglia cells immunostained for Mac-3 (in **e**; age, 1.5 years; boxed area magnified on the right) and enhanced vascularization (boxed area in **e** magnified on the right and further magnified in inset). Cerebellar lobes I-X are marked in **c**.

4. Discussion

4.1 Axon caliber and PI3K dependent induction of myelination

During myelination but also in remyelination, a plethora of cell intrinsic and extrinsic signaling molecules have been suggested as modulators and coordinators of the complex process of axonal ensheathment by oligodendrocytes (Hsieh et al., 2004; Mcmorris et al., 1986; Miron et al., 2013; Van't Veer et al., 2009; Vanderpal et al., 1988; Xiao et al., 2010; Xiao et al., 2012). However, recent data challenged the idea that axonal signals are at all required to initiate and coordinate this process. Here, in experiments by Lee, 2012, even artificial nanofibers with threshold caliber diameters above 0.4 µm became myelinated by oligodendrocytes in the absence of any axonally derived guidance signals *in vitro*. This study effectively uncoupled the role of molecular cues from biophysical properties of the axon and demonstrated a dependency of myelination on axon caliber in the CNS (Lee et al., 2013; Lee et al., 2012). Thus, one obvious possibility would be that an axonal caliber above a certain key-threshold, is sufficient to instruct myelination *in vivo*.

Several approaches in PNS analyses have addressed the correlation between myelination and axon caliber (Duncan and Hoffman, 1997; Matthews, 1968). Indeed, axons larger than 1 µm are preferentially myelinated (Duncan and Hoffman, 1997; Matthews, 1968; Salzer, 2003). Back in 1989, *Voyvodic* increased the caliber of normally unmyelinated sympathetic postganglionic axons in the PNS, by increasing the size of the peripheral target tissue they innervate (Voyvodic, 1989). Subsequently, this axonal caliber increase induced *de novo* myelination by Schwann cells. Based on this observation, it was concluded, that i) axon caliber in the PNS is in fact the crucial determinant of whether or not an axon becomes myelinated and that ii) the production of myelin is likely determined by a signal from the axon that increases along with axon caliber (Aguayo et al., 1976; Voyvodic, 1989; Weinberg and Spencer, 1976). Meanwhile, the instructive signal on the axon has been identified as Neuregulin 1 that activates ErbB downstream signaling in Schwann cells and is the key trigger for myelination in the PNS (Michailov et al., 2004; Taveggia et al., 2010). Neuronal overexpression of Nrg1 induces hypermyelination and the reduction of Nrg1 expression causes a hypomyelination (Michailov et al., 2004). However, this axonal growth factor is dispensable for CNS myelination (Brinkmann et al., 2008), which leaves the neuronal factors that control OPC development and myelination *in vivo* poorly understood. Nevertheless, and in contrast to Schwann cells, oligodendrocytes are able to follow a more “default” pathway and even myelinate artificial carbon nanofibers (Lee et al., 2013; Lee et al., 2012). However, in this artificial model, oligodendrocytes engage with the nanofibers, start membrane ensheatment, but they fail to generate multiple wraps and compact myelin (Karadottir and Stockley, 2012; Lee et al., 2013). Over the last two decades, different growth

factors and cytokines, including Pdgf, Fgf2, Igf1, Bdnf, Nt3, Cntf and Lif, have been identified as regulators of the proliferation and differentiation of oligodendrocyte lineage cells. A role for IGF1 (insulin-like growth factor 1) was for example demonstrated by the analysis of mouse mutants. Homozygous *Igf1*$^{-/-}$ mice, exhibited decreased numbers of oligodendrocytes and a reduction of white matter structures (Beck et al., 1995), while transgenic mice overexpressing *Igf1* developed an upregulation of oligodendroglial myelin synthesis (Carson et al., 1993). This strengthens the hypothesis, that beside the axon caliber an big orchestra of many different positive and negative signals from various cells and the extracellular environment is needed to modulate and control for proper and timely myelination. As mentioned in the introduction, most of the already known signals and growth factors, with putative effects on oligodendrocyte lineage cells, are produced and secreted by astrocytes and endothelia cells or are of unknown origin. Signal cues directly from axons are largely unknown and need to be discovered. To resolve this lack of knowledge, we genetically induced, in analogy to the classical work from *Voyvodic* (1989), an axonal caliber increase (by hyperactivating Akt/mTOR-dependent downstream signaling in normally unmyelinated neurons), which was followed by the proliferation of wt OPCs in the molecular layer, their maturation to oligodendrocytes, and the *de novo* myelination of parallel fibers starting at around postnatal day 40 (P40) and progressing with age. Interestingly, once the caliber threshold (0.25 µm) for being myelinated was achieved, oligodendrocytes showed no general preference for especially larger caliber axons. This is consistent with previous electron microscopy findings in spinal cords from rats, where single oligodendrocytes myelinated axons with different calibers (Waxman and Sims, 1984). The average diameter of a wildtype parallel fiber is around 0.2 µm and it is normally unmyelinated. Nevertheless, some parallel fibers in larger mammals, such as cats and macaques surpass the critical size limit and become myelinated (Lange, 1976). This may suggest that parallel fibers are in principle quite susceptible to myelination but they are simply not preferentially because of their small caliber. Furthermore, since the ML is anyway not populated by oligodendrocytes there may also be no need for the Pf to express an additional battery of molecules that would actively hinder myelination. This uniqueness of Pf might explain, why we were not able to induce *de novo* myelination of other normally unmyelinated CNS axons, the Schaffer collaterals of the hippocampus, with the very same genetic mutation of the *Pten* gene. We hypothesize that Schaffer collaterals likely have a higher need to express more inhibitory signals than Pf, in order to exclude their axons from myelination, since their surrounding is filled with oligodendrocytes and other myelinated axons.

4.2 Regulation of OPC proliferation, differentiation and CNS myelination

Understanding the signaling mechanisms that trigger oligodendrocyte precursor cell (OPC) proliferation and myelination in the central nervous system (CNS) *in vivo* is of key importance for the therapy of diseases, such as multiple sclerosis, in which endogenous repair mechanisms fail. Numerous signaling cues must be considered, including myelination-promoting and inhibiting factors that could act on OPCs and oligodendrocytes, as well the size and electrical activity of putative target axons (Piaton et al., 2010; Taveggia et al., 2010).

Neurons release growth factors in an activity dependent manner and neuronal activity is known to promote myelination and proliferation of OPCs (Karadottir and Attwell, 2007). Moreover, OPCs receive synaptic input from Pf in the cerebellar ML (Lin and Bergles, 2004) and synaptic input from unmyelinated axons to OPCs modulates their proliferation (Mangin et al., 2012) and myelination (Wake et al., 2011). Thus we asked in our mutant mouse model, if increased OPC proliferation and myelination was induced by changes resulting from alterations in granular cell activity. However, we found no differences between mutants and controls in the frequency of the spontaneous synaptic input that OPCs receive from parallel fibers or in the frequency of spontaneous inputs in Purkinje cells at the age of P7-P100, i.e. at times of ongoing OPC proliferation and myelination in the *Pten* mutant ML. These results suggest, that none of the observed oligodendroglial phenotypes was induced by changes in granular cell electric activity.

Hypothetically, *de novo* parallel fiber myelination in the mutants could have been caused by down-regulating axon-bound inhibitory neuronal ligands that bind to known inhibitory pathways of oligodendrocyte development, such as the Notch1 pathway (Taveggia et al., 2010). It is well established, that at early developmental stages, OPC differentiation and myelination can be inhibited by the interaction of axonally expressed Jagged to oligodendroglially expressed Notch (Genoud et al., 2002; Givogri et al., 2002; Wang et al., 1998; Zhang et al., 2007). One specific Notch1 ligand that appeared 2.5 fold downregulated in our transcriptome analysis of laser captured GC layer of *Pten* mutants was Dner, a protein strongly expressed in several types of post-mitotic neurons (Eiraku et al., 2002). Whether this down regulation of the neuronal transmembrane protein Dner plays a role in the process of ectopic myelination of Pf has to be addressed in more detail in the future.

We concentrated instead more on the idea that also the down regulation of soluble/released inhibitory signals might have been instructive for *de novo* myelination of Pf. To test for this possibility, we intercrossed flox *Pten* mutants to a *Nex-CreERT2* driver line (Agarwal et al., 2012) that inactivates target genes only in a small subset of cerebellar granule cells

(Agarwal et al., 2012). However, when analyzed 28 weeks after tamoxifen injections, loss of *Pten* in this small fraction of granule cells was still sufficient to significantly increase the numbers of mature oligodendrocytes and the MBP positive area in the cerebellar molecular layer. This makes it unlikely that soluble inhibitory factors (still expressed by the vast majority of non-recombined granule cells) regulate Pf myelination. Hence, we focused next on genes for soluble growth factors and signaling molecules, for which the corresponding mRNAs were upregulated in the hypertrophic GL and which are ligands of established pathways in oligodendrocytes that instruct myelination (Goebbels et al., 2010; Ishii et al., 2013; Santra et al., 2012).

Transcriptome analysis resulted in a first list of candidate factors upregulated in *Pten* cKO and selected by annotation. mRNAs with higher expression in the mutants included for example Bdnf, which we selected for a proof-of-principle *in vivo* analysis, to address the significance of this list of candidates. Bdnf is already believed to be involved in oligodendroglia lineage cell development and myelination, although no clear picture has emerged yet. On the one hand, conditional inactivation of *Bdnf* in neurons did not induce a difference in the density of Olig2+ cells in the striatum and no effect on myelination in the optic nerve (Rauskolb et al., 2010). On the other hand it has been shown in *Bdnf* heterozygous mice that NG2+ cells as well as the protein amount of MBP, MAG and PLP were reduced in the basal forebrain (Vondran et al., 2010). When we analyzed double mutant mice, which lacked both *Pten* and *Bdnf* in cerebellar granule cells we obtained the unexpected result, that the mutants had more (not less) proliferating OPCs, oligodendrocytes and myelin sheaths in the ML, however the myelin sheath thickness of single sheaths was reduced.

We reasoned that Bdnf is a "pro-differentiation" signal with limited efficacy for OPCs in our mutants. Accordingly, it's loss in double mutants initially increased the weight of the "pro-proliferative" signals and thereby also the number of OPCs generated in the mutant ML. However, at a later stage the remaining "pro-differentiation" factors were still sufficient to trigger OPC differentiation and myelination, possibly with some temporal delay. This finding suggested that not one key factor but many factors (each with a measurable but limited range of efficacy) play a role in orchestrating oligodendrocyte lineage cell progression in our mutants. Inactivating one player, such as Bdnf has a moderate effect on imbalancing the whole system. In line with this finding, until now, not a single neuronal mutation has been reported in the literature that completely prevents CNS myelination, even in large screens (Deshmukh et al., 2013; Mei et al., 2014; Najm et al., 2015).

Because of the suggested complexity of the cocktail of orchestrating factors, we turned to *in vitro* assays to further validate some of our candidate factors. In these experiments recombinant forms of our upregulated candidate genes triggered different responses in oligodendrocyte lineage cells. Pleiotrophin is a member of the neurite growth-promoting factor family (Kretschmer et al., 1991). Adding the recombinant form of Pleiotrophin to our cocultures revealed an induction of myelination. This is in line with the recent finding that Pleiotrophin is expressed and released from demyelinated neurons and binds as an inhibitory ligand to PTPRZ (Protein tyrosine phosphatase receptor type z) in OPCs, which results in induced OPC differentiation for remyelination (Kuboyama et al., 2015). In our experiments, Fgf1, a member of the heparin growth factor family demonstrated a pro-proliferative role for OPCs, when tested in cocultures. It was the only factor, next to our positive control Pdgf that resulted in significantly more OPC proliferation in culture. This is in line with several *in vitro* studies, that showed similar findings for Fgf1 and Fgf2 (Engele and Bohn, 1992). Neurons and astrocytes are able to produce and secrete different Fgfs (Becker-Catania et al., 2011; Elde et al., 1991; Gomezpinilla et al., 1992; Matsuyama et al., 1992; Nakamua et al., 1999; Riva and Mocchetti, 1991), whereas oligodendrocyte lineage cells express the corresponding Fgf receptors in a developmentally regulated manner (Bansal et al., 1996; Fortin et al., 2005). Fgfr1 and Fgfr3 are expressed by OPCs, whereas Fgfr2 and additionally Fgfr1 are expressed by differentiated oligodendrocytes (Bansal, 2002). Mice lacking both Fgfr1 and Fgfr2 in oligodendrocyte lineage cells, revealed surprisingly no phenotype in OPC proliferation and differentiation. Although, the growth of CNS myelin was strongly inhibited (Furusho et al., 2012). This suggest, that the *in vivo* function of Fgf signaling is more complex and probably not limited on proliferation (Furusho et al., 2012). Timp3, one out of four members of the tissue inhibitor metalloproteinases family, induced myelination in our cocultures. This function of Timp3 on promoting myelination is novel. However it has been shown before that inactivation of Timp1, a member of the same family, induced a reduced myelin repair following a demyelinating injury in mice (Crocker et al., 2006). Additionally, the formation of compact myelin was delayed accompanied by a reduction of NG2+ OPCs (Moore et al., 2011). Tmsb4x is a G-actin sequestering peptide (Moon et al., 2010) and is known to increase oligodendrogenesis, although the molecular mechanisms are unclear (Santra et al., 2012). Threating cocultures with the recombinant form of Tmsb4x increased the myelination index in our experiments, suggesting (in line with the literature) a positive effect on myelination. Activin A (Inhba, forming the biologically active dimer Activin A) belongs to the TGF-β protein superfamily (Kingsley, 1994). Myelination *in vitro* was induced in our cocultures by adding recombinant Activin A. More importantly Activin A also emerged as a differentiation factor in our primary oligodendrocyte cultures. This finding is in agreement with a recent

report, in which Activin A was identified as a microglia (M2) cell-derived oligodendrocyte differentiation factor. Blocking Activin A resulted in the inhibition of remyelination in cerebellar slice cultures (Miron et al., 2013). Activin A is in principle able to signal through a combination of type I and II transmembrane serine/threonine kinase receptors (Harrison et al., 2005; Tsuchida et al., 2008), via Smad2/3/4 dependent complexes or Smad-independent pathways such as MAPK (ERK1 and ERK2), or PI3K pathway (Tsuchida et al., 2009). By blocking the specific signaling pathways one by one, we could demonstrate that the pro-differentiation activity of Activin A on oligodendrocyte lineage cells required the activation of MAPK, but not PI3K or SMAD3, to be effective.

Our experimental setup and the emerged *de novo* myelination of the cerebellar molecular layer in *Pten* mutant mice, suggested the instructive role of a primarily neuronal (PI3K/Akt/mTOR-dependent) developmental program for myelination. Although, down-stream of this switch, as noted in the results part and annotated by the database from http://web.stanford.edu/group/barres_lab/brain_rnaseq.html (Zhang et al., 2014) not all newly identified differentiation/myelination factors are necessarily of neuronal origin. Several upregulated immune modulatory factors were revealed by our transcriptome analysis (like. Nts and Ninj1) with a role in immune cell migration (Ifergan et al., 2011; Katsanos et al., 2008). However, as shown in the results part, general microglia and macrophage marker antigens, including *Aif1*/*Iba1*, *Cd68* and *Itgam*/*CD11B* were not differentially regulated. This is in line with immunohistochemical analysis of microglial marker antigens and respective quantifications, which revealed no difference in cell numbers of Iba1+, Mac-3+ and GFAP+ cells in the GL between mutants and controls at the age of 2.5 months. However, *Cd163* a marker of anti-inflammatory (M2 type) microglia/macrophages was 7-fold upregulated at the mRNA level in the mutant GL and the ML contained significantly more microglial cells and astrocytes, when quantified by immunohistochemistry. This prompted the idea to analyze the potential impact of microglial cells more in detail in *Nex-CreERT2*Pten*$^{loxP/loxP}$ mutants in which less cells were recombined (only 4% of GC recombination, but significant *de novo* myelination). No elevation of gliosis markers were visible in the ML nor in the GL in *Nex-CreERT2*Pten*$^{loxP/loxP}$ mutants. Thus, we conclude that the *de novo* myelination of the ML in *Pten* cKO is not initiated by microgliosis. However, subtle gene regulation changes in existing microglia or astrocytes may have had secondary impact but were for sure downstream of the primary instructive signal, which is for sure neuronal as defined by the specific genetic intervention in GC. Interestingly we also identified several factors (Vegfc, Apcdd1, Igfbp7) in our genetic screen that are exclusively expressed in endothelial cells. Accordingly, immunohistochemistry for CD31 (cluster of differentiation 31/ PECAM-1, platelet endothelial cell adhesion molecule), a marker for early and mature endothelial cells (Thomas et al.,

2009) demonstrated a significantly higher angiogenesis in the mutant GL at the age of 2.5 months. This finding seems interesting, since recent studies suggested an instructive role of endothelia cells in the regulation of oligodendrocyte lineage cells. For example, the proliferation of OPCs was induced by the presence of endothelia cells in a trans-well culture system. Since the different cell types were cultured with no direct cell-cell contact, the finding indicated a secretion of putative oligo-supportive factors by endothelia cells (Arai and Lo, 2009). In summary the role specifically of microglial cells and vasculature as bystanders of myelination awaits to be further explored.

4.3 Utilization of acquired knowledge from PI3K dependent *de novo* myelination

We identified a neuronal, PIP3-dependent switch, that instructed the entire cascade of oligodendrocyte lineage cell development and *de novo* myelination, at least in part by direct or indirect upregulation of newly identified factors, such as Fgf1, Pleiotrophin, Timp3, Thymosin beta 4, and Activin A. One major dispute in demyelinating diseases like multiple sclerosis is about the failure to repair lesioned areas. Although OPCs are present, they often fail to differentiate into mature oligodendrocytes and to remyelinate axons that lost their myelin sheaths. Remyelination is a regenerative mechanism, protecting demyelinated axons by restoring myelin sheaths (Irvine and Blakemore, 2008). Genetic lineage tracing in transgenic mice identified oligodendrocyte lineage cells as an endogenous source of mature and myelinating oligodendrocytes in the healthy adult CNS (Rivers et al., 2008). It would be important to unveil the signals that promote oligodendrocyte differentiation during development and to use this knowledge to promote remyelination. With the help of our transcriptomic approach, we identified several known and also novel signaling cues with a putative effect on the oligodendrocyte lineage cell development. The application of these factors in demyelinating disorders, such as mouse models of multiple sclerosis would be a promising strategy in preclinical studies to protect degenerating axons by promoting remyelination. Nevertheless, a major problem is to administer factors like Bdnf, Fgf1, Timp3, Pleiotrophin, Tmsb4x or Activin A. Bdnf, for example cannot be transcytosed through the blood-brain barrier (BBB) in vivo (Pardridge et al., 1994). For the other identified factors, not much is known about their ability to pass the blood brain barrier. Some studies in rats/mice implanted miniosmotic pumps or used intraventricular infusion of growth factors like VEGF (Proescholdt et al., 1999) or BMP4 (bone morphogenic protein) (Sabo et al., 2011). Intraventricular infusion of BMP4 during demyelination increased the proliferation of OPCs (Sabo et al., 2011). In a very recent study, Bdnf was injected intravenously in rats after white matter injury in subcortical stroke. Induction of ischemia enabled Bdnf to cross the blood

brain barrier (Schabitz et al., 2007). Bdnf treated animals showed less functional deficits and depicted an increased proliferation of OPCs (Ramos-Cejudo et al., 2015). These data support the concept of growth factor mediated oligodendrogenesis and treatment of demyelination in mouse models and patients.

4.4 *Pten* deficiency in granular cells: A new mouse model for Lhermitte-Duclos disease

Especially upon aging, our conditional *Pten* mutant mice are a novel and suitable model for Lhermitte Duclos disease (LDD), which is superior to the existing ones (Backman et al., 2001; Kwon et al., 2001). LDD is characterized by diffuse hypertrophy of the granular layer, loss of white matter and slowly growing tumors (hamartoma) of the cerebellum (Eng, 2000). Patients develop a macrocephaly accompanied by ataxia and seizures, usually affecting patients aged 30-50 years (Giorgianni et al., 2013). The normal architecture of the cerebellar cortex is abrogated and a secondary Purkinje cell loss can be observed (Backman et al., 2001). Although the exact cause in patients is unknown, mutations in the *PTEN* gene have been identified (Blumenthal and Dennis, 2008). By inactivating a loxP flanked *Pten gene by using a GFAP-Cre driver line*, two mouse models were created that mimic some of the characteristic symptoms of the disease, such as ataxia, seizures, Purkinje cell loss and hypertrophy of granule cells (Backman et al., 2001; Kwon et al., 2006). However, none of the animals developed hamartomas, possibly due to the short life span of this mutants, that was owed to the fact that rather general Cre driver lines targeting primarily astroglial cells were used. Most of the mutants died around 29 weeks (Backman et al., 2001) or between 9 and 48 weeks (Kwon et al., 2001) in consequence of seizures and ataxia. In contrast, our model closely resembles the pathology of human patients, including hamartoma formation, white matter reduction and massive Purkinje cell loss and may contribute in further experiments to a better understanding of this disease. Also a further assessment of the transcriptomic profiles of the mutants including the upregulated soluble factors might be interesting, since they may qualify as specific tumor markers with diagnostic value for LDD.

5. Material and Methods

5.1 Mouse mutants

All experiments were conducted according to the Lower Saxony State regulations for the use of experimental animals in Germany as approved by the Niedersächsisches Landesamt für Verbraucherschutz und Lebensmittelsicherheit (LAVES) and according to UK government animal use regulations. Mice were housed in groups in individually ventilated cages under a 12:12h light/dark cycle with access to food and water *ad libitum*. If not stated otherwise, for molecular, histological, electrophysiological, electron microscopical and biochemical experiments, female and male mice were included in the experiments and were randomly allocated to experimental groups according to age and genotype. All animal experiments were conducted in a single blinded fashion towards the investigator. Inclusion/exclusion criteria were pre-established. Animals were excluded from the experiment when showing impaired health conditions not attributable to genotype or experiment or when the weight difference to the average group weight was larger than 10%. With respect to the outcome assessment, exclusion criteria were determined with Grubbs' test (ESD method), using the statistical software GraphPad (Prism). No animals or samples had to be excluded with these criteria in any of the experiments.

Mice mutant for *Pten*$^{loxP/loxP}$, Tg(mα6-Cre)B1LFR, *Nex-CreERT2, Nrg1*$^{loxP/loxP}$, *Bdnf*$^{loxP/loxP}$, *Plp1-DsRed*, *Rosa26*-lacZ and *Ng2-EYFP* were genotyped as described (Agarwal et al., 2012; Funfschilling and Reichardt, 2002; Hirrlinger et al., 2005; Karram et al., 2008; Lesche et al., 2002; Li et al., 2002; Rauskolb et al., 2010; Soriano, 1999). Tg(mα6-Cre)B1LFR, *Nex-CreERT2, Nrg1*$^{loxP/loxP}$, *Bdnf*$^{loxP/loxP}$, *Plp1-DsRed*, *Rosa26*-lacZ and *Ng2*-EYFP mutants were on C57BL/6N background, whereas *Pten*$^{loxP/loxP}$ mutants and thus all compound mutants harboring *Pten*^{loxP} *alleles* were on mixed C57BL/6N-SV129 background. For genotyping, genomic DNA was isolated from tail biopsies (InvisorbSpin Tissue Mini kit, Invitek) according to the manufacturer's directions and subjected to routine PCR methods.

5.1.1 Genotyping primer for various mouse lines

Pten

sense *5'*-ACTCAAGGCAGGGATGAGC-3'

antisense 5'-CAGAGTTAAGTTTTTGAAGGCAAG-3'

Tg(mα6-Cre)B1LFR

sense 5'-TAGAGCATTAGGGTGGGAG-3'

antisense 5'-TGCCGCCTTTGCAGGTGTGTCTTAC-3'

Nrg1

sense 5'-GCACCAAGTGGTTGCGATTGTTGCT-3'

antisense 5'-TCCTTTTGTGTGTGTTCAGCACCGG-3'

Bdnf

sense 5'-GTTGCGTAAGCTGTCTGTGCACTGTGC-3'

antisense 5'-CAGACTCAGAGGGCACTTTGATGGCTTG-3'

Plp1-DsRed

sense 5'-CGCCGACATCCCCGACTACAA-3'

antisense 5'-GCGGCCGCTACAGGAACAGGT-3'

Rosa26-lacZ

sense 5'-AAAGTCGCTCTGAGTTGTTAT-3'

antisense 5'-GCGAAGAGTTTGTCCTCAACC-3'

Ng2-EYFP

sense 5'-TGACCTTGGATTCTGAGC-3'

antisense 5'-CGCTGAACTTGTGGCCGTTTA-3'

5.2 BrdU labeling

Mice received 5’-bromo-deoxyuridine (BrdU, Sigma Aldrich) by daily intraperitoneal injections (50 µg/g of body weight) for 20 consecutive days. Mice were sacrificed 4 hours post final injection.

5.3 Histology and immunohistochemistry

Mice were anaesthetized with avertin (Sigma–Aldrich) and perfused with 15 ml of Hanks balanced salt solution (HBSS, PAA laboratories, Pasching, Austria) followed by fixative (4% PFA, 0.1M Phosphate buffer, 0.5% NaCl). Paraffin sections of the brain (5 µm) were deparaffinized using xylene and isopropanol and rehydrated in a descending ethanol series. Antigen unmasking was performed by boiling for 10–40 min in citric buffer, pH 6, or Tris EDTA, pH 9. Sections were blocked in 20% goat serum in PBS/BSA for 1 h and incubated with primary antibodies in 5% goat serum in PBS/BSA for 2 h at 37°C or overnight at 4°C. Detection was performed by using Alexa Fluor 488-, 555- and 633-conjugated secondary antibodies (1:1000, Thermo Fisher Scientific, #A-28175, #A-11034, #A-21212, #A-21422, #A-27039 and #A-21094) and by using biotinylated secondary antibodies, followed by diaminobenzidine (DAB) (LSAB2 Kit, Dako, #K0675; Vectastain Kit, Vector Laboratories, #BA-9400, #PK-6100). Primary antibodies were directed against BrdU (1:200, Chemicon, #MAB3424), CAII (1:200, kindly provided by S. Ghandour, Strasbourg, PMID: 118210), Calbindin (1:600, Sigma, #C9848), Caspr (1:100, NeuroMab, #75-001), CD31 (1:100, Dianova, #DIA-310), CNPase (1:150, Sigma, #C5922), $GABA_A$ receptor α6 subunit (1:500, Chemicon, #AB5610), GFAP (1:200, Novocastra, #NCL-GFAP-GA5), Iba1 (1:1000, Wako, #019-19741), MBP (1:200, Covance, #SMI-94R); $Na_V1.6$ (1:500, Alomone Labs, #ASC-009); NeuN (1:200, Chemicon, #MAB377); Olig2 (1:200, kindly provided by J. Alberta, PMID: 15198128), and Mac-3 (1:500, BD Pharmingen, #553322). 5 µm microtome sections (Microm HM400) were also stained by hematoxylin–eosin (HE) to study cytoarchitecture. Myelinated fibers were visualized by Gallyas silver impregnation as described (Lappe-Siefke et al., 2003). All images showing immunohistochemical analyses and stainings were successfully repeated at least three times.

5.4 In situ hybridization

In situ hybridization was performed as described (Bormuth et al., 2013), by our collaborators Kuo Yan and Dr. Ingo Bormuth. A *Myrf* probe corresponding to 941bp from *Myrf* 3' UTR was kindly provided by B. Emery (Jungers Center for Neurosciences Research, Department of Neurology, Oregon USA).

5.5 Electron microscopy

Mice were anaesthetized with avertin (Sigma–Aldrich) and perfused with 15 ml of Hanks balanced salt solution (HBSS, PAA laboratories, Pasching, Austria) followed by fixative (4% PFA, 0.1M Phosphate buffer, 0.5% NaCl, 2.5% glutaraldehyde). At parasagittal plane, cerebellar lobulus 5 was dissected, contrasted with 1% osmium tetraoxide and embedded in epoxy resin. Semi-thin (0.5mm) and ultra-thin (50–60 nm) sections were cut, using a microtome (RM 2155, Leica Microsystems, Wetzlar, Germany) with a diamond knife (Histo HI 4317, Diatome, Biel, Switzerland). Semi-thin sections were stained with azur-II-methylenblue for 1 min at 60°C. Ultra-thin sections were stained with 2% uranylacetate (30 min) and 1% lead citrate solution (12 min) and analysed using a LEO EM912AB electron microscope (Carl Zeiss NTS, Oberkochen, Germany). Images were taken with an on-axis 2048x2048 CCD camera (Proscan, Scheuring, Germany).

5.6 Electrophysiology

Electrophysiology was performed by our collaborators Sonia Spitzer and Ragnhildur Thóra Káradóttir by cuting parasagittal cerebellar slices (225 µm) using a vibrating blade microtome (Leica VT1200S) from P7-P100 *Ng2-EYFP*$^{+/-}$**Tg(mα6)-Cre*Pten*$^{loxP/loxP}$ mice (mutants) and *Ng2-EYFP*$^{+/-}$**Pten* $^{loxP/loxP}$ mice (controls), culled by cervical dislocation in accordance with UK government animal use regulations. After dissection, the brain was placed in a cooled (~1ºC) oxygenated (95% O2–5% CO2) Krebs solution containing (mM): 126 NaCl, 24 NaHCO3, 1 NaH2PO4, 2.5 KCl, 2.5 CaCl2, 2 MgCl2, 10 D-glucose (pH 7.4). In addition, kynurenic acid was included in order to block glutamate receptors, which might be activated during the dissection procedure and cause cell damage. During experiments slices were superfused at 22±1ºC with HEPES- buffered external solution containing (mM): 144 NaCl, 2.5 KCl, 10 HEPES, 1 NaH2PO4, 2.5 CaCl2, 10 glucose, 0.1 glycine (to co-activate NMDA receptors), 0.005 strychnine (to block glycine receptors), pH set to 7.4 with NaOH, bubbled with 100% O2. OPCs were identified by EYFP expression and whole-cell voltage clamped. Recording electrodes had a resistance between 5-9MΩ when filled with an internal solution comprising (mM): 130 K-gluconate, 4 NaCl, 0.5 CaCl2, 10 HEPES, 10 BAPTA, 4 MgATP, 0.5 Na2GTP, 2 K-Lucifer yellow, pH set to 7.3 with KOH and the uncompensated series resistance was 40±1MΩ and electrode junction potentials (- 14mV) were compensated for. A Multiclamp 700B (Molecular Devices) was used for voltage clamp data acquisition. Data were sampled at 50kHz and filtered at 10kHz using pClamp10.3 (Molecular Devices).

5.7 Synaptic current analysis

A synaptic current was defined to occur if its amplitude was bigger than twice the standard deviation of the baseline current noise and its 10-90% decay time was longer than its rise time. Events were detected and analysed with pClamp 10.3 (Molecular Devices) and the Strathclyde Electrophysiology Software package WinEDR V3.3.7 WinWCP V4.6.2.

5.8 Laser-capture microdissection, RNA isolation and linear amplification, and microarray hybridization

Mice were killed at 3 months of age by cervical dislocation, total brains were dissected and frozen on dry ice, protected with parafilm and stored at -80°C. Serial coronal cryosections (20 µm) were prepared using a Leica CM3000 Cryostat, mounted on polyethylene naphthalate membrane frame slides (Arcturus), stained with thionin, and dried in an ascending ethanol/xylene series. For laser-capture microdissection (LCM), a Veritas Microdissection System (Arcturus) was used with slides mounted and stained the same day. Cerebellar GL were dissected by ultraviolet laser (laser power set to 3.2–4.2) and attached to CapSure LCM caps using an infrared laser (power set to 80%). Caps were collected in 0.5 ml Eppendorf tubes containing 100 µl of RNeasy Lysis Buffer (Qiagen) and stored at -80°C. Total RNA was isolated from LCM tissue using the Micro RNeasy Kit (Qiagen) according to the instructions of the manufacturer except that RNA was eluted from the column with 10µl of water followed by precipitation with NaAcetate (pH 5.2, f.c. 0.3M) and PelletPaint (Novagen) as carrier. Two-round amplification and biotin-labeling, hybridization to mouse MOE230A 2.0 genechips (Affymetrix), washing and scanning was essentially as described (Rossner et al., 2006) with 3 biological replicates for each genotype. Data analysis was performed using Genomics Suite (Partek Inc.). Raw data were normalized using the RMA algorithm and differentially expressed genes were identified with ANOVA according to the workflow suggested by the manufacturer (Partek Inc.). Differentially expressed genes with signal intensities in mutants > control were selected with >1.4-fold change and adjusted P-values <0.05.

5.9 RNA isolation, cDNA synthesis, and qRT-PCR.

Total RNA was isolated from LCM tissue using the Transcriptor High Fidelity Kit (Roche) according to the instructions of the manufacturer. cDNA was synthesized using a mixture of random nonamer primers and anchored poly-dT primers and SuperScript III RNase H reverse transcriptase (Invitrogen) according to the instructions of the manufacturer. qRT-

PCR was performed using SYBR green master mix (Applied Biosystems) and a 7500 Fast Real-Time PCR System (Applied Biosystems). Primers were designed using the Roche Universal ProbeLibrary website (http://qpcr.probefinder.com). Relative mRNA concentrations were normalized to Actin and Atp5b. Data were analyzed using qBase software version 1.3.5 (Center for Medical Genetics, Ghent University, Ghent, Belgium).

5.9.1 Quantitative real-time PCR primers

Pten
Forward: 5'-TGGGGAAGTAAGGACCAG -3'
Reverse: 5'-TATCTGCACGCTCTATAC -3'

Neurotensin
Forward: 5'-AGCTGGTGTGCCTGACTCTC -3'
Reverse: 5'-CCAGGGCTCTCACATCTTCT -3'

Fgf1
Forward: 5'-CCGAAGGGCTTTTATACGG -3'
Reverse: 5'-TCTTGGAGGTGTAAGTGTTATAATGG -3'

Pleiotrophin
Forward: 5'-CCTCAAGCGGAGTCAAAGAA -3''
Reverse: 5'-CTTTTCCTGGTCCACAGACG -3'

Timp3
Forward: 5'-CACGGAAGCCTCTGAAAGTC -3'
Reverse: 5'-TCCCACCTCTCCACAAAGTT -3'

Inhba
Forward: 5'-GGGAGTGATCCCTGGAAAC -3'
Reverse: 5'-TCCTCTTCATGGTATTGGCACT -3'

5.10 Mixed myelinating cocultures from mouse spinal cord

Wild-type C57BL/6N mice were time-mated, with the day of plugging denoted as embryonic day 0.5 (E0.5), and embryos were collected on embryonic day 13.5 (E13.5). The spinal cord was dissected, and dissociated mechanically and enzymatically (0.25% trypsin, Invitrogen).

Enzymatic activity was stopped by the addition of plating medium (50% DMEM, 25% horse serum, 25% Hanks balanced salt solution without Ca^{2+} and Mg^{2+}) containing 2.5 µg/ml DNAse I. Cells were dissociated into a single cell suspension by triturating through 20- and 23-gauge needles (4 and 2 times, respectively) and spun at 800 rpm for 5 min. The pellet was resuspended in plating medium. Dissociated spinal cord cells were plated initially onto poly-L-lysine (PLL, in boric acid buffer, pH8.4) coated coverslips at a density of 150.000 cells/100 µl, which were then placed into a 35-mm Petri dish. The cells were left to attach for 2–3 hours, when 150 µl of plating medium and 500 µl of differentiation medium was added. This medium contained DMEM (4,500 mg/L glucose), 10 mg/ml biotin, 0.5% hormone mixture (1 mg/mL apotransferrin, 20 mM putrescine, 4 µM progesterone, and 6 µM selenium), 50 nM hydrocortisone, and 10 µg/ml insulin (all reagents were from Sigma). Cultures were maintained by replacing half of the medium with fresh medium three times a week. After 12 days in culture, cells were fed with differentiation medium with (or without) recombinant human Pdgf (100ng/ml), Sparcl1 (10ng/ml), Vegfc (100ng/ml), Fgf1 (100ng/ml), Ptn (10ng/ml), Timp3 (100ng/ml), Tmsb4x (50ng/ml) or Activin A (100 ng/ml) and reduced concentration of Insulin (0.2 µg/ml). Cultures were maintained for up to 25 days in a humidified atmosphere of 5% CO_2 at 37°C.

5.11 Mixed primary oligodendrocyte cultures

Mixed primary oligodendrocyte cultures were prepared from (7 pooled) spinal cords of P4 mouse pups. Tissue chunks were incubated in 5 ml papain (200U) in papain buffer plus L-cysteine for 1 hour at ~35°C with constant gassing (95% oxygen and 5% carbon dioxide). The papain reaction was stopped with plating medium (30% horse serum in DMEM) containing 2.5 µg/ml DNAse I. Cells were dissociated into a single cell suspension by triturating through 20 and 23 gauge needles (4 and 2 times, respectively), spun at 800 rpm for 5 min, and the pellet was resuspended in plating medium. Cells were plated at a concentration of 80,000 cells/100 µl plating medium onto PLL coated 11 mm diameter glass coverslips, in 35 mm diameter Petri-dishes (2 coverslips/dish). Two hours later, differentiation medium containing DMEM (4,500 mg/L glucose), 10 ng/ml biotin, 0.5% hormone mixture (1 mg/mL apotransferrin, 20 mM putrescine, 4 µM progesterone, and 6 µM selenium), 50 nM hydrocortisone, and 10 µg/ml insulin (all reagents from Sigma) was added to each 35 mm Petri dish to yield a mix of 50% plating medium: 50% differentiation medium. The following day all medium and myelin debris was removed from the coverslips by rinsing briefly in medium, and fresh differentiation medium was added to each 35 mm Petri dish, with or without human recombinant forms of Klotho (400ng/ml), Ptn (10ng/ml),

Timp3 (100ng/ml) or Activin A (100ng/ml). Cells were fed every second day by replacing half the medium with fresh differentiation medium including the recombinant proteins. Cultures were maintained for 3 and 5 days in a humidified atmosphere of 5% CO_2 at 37°C.

5.12 Recombinant proteins

Human recombinant proteins were Sparcl1, Vegfc, Klotho, Timp3, and Activin A (R&D Systems), Pdgf and Ptn (Sigma Aldrich), Tmsb4x (Novus Biologicals) and Fgf1 (Invitrogen). Recombinant proteins were dissolved in ddH_2O. Individual aliquots were thawed only once and diluted in cell culture medium immediately before use. PI3K inhibitor LY294002 and MEK1/2 inhibitor UO126 were from Cell Signaling Technology, SMAD3 inhibitor SIS3 was from Calbiochem.

5.13 Immunocytochemistry

Cells were fixed with 4% PFA for 5 min at 37°C. After fixation, cultures were washed in PBS three times, permeabilized with ice cold methanol for 5 min, and blocked in blocking buffer (2% fish skin gelatin, 2% FCS, 2% BSA in PBS) for 60 min. Primary antibodies (diluted in 10% blocking buffer) were directed against GFAP (1:200, Novocastra, #NCL-GFAP-GA5), KI-67 (1:10, Dako, #M7249), MBP (1:200, Covance, #SMI-94R), Olig2 (1:200, kindly provided by J. Alberta, PMID: 15198128) SMI31 (1:1000, Covance, #SMI-31P), and APC-CC1 (1:100, Calbiochem, #OP80) and incubated overnight at 4°C. Coverslips were washed in PBS three times. Corresponding secondary Alexa Fluor 488-, 555- and 633-conjunated antibodies (1:1000, Thermo Fisher Scientific, #A-28175, #A-21422, #A-27039 and #A-21094) were diluted in 10% blocking buffer and added for 1 h. Coverslips were washed in ddH_2O three times and mounted in Aqua-Poly/Mount (Polysciences).

5.14 Morphometry

Digitized overlapping light microscopic images (20x) were fused to a continuous image of a complete parasagittal cerebellum (Lateral, 0.12 mm) by using Zeiss Zen software and analyzed for absolute numbers of CNP+, CAII+, Olig2+, Iba1+, Mac-3+, and BrdU+ cells. The number of Iba1+ and Mac-3+ cells was normalized to the area of ML and GL, respectively. Endothelial cells positive for CD31 were traced with ImageJ and normalized to the area of the ML. To quantify MBP+ and GFAP+ areas, two ImageJ plugins for semi-automated analysis were implemented (“MBP” and “GFAP” can be found on the included

CD-ROM). Average diameter of hippocampal CA3 neuronal cell bodies of *Nex-CreERT2*Pten*$^{loxP/loxP}$ mice was determined by using ImageJ software. Two independent sections per mouse and staining were quantified. In cell culture experiments, the differentiation and proliferation state of oligodendrocyte lineage cells was analyzed within the given fields of 11 randomly taken images (20x) per coverslip (mixed myelinating cultures: myelination assay, 3-11 independent experiments with 2 coverslips per condition; proliferation assay, 3-11 independent experiments with 1 coverslip per condition; mixed primary oligodendrocyte cultures: 3-5 independent experiments with 2 coverslips per condition). For quantitative assessment of *in vitro* myelination a "myelination index" was calculated by dividing the MBP+ area (as identified by generating a "mask" outlining the myelin sheaths; "CoCultureMBP", can be found on the included CD-ROM). by the axonal area (Smi31+ axons; "CoCultureSmi31", can be found on the included CD-ROM). For the proliferation assay the percentage of semi-automatically quantified Olig2$^+$ cells was determined in relation to all DAPI+ cells ("CoCultureOlig2 and "CoCultureDAPI", can be found on the included CD-ROM) and the number of Ki67$^+$, Olig2$^+$ cells was set in relation to the total number of Olig2$^+$ cells. For the differentiation assay, the percentage of postmitotic oligodendrocytes was determined by quantifying and dividing the numbers of CC1$^+$ cells by the total number of Olig2$^+$ oligodendrocyte lineage cells. All analyses were performed in a single blinded fashion towards the investigator who was unaware of the treatment regimen.

5.15 G-ratio measurement

Digitized images (magnification 7000x) of ultrathin cerebellum lobe 5 sections were used to determine the numbers of myelinated axons, axon calibers and g-ratios (>100 randomly chosen myelinated axons in the molecular layer). g-ratios were determined by dividing the inner myelin diameter by the diameter of the entire fiber. Quantitations were performed from ≥3 age-matched male mice per genotype and age.

5.16 Protein analysis

Cerebellum lysates were homogenized in lysis-buffer (50 mM HEPES, pH 7.5, 150 mM NaCl, 1.5 mM MgCl2, 5 mM EGTA, 10% glycerol, 1% triton X-100, 2mM Na3VO4) containing phosphatase (Phos*STOP* Inhibitor Cocktail, Roche, Basel, Switzerland) and protease (Complete tablets, Roche, Basel, Switzerland) inhibitors using an Ultraturrax (T8, Ika, Staufen, Germany) at highest settings (30–60 s). After incubation for 15 min on ice insoluble material was removed by centrifugation at 16.000 g, 4°C for 15 min. For

Westernblot analysis, 10 µg of protein lysate was size-separated on 12% of SDS-polyacrylamide gels and blotted onto PVDF membranes (HybondTM-P, Amersham Biosciences, UK) by Bio-Rad western blotting method. Membranes were blocked in 5% milk powder (in PBS) for 1h at room temperature. Primary antibodies were directed against p-AKT (Cell Signaling, mRb, 1:1000, #4060), AKT (Cell Signaling, mRb, 1:1000, #4691), PTEN (Cell Signaling, mRb, 1:1000, #9188), p-PDK1 (Cell Signaling, mRb, 1:1000, #3438), p-mTOR (Cell Signaling, mRb, 1:1000, #5536), p-S6 (Cell Signaling, mRb, 1:1000, #4858), and Actin (Sigma–Aldrich, mM, 1:1000, #A3853). Antibodies were diluted in blocking buffer and incubated overnight at 4°C. Membranes were washed 3 x 10 min in TBS-T buffer (50 mM Tris-HCl, pH 7.4, 150 mM NaCl and 0.05% Tween-20), followed by an incubation with horse-radish peroxidase-conjugated secondary antibodies (1:5000, Dianova, #111-035-003, #115-035-003). After three more washing steps with TBS-T buffer, immunoreactive proteins were detected with an enhanced chemiluminescence kit (Western LightningTM, Westernblot Chemiluminescence Reagent Plus, PerkinElmer Life Sciences, Waltham, MA) according to the manufacturer's instructions.

5.17 Statistical analysis

For Power analysis the software G*Power Version 3.1.7. was used. Power analyses were performed before conducting experiments (a priori). Adequate Power (1 – beta-error) was defined as ≥ 80% and the alpha error as 5%. The sample size was calculated with the following pre-specified effect sizes: 1. mRNA expression analysis: effect size d of approximately 2.5 (estimated mean difference of 50% and standard deviation of 15%). 2. Analysis of mature oligodendrocyte numbers in GL (effect size d of approximately 3.5, estimated mean difference of 30% and standard deviation of 10%) and ML (effect size d of approximately 6.5, estimated mean difference of 400% and standard deviation of 30%) and myelinated area in the ML of wildtype and *Pten* mutants (effect size d of approximately 6.0, estimated mean difference of 170% and standard deviation of 40%). 3. Proliferation analysis of oligodendrocyte lineage cells: effect size d of approximately 9.0 (estimated mean difference of 330% and standard deviation of 15%). 4. *In vivo* analysis of candidate genes. Analysis of mature oligodendrocyte numbers: effect size d of approximately 5.5 (estimated mean difference of 30% and standard deviation of 15%). Analysis of myelinated area: effect size d of approximately 4.0 (estimated mean difference of 30% and standard deviation of 13%). Proliferation analysis of oligodendrocyte lineage cells: effect size d of approximately 3.5 (estimated mean difference of 20% and standard deviation of 10%). Analysis of (i) myelinated and (ii) unmyelinated pf diameters: (i) effect size d of approximately 2.6 (estimated mean difference of 20% and standard deviation of 13%). (ii) Effect size d of

approximately 1.5 (estimated mean difference of 15% and standard deviation of 13%). G-ratio analysis: effect size d of approximately 4.5 (estimated mean difference of 6% and standard deviation of 2%). 5. Microglia (ML: Effect size d of approximately 4.7, estimated mean difference of 100% and standard deviation of 20%; GL: effect size d of approximately 1.2, estimated mean difference of 10% and standard deviation of 5%), astrocytes (ML: effect size d of approximately 4.0, estimated mean difference of 150% and standard deviation of 15%; GL: effect size d of approximately 1.3, estimated mean difference of 10% and standard deviation of 5%) and vascular endothelia cells (effect size d of approximately 3.7, estimated mean difference of 40% and standard deviation of 15%) in *Pten* mutant mice. 6. Microglia (ML: effect size d of approximately 1.0, estimated mean difference of 10% and standard deviation of 9%; GL: effect size d of approximately 1.3, estimated mean difference of 10% and standard deviation of 7%) and astrocytes (ML: effect size d of approximately 1.2, estimated mean difference of 20% and standard deviation of 15%; GL: effect size d of approximately 1.1, estimated mean difference of 10% and standard deviation of 5%) in *NEX-CreERT2*Pten*$^{loxP/loxP}$ mice. 7. Average diameter of hippocampal CA3 neuronal cell bodies from *Nex-CreERT2*Pten*$^{loxP/loxP}$ mice: effect size d of approximately 12.0 (estimated mean difference of 25% and standard deviation of 2%) 8. *In vitro* analysis of candidate factors. Analysis of oligodendrocyte lineage cell numbers: effect size d of approximately 4.0 (estimated mean difference of 80% and standard deviation of 30%). Proliferation analysis: effect size d of approximately 2.3 (estimated mean difference of 60% and standard deviation of 36%). Myelination index: effect size d of approximately 2.0 (estimated mean difference of 65% and standard deviation of 50%). Analysis of oligodendrocyte differentiation: effect size d of approximately 9.0 (estimated mean difference of 40% and standard deviation of 10%). For electrophysiology experiments we determined the sample size by utilizing previous data distributions.

Data are expressed as means +/- s.e.m. In order to select appropriate statistical tests all data have been tested for normal distribution with Kolmogorov-Smirnov test or Shapiro-Wilk test. For normally distributed data with comparable variances we used two-tailed unpaired Student's t-tests and Chi-square tests to determine the statistical significance between two groups. For data not showing normal distribution or in case that no normality test could be conducted the nonparametric Wilcoxon matched pairs test was applied. Data sets containing more than two groups were tested by applying analysis of variance (ANOVA) and Bonferroni post hoc test. Analysis of co-variance (ANCOVA) was used to analyse the differences between slopes of regression lines. Applied statistical tests are indicated in the respective figure legends. Statistical differences were considered significant when $p<0.05$

(*p<0.05, **p<0.01, ***p<0.001) and tests and fitting of regression lines were performed by using GraphPad (Prism) and MS Excel.

6. References

Acheson, A., Conover, J.C., Fandl, J.P., Dechiara, T.M., Russell, M., Thadani, A., Squinto, S.P., Yancopoulos, G.D., and Lindsay, R.M. (1995). A Bdnf Autocrine Loop in Adult Sensory Neurons Prevents Cell Death. Nature 374, 450-453.

Agarwal, A., Dibaj, P., Kassmann, C.M., Goebbels, S., Nave, K.A., and Schwab, M.H. (2012). In vivo imaging and noninvasive ablation of pyramidal neurons in adult NEX-CreERT2 mice. Cereb Cortex 22, 1473-1486.

Aguayo, A.J., Charron, L., and Bray, G.M. (1976). Potential of Schwann cells from unmyelinated nerves to produce myelin: a quantitative ultrastructural and radiographic study. J Neurocytol 5, 565-573.

Arai, K., and Lo, E.H. (2009). An oligovascular niche: cerebral endothelial cells promote the survival and proliferation of oligodendrocyte precursor cells. J Neurosci 29, 4351-4355.

Arroyo, E.J., and Scherer, S.S. (2000). On the molecular architecture of myelinated fibers. Histochem Cell Biol 113, 1-18.

Backman, S.A., Stambolic, V., Suzuki, A., Haight, J., Elia, A., Pretorius, J., Tsao, M.S., Shannon, P., Bolon, B., Ivy, G.O., and Mak, T.W. (2001). Deletion of Pten in mouse brain causes seizures, ataxia and defects in soma size resembling Lhermitte-Duclos disease. Nat Genet 29, 396-403.

Bansal, R. (2002). Fibroblast growth factors and their receptors in oligodendrocyte development: Implications for demyelination and remyelination. Dev Neurosci-Basel 24, 35-46.

Bansal, R., Kumar, M., Murray, K., Morrison, R.S., and Pfeiffer, S.E. (1996). Regulation of FGF receptors in the oligodendrocyte lineage. Molecular and Cellular Neuroscience 7, 263-275.

Barmack, N.H., and Yakhnitsa, V. (2011). Topsy Turvy: Functions of Climbing and Mossy Fibers in the Vestibulo-Cerebellum. Neuroscientist 17, 221-236.

Baron, W., Colognato, H., and Ffrench-Constant, C. (2005). Integrin-growth factor interactions,as regulators of oligodendroglial development and function. Glia 49, 467-479.

Barres, B.A., Jacobson, M.D., Schmid, R., Sendtner, M., and Raff, M.C. (1993). Does Oligodendrocyte Survival Depend on Axons. Current Biology 3, 489-497.

Barres, B.A., and Raff, M.C. (1993). Proliferation of Oligodendrocyte Precursor Cells Depends on Electrical-Activity in Axons. Nature 361, 258-260.

Barres, B.A., and Raff, M.C. (1994). Control of Oligodendrocyte Number in the Developing Rat Optic-Nerve. Neuron 12, 935-942.

Barres, B.A., and Raff, M.C. (1999). Axonal control of oligodendrocyte development. Journal of Cell Biology 147, 1123-1128.

Bauer, N.M., Moos, C., van Horssen, J., Witte, M., van der Valk, P., Altenhein, B., Luhmann, H.J., and White, R. (2012). Myelin basic protein synthesis is regulated by small non-coding RNA 715. EMBO Rep 13, 827-834.

Baumann, N., and Pham-Dinh, D. (2001). Biology of oligodendrocyte and myelin in the mammalian central nervous system. Physiol Rev 81, 871-927.

Beck, K.D., Powellbraxton, L., Widmer, H.R., Valverde, J., and Hefti, F. (1995). Igf1 Gene Disruption Results in Reduced Brain Size, Cns Hypomyelination, and Loss of Hippocampal Granule and Striatal Parvalbumin-Containing Neurons. Neuron 14, 717-730.

Becker-Catania, S.G., Nelson, J.K., Olivares, S., Chen, S.J., and DeVries, G.H. (2011). Oligodendrocyte progenitor cells proliferate and survive in an immature state following treatment with an axolemma-enriched fraction. Asn Neuro 3, 51-67.

Bercury, K.K., and Macklin, W.B. (2015). Dynamics and Mechanisms of CNS Myelination. Dev Cell 32, 447-458.

Bergles, D.E., and Richardson, W.D. (2016). Oligodendrocyte Development and Plasticity. Csh Perspect Biol 8.

Blumenthal, G.M., and Dennis, P.A. (2008). PTEN hamartoma tumor syndromes. Eur J Hum Genet 16, 1289-1300.

Boespflug-Tanguy, O., Labauge, P., Fogli, A., and Vaurs-Barriere, C. (2008). Genes involved in leukodystrophies: a glance at glial functions. Curr Neurol Neurosci Rep 8, 217-229.

Boison, D., Bussow, H., D'Urso, D., Muller, H.W., and Stoffel, W. (1995). Adhesive properties of proteolipid protein are responsible for the compaction of CNS myelin sheaths. J Neurosci 15, 5502-5513.

Bormuth, I., Yan, K., Yonemasu, T., Gummert, M., Zhang, M., Wichert, S., Grishina, O., Pieper, A., Zhang, W., Goebbels, S*., et al.* (2013). Neuronal basic helix-loop-helix proteins Neurod2/6 regulate cortical commissure formation before midline interactions. J Neurosci 33, 641-651.

Brinkmann, B.G., Agarwal, A., Sereda, M.W., Garratt, A.N., Mueller, T., Wende, H., Stassart, R.M., Nawaz, S., Humml, C., Velanac, V*., et al.* (2008). Neuregulin-1/ErbB signaling serves distinct functions in myelination of the peripheral and central nervous system. Neuron 59, 581-595.

Bujalka, H., Koenning, M., Jackson, S., Perreau, V.M., Pope, B., Hay, C.M., Mitew, S., Hill, A.F., Lu, Q.R., Wegner, M*., et al.* (2013). MYRF Is a Membrane-Associated Transcription Factor That Autoproteolytically Cleaves to Directly Activate Myelin Genes. Plos Biol 11.

Burne, J.F., Staple, J.K., and Raff, M.C. (1996). Glial cells are increased proportionally in transgenic optic nerves with increased numbers of axons. Journal of Neuroscience 16, 2064-2073.

Cantley, L.C., and Neel, B.G. (1999). New insights into tumor suppression: PTEN suppresses tumor formation by restraining the phosphoinositide 3-kinase AKT pathway. P Natl Acad Sci USA 96, 4240-4245.

Carson, M.J., Behringer, R.R., Brinster, R.L., and McMorris, F.A. (1993). Insulin-like growth factor I increases brain growth and central nervous system myelination in transgenic mice. Neuron 10, 729-740.

Chen, C.D., Sloane, J.A., Li, H., Aytan, N., Giannaris, E.L., Zeldich, E., Hinman, J.D., Dedeoglu, A., Rosene, D.L., Bansal, R*., et al.* (2013). The antiaging protein Klotho

enhances oligodendrocyte maturation and myelination of the CNS. J Neurosci 33, 1927-1939.

Chong, S.Y., Rosenberg, S.S., Fancy, S.P., Zhao, C., Shen, Y.A., Hahn, A.T., McGee, A.W., Xu, X., Zheng, B., Zhang, L.I.*, et al.* (2012). Neurite outgrowth inhibitor Nogo-A establishes spatial segregation and extent of oligodendrocyte myelination. Proc Natl Acad Sci U S A 109, 1299-1304.

Crocker, S.J., Whitmire, J.K., Frausto, R.F., Chertboonmuang, P., Soloway, P.D., Whitton, J.L., and Campbell, I.L. (2006). Persistent macrophage/microglial activation and myelin disruption after experimental autoimmune encephalomyelitis in tissue inhibitor of metalloproteinase-1-deficient mice. Am J Pathol 169, 2104-2116.

Cruciat, C.M., and Niehrs, C. (2013). Secreted and transmembrane wnt inhibitors and activators. Cold Spring Harb Perspect Biol 5, a015081.

Czopka, T., Ffrench-Constant, C., and Lyons, D.A. (2013). Individual Oligodendrocytes Have Only a Few Hours in which to Generate New Myelin Sheaths In Vivo. Dev Cell 25, 599-609.

Demerens, C., Stankoff, B., Logak, M., Anglade, P., Allinquant, B., Couraud, F., Zalc, B., and Lubetzki, C. (1996). Induction of myelination in the central nervous system by electrical activity. P Natl Acad Sci USA 93, 9887-9892.

Deshmukh, V.A., Tardif, V., Lyssiotis, C.A., Green, C.C., Kerman, B., Kim, H.J., Padmanabhan, K., Swoboda, J.G., Ahmad, I., Kondo, T.*, et al.* (2013). A regenerative approach to the treatment of multiple sclerosis. Nature 502, 327-332.

Do, T.V., Kubba, L.A., Antenos, M., Rademaker, A.W., Sturgis, C.D., and Woodruff, T.K. (2008). The role of activin A and Akt/GSK signaling in ovarian tumor biology. Endocrinology 149, 3809-3816.

Dubois-Dalcq, M., Behar, T., Hudson, L., and Lazzarini, R.A. (1986). Emergence of three myelin proteins in oligodendrocytes cultured without neurons. J Cell Biol 102, 384-392.

Duncan, I.D., and Hoffman, R.L. (1997). Schwann cell invasion of the central nervous system of the myelin mutants (vol 190, pg 35, 1996). J Anat 191, 318-319.

Dupouey, P., Jacque, C., Bourre, J.M., Cesselin, F., Privat, A., and Baumann, N. (1979). Immunochemical Studies of Myelin Basic-Protein in Shiverer Mouse Devoid of Major Dense Line of Myelin. Neuroscience Letters 12, 113-118.

Eiraku, M., Hirata, Y., Takeshima, H., Hirano, T., and Kengaku, M. (2002). Delta/Notch-like epidermal growth factor (EGF)-related receptor, a novel EGF-like ReDeat-cont ining protein T ryeted to dendrites of developing and adult central nervous system neurons. J Biol Chem 277, 25400-25407.

Elde, R., Cao, Y., Cintra, A., Brelje, T.C., Peltohuikko, M., Junttila, T., Fuxe, K., Pettersson, R.F., and Hokfelt, T. (1991). Prominent Expression of Acidic Fibroblast Growth-Factor in Motor and Sensory Neurons. Neuron 7, 349-364.

Eng, C. (2000). Will the real Cowden syndrome please stand up: revised diagnostic criteria. Journal of Medical Genetics 37, 828-830.

Engele, J., and Bohn, M.C. (1992). Effects of Acidic and Basic Fibroblast Growth-Factors (Afgf, Bfgf) on Glial Precursor Cell-Proliferation - Age Dependency and Brain Region Specificity. Developmental Biology 152, 363-372.

Flores, A.I., Narayanan, S.P., Morse, E.N., Shick, H.E., Yin, X., Kidd, G., Avila, R.L., Kirschner, D.A., and Macklin, W.B. (2008). Constitutively active Akt induces enhanced myelination in the CNS. J Neurosci 28, 7174-7183.

Fortin, D., Rom, E., Sun, H.J., Yayon, A., and Bansal, R. (2005). Distinct fibroblast growth factor (FGF)/FGF receptor signaling pairs initiate diverse cellular responses in the oligodendrocyte lineage. Journal of Neuroscience 25, 7470-7479.

Franklin, R.J., and Ffrench-Constant, C. (2008). Remyelination in the CNS: from biology to therapy. Nat Rev Neurosci 9, 839-855.

Fraser, M.M., Zhu, X.Y., Kwon, C.H., Uhlmann, E.J., Gutmann, D.H., and Baker, S.J. (2004). Pten loss causes hypertrophy and increased proliferation of astrocytes in vivo. Cancer Res 64, 7773-7779.

Funfschilling, U., and Reichardt, L.F. (2002). Cre-mediated recombination in rhombic lip derivatives. Genesis 33, 160-169.

Funfschilling, U., Supplie, L.M., Mahad, D., Boretius, S., Saab, A.S., Edgar, J., Brinkmann, B.G., Kassmann, C.M., Tzvetanova, I.D., Mobius, W.*, et al.* (2012). Glycolytic oligodendrocytes maintain myelin and long-term axonal integrity. Nature 485, 517-521.

Furusho, M., Dupree, J.L., Nave, K.A., and Bansal, R. (2012). Fibroblast Growth Factor Receptor Signaling in Oligodendrocytes Regulates Myelin Sheath Thickness. Journal of Neuroscience 32, 6631-6641.

Gallyas, F. (1979). Silver staining of myelin by means of physical development. Neurol Res 1, 203-209.

Genoud, S., Lappe-Siefke, C., Goebbels, S., Radtke, F., Aguet, M., Scherer, S.S., Suter, U., Nave, K.A., and Mantei, N. (2002). Notch1 control of oligodendrocyte differentiation in the spinal cord. Journal of Cell Biology 158, 709-718.

Gibson, E.M., Purger, D., Mount, C.W., Goldstein, A.K., Lin, G.L., Wood, L.S., Inema, I., Miller, S.E., Bieri, G., Zuchero, J.B.*, et al.* (2014). Neuronal Activity Promotes Oligodendrogenesis and Adaptive Myelination in the Mammalian Brain. Science 344, 487-+.

Giorgianni, A., Pellegrino, C., De Benedictis, A., Mercuri, A., Baruzzi, F., Minotto, R., Tabano, A., and Balbi, S. (2013). Lhermitte-Duclos Disease: A Case Report. The neuroradiology journal 26, 655-660.

Givogri, M.I., Costa, R.M., Schonmann, V., Silva, A.J., Campagnoni, A.T., and Bongarzone, E.R. (2002). Central nervous system myelination in mice with deficient expression of notch1 receptor. Journal of Neuroscience Research 67, 309-320.

Goebbels, S., Oltrogge, J.H., Kemper, R., Heilmann, I., Bormuth, I., Wolfer, S., Wichert, S.P., Mobius, W., Liu, X., Lappe-Siefke, C.*, et al.* (2010). Elevated phosphatidylinositol 3,4,5-trisphosphate in glia triggers cell-autonomous membrane wrapping and myelination. J Neurosci 30, 8953-8964.

Goebbels, S., Oltrogge, J.H., Wolfer, S., Wieser, G.L., Nientiedt, T., Pieper, A., Ruhwedel, T., Groszer, M., Sereda, M.W., and Nave, K.A. (2012). Genetic disruption of Pten in a novel mouse model of tomaculous neuropathy. Embo Mol Med 4, 486-499.

Gomezpinilla, F., Lee, J.W.K., and Cotman, C.W. (1992). Basic Fgf in Adult-Rat Brain - Cellular-Distribution and Response to Entorhinal Lesion and Fimbria Fornix Transection. Journal of Neuroscience 12, 345-355.

Groszer, M., Erickson, R., Scripture-Adams, D.D., Lesche, R., Trumpp, A., Zack, J.A., Kornblum, H.I., Liu, X., and Wu, H. (2001). Negative regulation of neural stem/progenitor cell proliferation by the Pten tumor suppressor gene in vivo. Science 294, 2186-2189.

Harrison, C.A., Gray, P.C., Vale, W.W., and Robertson, D.M. (2005). Antagonists of activin signaling: mechanisms and potential biological applications. Trends Endocrin Met 16, 73-78.

He, L., and Lu, Q.R. (2013). Coordinated control of oligodendrocyte development by extrinsic and intrinsic signaling cues. Neurosci Bull 29, 129-143.

Hemmings, B.A., and Restuccia, D.F. (2015). The PI3K-PKB/Akt Pathway (vol 4, a011189, 2012). Csh Perspect Biol 7.

Hildebrand, C., Remahl, S., Persson, H., and Bjartmar, C. (1993). Myelinated nerve fibres in the CNS. Prog Neurobiol 40, 319-384.

Hirrlinger, P.G., Scheller, A., Braun, C., Quintela-Schneider, M., Fuss, B., Hirrlinger, J., and Kirchhoff, F. (2005). Expression of reef coral fluorescent proteins in the central nervous system of transgenic mice. Mol Cell Neurosci 30, 291-303.

Hsieh, J., Aimone, J.B., Kaspar, B.K., Kuwabara, T., Nakashima, K., and Gage, F.H. (2004). IGF-1 instructs multipotent adult neural progenitor cells to become oligodendrocytes. Journal of Cell Biology 164, 111-122.

Hu, X.Y., Hicks, C.W., He, W.X., Wong, P., Macklin, W.B., Trapp, B.D., and Yan, R.Q. (2006). Bace1 modulates myelination in the central and peripheral nervous system. Nature Neuroscience 9, 1520-1525.

Hu, Y.Z., Geng, F.J., Tao, L.X., Hu, N., Du, F.L., Fu, K.A., and Chen, F.Y. (2011). Enhanced White Matter Tracts Integrity in Children With Abacus Training. Hum Brain Mapp 32, 10-21.

Huang, E.J., and Reichardt, L.F. (2001). Neurotrophins: Roles in neuronal development and function. Annu Rev Neurosci 24, 677-736.

Ifergan, I., Kebir, H., Terouz, S., Alvarez, J.I., Lecuyer, M.A., Gendron, S., Bourbonniere, L., Dunay, I.R., Bouthillier, A., Moumdjian, R.*, et al.* (2011). Role of Ninjurin-1 in the migration of myeloid cells to central nervous system inflammatory lesions. Ann Neurol 70, 751-763.

Inoue, K., Osaka, H., Sugiyama, N., Kawanishi, C., Onishi, H., Nezu, A., Kimura, K., Yamada, Y., and Kosaka, K. (1996). A duplicated PLP gene causing Pelizaeus-Merzbacher disease detected by comparative multiplex PCR. Am J Hum Genet 59, 32-39.

Irvine, K.A., and Blakemore, W.F. (2008). Remyelination protects axons from demyelination-associated axon degeneration. Brain 131, 1464-1477.

Ishibashi, T., Dakin, K.A., Stevens, B., Lee, P.R., Kozlov, S.V., Stewart, C.L., and Fields, R.D. (2006). Astrocytes promote myelination in response to electrical impulses. Neuron 49, 823-832.

Ishii, A., Furusho, M., and Bansal, R. (2013). Sustained activation of ERK1/2 MAPK in oligodendrocytes and schwann cells enhances myelin growth and stimulates oligodendrocyte progenitor expansion. J Neurosci 33, 175-186.

Ito, M. (2006). Cerebellar circuitry as a neuronal machine. Prog Neurobiol 78, 272-303.

Jessen, K.R., and Mirsky, R. (2005). The origin and development of glial cells in peripheral nerves. Nat Rev Neurosci 6, 671-682.

Karadottir, R., and Attwell, D. (2007). Neurotransmitter receptors in the life and death of oligodendrocytes. Neuroscience 145, 1426-1438.

Karadottir, R.T., and Stockley, J.H. (2012). Deconstructing myelination: it all comes down to size. Nat Methods 9, 883-884.

Karram, K., Goebbels, S., Schwab, M., Jennissen, K., Seifert, G., Steinhauser, C., Nave, K.A., and Trotter, J. (2008). NG2-expressing cells in the nervous system revealed by the NG2-EYFP-knockin mouse. Genesis 46, 743-757.

Katsanos, G.S., Anogianaki, A., Castellani, M.L., Ciampoli, C., De Amicis, D., Orso, C., Pollice, R., Vecchiet, J., Tete, S., Salini, V.*, et al.* (2008). Biology of neurotensin: revisited study. Int J Immunopathol Pharmacol 21, 255-259.

Kettenmann, H., and Ransom, B.R. (2005). Neuroglia, 2nd edn (New York: Oxford University Press).

Kettenmann, H., and Verkhratsky, A. (2011). [Neuroglia--living nerve glue]. Fortschr Neurol Psychiatr 79, 588-597.

Kingsley, D.M. (1994). The Tgf-Beta Superfamily - New Members, New Receptors, and New Genetic Tests of Function in Different Organisms. Gene Dev 8, 133-146.

Kirby, B.B., Takada, N., Latimer, A.J., Shin, J., Carney, T.J., Kelsh, R.N., and Appel, B. (2006). In vivo time-lapse imaging shows dynamic oligodendrocyte progenitor behavior during zebrafish development. Nature Neuroscience 9, 1506-1511.

Klugmann, M., Schwab, M.H., Puhlhofer, A., Schneider, A., Zimmermann, F., Griffiths, I.R., and Nave, K.A. (1997). Assembly of CNS myelin in the absence of proteolipid protein. Neuron 18, 59-70.

Kretschmer, P.J., Fairhurst, J.L., Decker, M.M., Chan, C.P., Gluzman, Y., Bohlen, P., and Kovesdi, I. (1991). Cloning, Characterization and Developmental Regulation of Two Members of a Novel Human Gene Family of Neurite Outgrowth-Promoting Proteins. Growth Factors 5, 99-114.

Kuboyama, K., Fujikawa, A., Suzuki, R., and Noda, M. (2015). Inactivation of Protein Tyrosine Phosphatase Receptor Type Z by Pleiotrophin Promotes Remyelination through Activation of Differentiation of Oligodendrocyte Precursor Cells. Journal of Neuroscience 35, 12162-12171.

Kwon, C.H., Luikart, B.W., Powell, C.M., Zhou, J., Matheny, S.A., Zhang, W., Li, Y., Baker, S.J., and Parada, L.F. (2006). Pten regulates neuronal arborization and social interaction in mice. Neuron 50, 377-388.

Kwon, C.H., Zhu, X.Y., Zhang, J.Y., Knoop, L.L., Tharp, R., Smeyne, R.J., Eberhart, C.G., Burger, P.C., and Baker, S.J. (2001). Pten regulates neuronal soma size: a mouse model of Lhermitte-Duclos disease. Nature Genetics 29, 404-411.

Lange, W. (1976). The myelinated parallel fibers of the cerebellar cortex and their regional distribution. Cell and Tissue Research 166, 489-496.

Laplante, M., and Sabatini, D.M. (2012). mTOR signaling in growth control and disease. Cell 149, 274-293.

Lappe-Siefke, C., Goebbels, S., Gravel, M., Nicksch, E., Lee, J., Braun, P.E., Griffiths, I.R., and Nave, K.A. (2003). Disruption of Cnp1 uncouples oligodendroglial functions in axonal support and myelination. Nat Genet 33, 366-374.

Lau, L.W., Cua, R., Keough, M.B., Haylock-Jacobs, S., and Yong, V.W. (2013). Pathophysiology of the brain extracellular matrix: a new target for remyelination. Nat Rev Neurosci 14, 722-729.

Le Bras, B., Barallobre, M.J., Homman-Ludiye, J., Ny, A., Wyns, S., Tammela, T., Haiko, P., Karkkainen, M.J., Yuan, L., Muriel, M.P.*, et al.* (2006). VEGF-C is a trophic factor for neural progenitors in the vertebrate embryonic brain. Nat Neurosci 9, 340-348.

Lee, S., Chong, S.Y.C., Tuck, S.J., Corey, J.M., and Chan, J.R. (2013). A rapid and reproducible assay for modeling myelination by oligodendrocytes using engineered nanofibers. Nat Protoc 8, 771-782.

Lee, S., Leach, M.K., Redmond, S.A., Chong, S.Y., Mellon, S.H., Tuck, S.J., Feng, Z.Q., Corey, J.M., and Chan, J.R. (2012). A culture system to study oligodendrocyte myelination processes using engineered nanofibers. Nat Methods 9, 917-922.

Lesche, R., Groszer, M., Gao, J., Wang, Y., Messing, A., Sun, H., Liu, X., and Wu, H. (2002). Cre/loxP-mediated inactivation of the murine Pten tumor suppressor gene. Genesis 32, 148-149.

Levimontalcini, R., and Angeletti, P.U. (1968). Nerve Growth Factor. Physiological Reviews 48, 534-+.

Li, J., Yen, C., Liaw, D., Podsypanina, K., Bose, S., Wang, S.I., Puc, J., Miliaresis, C., Rodgers, L., McCombie, R.*, et al.* (1997). PTEN, a putative protein tyrosine phosphatase gene mutated in human brain, breast, and prostate cancer. Science 275, 1943-1947.

Li, L., Cleary, S., Mandarano, M.A., Long, W., Birchmeier, C., and Jones, F.E. (2002). The breast proto-oncogene, HRGalpha regulates epithelial proliferation and lobuloalveolar development in the mouse mammary gland. Oncogene 21, 4900-4907.

Li, Q., Brus-Ramer, M., Martin, J.H., and McDonald, J.W. (2010). Electrical stimulation of the medullary pyramid promotes proliferation and differentiation of oligodendrocyte progenitor cells in the corticospinal tract of the adult rat. Neurosci Lett 479, 128-133.

Lin, S.C., and Bergles, D.E. (2004). Synaptic signaling between neurons and glia. Glia 47, 290-298.

Mangin, J.M., Li, P., Scafidi, J., and Gallo, V. (2012). Experience-dependent regulation of NG2 progenitors in the developing barrel cortex. Nat Neurosci 15, 1192-1194.

Matsuyama, A., Iwata, H., Okumura, N., Yoshida, S., Imaizumi, K., Lee, Y., Shiraishi, S., and Shiosaka, S. (1992). Localization of Basic Fibroblast Growth Factor-Like Immunoreactivity in the Rat-Brain. Brain Research 587, 49-65.

Matthews, M.A. (1968). An electron microscopic study of the relationship between axon diameter and the initiation of myelin production in the peripheral nervous system. The Anatomical Record 161, 337-351.

Matthews, M.A., and Duncan, D. (1971). A quantitative study of morphological changes accompanying the initiation and progress of myelin production in the dorsal funiculus of the rat spinal cord. J Comp Neurol 142, 1-22.

McKenzie, I.A., Ohayon, D., Li, H.L., de Faria, J.P., Emery, B., Tohyama, K., and Richardson, W.D. (2014). Motor skill learning requires active central myelination. Science 346, 318-322.

Mcmorris, F.A., Smith, T.M., Desalvo, S., and Furlanetto, R.W. (1986). Insulin-Like Growth Factor-I Somatomedin-C - a Potent Inducer of Oligodendrocyte Development. P Natl Acad Sci USA 83, 822-826.

Mei, F., Fancy, S.P., Shen, Y.A., Niu, J., Zhao, C., Presley, B., Miao, E., Lee, S., Mayoral, S.R., Redmond, S.A.*, et al.* (2014). Micropillar arrays as a high-throughput screening platform for therapeutics in multiple sclerosis. Nat Med 20, 954-960.

Michailov, G.V., Sereda, M.W., Brinkmann, B.G., Fischer, T.M., Haug, B., Birchmeier, C., Role, L., Lai, C., Schwab, M.H., and Nave, K.A. (2004). Axonal neuregulin-1 regulates myelin sheath thickness. Science 304, 700-703.

Miller, D.J., Duka, T., Stimpson, C.D., Schapiro, S.J., Baze, W.B., McArthur, M.J., Fobbs, A.J., Sousa, A.M.M., Sestan, N., Wildman, D.E.*, et al.* (2012). Prolonged myelination in human neocortical evolution. P Natl Acad Sci USA 109, 16480-16485.

Miller, R.H. (2002). Regulation of oligodendrocyte development in the vertebrate CNS. Prog Neurobiol 67, 451-467.

Miron, V.E., Boyd, A., Zhao, J.W., Yuen, T.J., Ruckh, J.M., Shadrach, J.L., van Wijngaarden, P., Wagers, A.J., Williams, A., Franklin, R.J., and ffrench-Constant, C. (2013). M2 microglia and macrophages drive oligodendrocyte differentiation during CNS remyelination. Nat Neurosci 16, 1211-1218.

Mirsky, R., Winter, J., Abney, E.R., Pruss, R.M., Gavrilovic, J., and Raff, M.C. (1980). Myelin-specific proteins and glycolipids in rat Schwann cells and oligodendrocytes in culture. J Cell Biol 84, 483-494.

Moon, E.Y., Im, Y.S., Ryu, Y.K., and Kang, J.H. (2010). Actin-sequestering protein, thymosin beta-4, is a novel hypoxia responsive regulator. Clin Exp Metastas 27, 601-609.

Moore, C.S., Milner, R., Nishiyama, A., Frausto, R.F., Serwanski, D.R., Pagarigan, R.R., Whitton, J.L., Miller, R.H., and Crocker, S.J. (2011). Astrocytic Tissue Inhibitor of Metalloproteinase-1 (TIMP-1) Promotes Oligodendrocyte Differentiation and Enhances CNS Myelination. Journal of Neuroscience 31, 6247-6254.

Najm, F.J., Madhavan, M., Zaremba, A., Shick, E., Karl, R.T., Factor, D.C., Miller, T.E., Nevin, Z.S., Kantor, C., Sargent, A.*, et al.* (2015). Drug-based modulation of endogenous stem cells promotes functional remyelination in vivo. Nature 522, 216-220.

Nakamua, S., Todo, T., Motoi, Y., Haga, S., Aizawa, T., Ueki, A., and Ikeda, K. (1999). Glial expression of fibroblast growth factor-9 in rat central nervous system. Glia 28, 53-65.

Nave, K.A. (2010). Myelination and support of axonal integrity by glia. Nature 468, 244-252.

Nave, K.A., and Salzer, J.L. (2006). Axonal regulation of myelination by neuregulin 1. Curr Opin Neurobiol 16, 492-500.

Nave, K.A., and Werner, H.B. (2014). Myelination of the nervous system: mechanisms and functions. Annu Rev Cell Dev Biol 30, 503-533.

Nawaz, S., Kippert, A., Saab, A.S., Werner, H.B., Lang, T., Nave, K.A., and Simons, M. (2009). Phosphatidylinositol 4,5-bisphosphate-dependent interaction of myelin basic protein with the plasma membrane in oligodendroglial cells and its rapid perturbation by elevated calcium. J Neurosci 29, 4794-4807.

Nicoll, R.A., and Schmitz, D. (2005). Synaptic plasticity at hippocampal mossy fibre synapses. Nature Reviews Neuroscience 6, 863-876.

Pardridge, W.M., Kang, Y.S., and Buciak, J.L. (1994). Transport of Human Recombinant Brain-Derived Neurotrophic Factor (Bdnf) through the Rat Blood-Brain-Barrier in-Vivo Using Vector-Mediated Peptide Drug-Delivery. Pharmaceut Res 11, 738-746.

Piaton, G., Gould, R.M., and Lubetzki, C. (2010). Axon-oligodendrocyte interactions during developmental myelination, demyelination and repair. J Neurochem 114, 1243-1260.

Poliak, S., and Peles, E. (2003). The local differentiation of myelinated axons at nodes of Ranvier. Nature Reviews Neuroscience 4, 968-980.

Proescholdt, M.A., Heiss, J.D., Walbridge, S., Muhlhauser, J., Capogrossi, M.C., Oldfield, E.H., and Merrill, M.J. (1999). Vascular endothelial growth factor (VEGF) modulates vascular permeability and inflammation in rat brain. J Neuropath Exp Neur 58, 613-627.

Purves, D. (2012). Circuits within the Cerebellum. In Neuroscience (Sunderland, Mass.: Sinauer Associates).

Ramos-Cejudo, J., Gutierrez-Fernandez, M., Otero-Ortega, L., Rodriguez-Frutos, B., Fuentes, B., Vallejo-Cremades, M.T., Hernanz, T.N., Cerdan, S., and Diez-Tejedor, E. (2015). Brain-Derived Neurotrophic Factor Administration Mediated Oligodendrocyte Differentiation and Myelin Formation in Subcortical Ischemic Stroke. Stroke 46, 221-+.

Rasband, M.N. (2011). Composition, assembly, and maintenance of excitable membrane domains in myelinated axons. Semin Cell Dev Biol 22, 178-184.

Rauskolb, S., Zagrebelsky, M., Dreznjak, A., Deogracias, R., Matsumoto, T., Wiese, S., Erne, B., Sendtner, M., Schaeren-Wiemers, N., Korte, M., and Barde, Y.A. (2010). Global deprivation of brain-derived neurotrophic factor in the CNS reveals an area-specific requirement for dendritic growth. J Neurosci 30, 1739-1749.

Richardson, W.D., Young, K.M., Tripathi, R.B., and McKenzie, I. (2011). NG2-glia as Multipotent Neural Stem Cells: Fact or Fantasy? Neuron 70, 661-673.

Riva, M.A., and Mocchetti, I. (1991). Developmental Expression of the Basic Fibroblast Growth-Factor Gene in Rat-Brain. Dev Brain Res 62, 45-50.

Rivers, L.E., Young, K.M., Rizzi, M., Jamen, F., Psachoulia, K., Wade, A., Kessaris, N., and Richardson, W.D. (2008). PDGFRA/NG2 glia generate myelinating oligodendrocytes and piriform projection neurons in adult mice. Nature Neuroscience 11, 1392-1401.

Rosenbluth, J. (1980). Central myelin in the mouse mutant shiverer. J Comp Neurol 194, 639-648.

Rossner, M.J., Hirrlinger, J., Wichert, S.P., Boehm, C., Newrzella, D., Hiemisch, H., Eisenhardt, G., Stuenkel, C., von Ahsen, O., and Nave, K.A. (2006). Global transcriptome analysis of genetically identified neurons in the adult cortex. J Neurosci 26, 9956-9966.

Rowitch, D.H., and Kriegstein, A.R. (2010). Developmental genetics of vertebrate glial-cell specification. Nature 468, 214-222.

Sabo, J.K., Aumann, T.D., Merlo, D., Kilpatrick, T.J., and Cate, H.S. (2011). Remyelination Is Altered by Bone Morphogenic Protein Signaling in Demyelinated Lesions. Journal of Neuroscience 31, 4504-4510.

Sagane, K., Hayakawa, K., Kai, J., Hirohashi, T., Takahashi, E., Miyamoto, N., Ino, M., Oki, T., Yamazaki, K., and Nagasu, T. (2005). Ataxia and peripheral nerve hypomyelination in ADAM22-deficient mice. Bmc Neurosci 6.

Salzer, J.L. (2003). Polarized Domains of Myelinated Axons. Neuron 40, 297-318.

Santra, M., Chopp, M., Zhang, Z.G., Lu, M., Santra, S., Nalani, A., Santra, S., and Morris, D.C. (2012). Thymosin beta 4 mediates oligodendrocyte differentiation by upregulating p38 MAPK. Glia 60, 1826-1838.

Savas, J.N., Toyama, B.H., Xu, T., Yates, J.R., and Hetzer, M.W. (2012). Extremely Long-Lived Nuclear Pore Proteins in the Rat Brain. Science 335, 942-942.

Schabitz, W.R., Steigleder, T., Cooper-Kuhn, C.M., Schwab, S., Sommer, C., Schneider, A., and Kuhn, H.G. (2007). Intravenous brain-derived neurotrophic factor enhances poststroke sensorimotor recovery and stimulates neurogenesis. Stroke 38, 2165-2172.

Scholz, J., Klein, M.C., Behrens, T.E.J., and Johansen-Berg, H. (2009). Training induces changes in white-matter architecture. Nature Neuroscience 12, 1370-1371.

Schwab, M.E., and Strittmatter, S.M. (2014). Nogo limits neural plasticity and recovery from injury. Curr Opin Neurobiol 27, 53-60.

Simons, M., and Trajkovic, K. (2006). Neuron-glia communication in the control of oligodendrocyte function and myelin biogenesis. J Cell Sci 119, 4381-4389.

Soriano, P. (1999). Generalized lacZ expression with the ROSA26 Cre reporter strain. Nat Genet 21, 70-71.

Staugaitis, S.M., and Trapp, B.D. (2009). NG2-positive glia in the human central nervous system. Neuron Glia Biol 5, 35-44.

Stevens, B., Porta, S., Haak, L.L., Gallo, V., and Fields, R.D. (2002). Adenosine: A neuron-glial transmitter promoting myelination in the CNS in response to action potentials. Neuron 36, 855-868.

Stiles, B., Groszer, M., Wang, S., Jiao, J., and Wu, H. (2004a). PTENless means more. Dev Biol 273, 175-184.

Stiles, B., Groszer, M., Wang, S.Y., Jiao, J., and Wu, H. (2004b). PTENless means more. Developmental Biology 273, 175-184.

Stritt, C., Stern, S., Harting, K., Manke, T., Sinske, D., Schwarz, H., Vingron, M., Nordheim, A., and Knoll, B. (2009). Paracrine control of oligodendrocyte differentiation by SRF-directed neuronal gene expression. Nature Neuroscience 12, 418-427.

Suter, U., and Scherer, S.S. (2003). Disease mechanisms in inherited neuropathies. Nat Rev Neurosci 4, 714-726.

Suzuki, A., Nakano, T., Mak, T.W., and Sasaki, T. (2008). Portrait of PTEN: Messages from mutant mice. Cancer Sci 99, 209-213.

Sylva, M., Moorman, A.F., and van den Hoff, M.J. (2013). Follistatin-like 1 in vertebrate development. Birth Defects Res C Embryo Today 99, 61-69.

Taveggia, C., Feltri, M.L., and Wrabetz, L. (2010). Signals to promote myelin formation and repair. Nature Reviews Neurology 6, 276-287.

Taveggia, C., Thaker, P., Petrylak, A., Caporaso, G.L., Toews, A., Falls, D.L., Einheber, S., and Salzer, J.L. (2008). Type III neuregulin-1 promotes oligodendrocyte myelination. Glia 56, 284-293.

Taveggia, C., Zanazzi, G., Petrylak, A., Yano, H., Rosenbluth, J., Einheber, S., Xu, X.R., Esper, R.M., Loeb, J.A., Shrager, P.*, et al.* (2005). Neuregulin-1 type III determines the ensheathment fate of axons. Neuron 47, 681-694.

Temple, S., and Raff, M.C. (1986). Clonal analysis of oligodendrocyte development in culture: evidence for a developmental clock that counts cell divisions. Cell 44, 773-779.

Thomas, R.A., Pietrzak, D.C., Scicchitano, M.S., Thomas, H.C., McFarland, D.C., and Frazier, K.S. (2009). Detection and characterization of circulating endothelial progenitor cells in normal rat blood. Journal of Pharmacological and Toxicological Methods 60, 263-274.

Tsuchida, K., Nakatani, M., Hitachi, K., Uezumi, A., Sunada, Y., Ageta, H., and Inokuchi, K. (2009). Activin signaling as an emerging target for therapeutic interventions. Cell Commun Signal 7, 15.

Tsuchida, K., Nakatani, M., Ueztjmi, A., Murakami, T., and Cui, X.L. (2008). Signal transduction pathway through activin receptors as a therapeutic target of musculoskeletal diseases and cancer. Endocr J 55, 11-21.

Van't Veer, A., Du, Y., Fischer, T.Z., Boetig, D.R., Wood, M.R., and Dreyfus, C.F. (2009). Brain-Derived Neurotrophic Factor Effects on Oligodendrocyte Progenitors of the Basal Forebrain Are Mediated Through TrkB and the MAP Kinase Pathway. Journal of Neuroscience Research 87, 69-78.

Vanderpal, R.H.M., Koper, J.W., Vangolde, L.M.G., and Lopescardozo, M. (1988). Effects of Insulin and Insulin-Like Growth-Factor (Igf-I) on Oligodendrocyte-Enriched Glial Cultures. Journal of Neuroscience Research 19, 483-490.

Vartanian, T., Fischbach, G., and Miller, R. (1999). Failure of spinal cord oligodendrocyte development in mice lacking neuregulin. P Natl Acad Sci USA 96, 731-735.

Vondran, M.W., Clinton-Luke, P., Honeywell, J.Z., and Dreyfus, C.F. (2010). BDNF+/- Mice Exhibit Deficits in Oligodendrocyte Lineage Cells of the Basal Forebrain. Glia 58, 848-856.

Voyvodic, J.T. (1989). Target size regulates calibre and myelination of sympathetic axons. Nature 342, 430-433.

Wakatsuki, S., Yumoto, N., Komatsu, K., Araki, T., and Sehara-Fujisawa, A. (2009). Roles of Meltrin-beta/ADAM19 in Progression of Schwann Cell Differentiation and Myelination during Sciatic Nerve Regeneration. J Biol Chem 284, 2957-2966.

Wake, H., Lee, P.R., and Fields, R.D. (2011). Control of local protein synthesis and initial events in myelination by action potentials. Science 333, 1647-1651.

Wang, S.L., Sdrulla, A.D., diSibio, G., Bush, G., Nofziger, D., Hicks, C., Weinmaster, G., and Barres, B.A. (1998). Notch receptor activation inhibits oligodendrocyte differentiation. Neuron 21, 63-75.

Waxman, S.G., and Sims, T.J. (1984). Specificity in Central Myelination - Evidence for Local-Regulation of Myelin Thickness. Brain Research 292, 179-185.

Weinberg, H.J., and Spencer, P.S. (1976). Studies on the control of myelinogenesis. II. Evidence for neuronal regulation of myelin production. Brain Res 113, 363-378.

Willem, M., Garratt, A.N., Novak, B., Citron, M., Kaufmann, S., Rittger, A., DeStrooper, B., Saftig, P., Birchmeier, C., and Haass, C. (2006). Control of peripheral nerve myelination by the beta-secretase BACE1. Science 314, 664-666.

Wojtowicz, J.M., and Kee, N. (2006). BrdU assay for neurogenesis in rodents. Nat Protoc 1, 1399-1405.

Wyatt, K.D., Tanapat, P., and Wang, S.S.H. (2005). Speed limits in the cerebellum: constraints from myelinated and unmyelinated parallel fibers. European Journal of Neuroscience 21, 2285-2290.

Xiao, J., Wong, A.W., Willingham, M.M., van den Buuse, M., Kilpatrick, T.J., and Murray, S.S. (2010). Brain-derived neurotrophic factor promotes central nervous system myelination via a direct effect upon oligodendrocytes. Neurosignals 18, 186-202.

Xiao, J.H., Ferner, A.H., Wong, A.W., Denham, M., Kilpatrick, T.J., and Murray, S.S. (2012). Extracellular signal-regulated kinase 1/2 signaling promotes oligodendrocyte myelination in vitro. J Neurochem 122, 1167-1180.

Yeung, M.S.Y., Zdunek, S., Bergmann, O., Bernard, S., Salehpour, M., Alkass, K., Perl, S., Tisdale, J., Possnert, G., Brundin, L.*, et al.* (2014). Dynamics of Oligodendrocyte Generation and Myelination in the Human Brain. Cell 159, 766-774.

Young, K.M., Psachoulia, K., Tripathi, R.B., Dunn, S.J., Cossell, L., Attwell, D., Tohyama, K., and Richardson, W.D. (2013). Oligodendrocyte Dynamics in the Healthy Adult CNS: Evidence for Myelin Remodeling. Neuron 77, 873-885.

Zhang, Y., Chen, K., Sloan, S.A., Bennett, M.L., Scholze, A.R., O'Keeffe, S., Phatnani, H.P., Guarnieri, P., Caneda, C., Ruderisch, N.*, et al.* (2014). An RNA-sequencing transcriptome

and splicing database of glia, neurons, and vascular cells of the cerebral cortex. J Neurosci 34, 11929-11947.

Zhang, Y.Q., Chen, Y.T., Xie, S.Z., Wang, L., Lee, Y.F., Chang, S.S., and Chang, C.S. (2007). Loss of testicular orphan receptor 4 impairs normal myelination in mouse forebrain. Mol Endocrinol 21, 908-920.